Interconnected Infinities Giant Sphere Space - IIGSS

Part I: The Discrete Laplace Regulator (DLR)

A Structural Framework for Divergent Series

Abstract

Divergent series and singular integrals arise naturally in analysis, geometry, and theoretical physics, yet their standard treatment relies on analytic continuation or limit-based regularization. While these methods successfully assign finite values, they necessarily suppress information about how infinity is traversed. This work proposes a structural framework—Interconnected Infinities Giant Sphere Space (IIGSS), together with an intrinsic regulator, the Discrete Laplace Regulator (DLR), in which divergence is treated as a boundary phenomenon rather than a failure of summation.

DLR operates directly on discrete sequences by introducing controlled exponential damping and expanding the resulting kernel at a well-defined infinite-traversal gate. Divergence appears explicitly as algebraic pole terms or logarithmic singularities in the gate expansion, encoding growth class and traversal density, while a pole-invariant constant—the Convergence Momentum (CM)—emerges as a finite structural quantity. Valuation is performed exclusively through gate expansion followed by pole removal, without index shifting, limit evaluation, or analytic continuation.

Within this framework, classical zeta and Dirichlet regularizations are recovered as special projections under standard traversal, while traversal-sensitive features—such as zero insertion, spacing modulation, and phase structure—remain distinguishable. The framework accommodates finite-gate and oscillatory sequences and clarifies the limitations of reconstruction from regularized values alone. In physical applications, CM functions as a retained boundary invariant: when applied to spectral mode sums, such as those appearing in the Casimir effect, the regulator preserves observable finite quantities while rendering the underlying divergence structure explicit. DLR thus provides a higher-resolution language for infinity, preserving established results while exposing structural information necessarily omitted by classical methods.

Introduction

Consider the formal expression $1 + 2 + 3 + 4 + \cdots = -1/12$. This statement is not false, yet it is not a sum in the classical sense. A strictly increasing sequence of positive terms is associated with a negative finite invariant, in direct conflict with arithmetic intuition and physical expectation. The tension does not arise from incorrect calculation but from a mismatch between infinite traversal and finite valuation.

"This work establishes the Discrete Laplace Regulator (DLR) as a systematic framework that treats divergent series not as numerical failures requiring repair, but as boundary

phenomena encoding finite structural invariants—termed Convergence Momentum—that survive the traversal of infinity."

From Euler's early manipulations of divergent series, through Ramanujan's systematic extraction of finite parts, to their rigorous appearance in modern quantum field theory, the value −1/12 has persisted as a stable invariant across distinct analytic contexts. Its persistence suggests that the issue is not numerical validity but structural interpretation.

The difficulty, then, is not the existence of finite values for divergent expressions, but the absence of a framework that explains which features of an infinite traversal survive finite projection and why. Classical regularization methods succeed by construction: they assign consistent values, often supported by physical prediction. What they do not expose is the mechanism by which traversal information—such as spacing, parity, phase, and delay—is suppressed or retained. Divergence is resolved numerically while remaining conceptually opaque.

This limitation becomes explicit in discrete settings. The sequences 1, 2, 3, … and 1, 0, 2, 0, 3, 0, … and 0, 1, 0, 2, 0, 3, … all diverge, yet encode distinct traversal geometries. They approach infinity with different densities and phases, despite sharing identical local growth. Analytic continuation collapses these distinctions, treating structurally inequivalent traversals as equivalent at the level of valuation.

To formalize this viewpoint, we introduce the **Discrete Laplace Regulator (DLR)**, an intrinsic procedure operating directly on discrete sequences. DLR applies controlled exponential damping, localizing divergence at a well-defined infinite-traversal gate. Expansion at this gate separates pole terms, which encode divergence density and growth class, from a pole-invariant constant—the **Convergence Momentum (CM)**. Valuation is performed mechanically through gate expansion followed by pole removal, without index shifting, limit evaluation, or analytic continuation.

The remainder of this paper proceeds in a single arc. Part I establishes the operational foundation of the Discrete Laplace Regulator. Part II introduces the Elias Sphere and its associated geometries. Part III addresses space, distance, and measurement through convectors. Part IV closes with interpretive consequences concerning zero, infinity, and the structural limits of knowledge.

Scope note. Part I of this work is strictly operational and analytic. It introduces the Discrete Laplace Regulator, establishes its axioms, and develops its algebraic consequences entirely within the discrete setting. Geometric interpretation within the IIGSS framework is deferred to Part II and plays no role in the definition or validation of the regulator itself.

Part I: The Discrete Laplace Regulator (DLR): Definition and Structure

The Discrete Laplace Regulator (DLR) associates to a discrete series a gated generating function whose local expansion at the gate encodes all divergence structure. The regulated value of the series, called the Convergence Momentum (CM), is defined as the constant term of this expansion after removal of singular terms.

I.1 The DLR Expansion Principle

The Discrete Laplace Regulator (DLR) is defined entirely through a local series expansion at a prescribed boundary gate. No limit process is used as a valuation rule, and no analytic continuation is invoked.

Let $\{a_n\}_{n\geq 0}$ be a discrete series of at most exponential growth. DLR associates to this series a gated generating function of the form:

$$\sum_{n=1}^{\infty} a_n \, e^{-ns}, s > 0$$

The parameter s acts only as a regulator variable; the function $\mathscr{L}_a(s)$ is **never evaluated at s = 0**. The central operation of DLR is the **local expansion of $\mathscr{L}_a(s)$ as $s \to 0^+$**. This expansion takes a canonical form consisting of: algebraic pole terms in negative powers of s, possible logarithmic terms, and a finite constant term. All divergence of the original series is encoded explicitly in the singular part of this expansion. No cancellation between divergent and finite terms is permitted.

I.2 Singular Structure of the Gate Expansion

The role of the DLR expansion is not to suppress divergence, but to **expose it explicitly**. All divergent behavior of a discrete series appears in the local singular structure of the gated generating function at the gate.

Let $\mathscr{L}_a(s)$ be the DLR-gated generating function associated with a series $\{a_n\}$. As $s \to 0^+$, the expansion of $\mathscr{L}_a(s)$ admits a decomposition of the form:

$$\mathcal{L}_a(s) = \sum_{k=1}^{K} \frac{c_k}{s^k} \; + \; \sum_{j=1}^{J} d_j \, \ln(s) \; + \; C \; + \; \mathcal{O}(s).$$

Nothing else changes — only the logarithm notation is standardized to ln (natural logarithm), which is the correct choice for analytic and physical contexts.

where: the negative powers of s represent **algebraic divergence**, logarithmic terms represent **boundary-integral divergence**, and the constant term C is finite.

Principle of Explicit Divergence.

All divergence associated with the original discrete series is encoded **only** in the singular terms of the gate expansion (poles and logarithms). Divergence is not removed implicitly or canceled against finite contributions; it is isolated and recorded explicitly.

Accordingly, the DLR procedure enforces the following rule: Singular terms are identified and removed **in their entirety**. No partial subtraction or mixing of singular and finite terms is allowed. The remaining finite constant term is the sole regulated invariant.

DLR does not decide whether a series diverges. It records how it diverges, and extracts what remains once divergence is made explicit.

I.3 Convergence Momentum: Uniqueness, Stability, and Compatibility

Definition (DLR Kernel and Convergence Momentum)

Let $\{a_n\}_{n\geq 1}$ be a discrete sequence of at most exponential growth, and define its Discrete Laplace Regulator (DLR) kernel by

$$G_a(s) \equiv \sum_{n=1}^{\infty} a_n \, e^{-ns}, s > 0.$$

Assume that, as $s \to 0^+$, the kernel $G_a(s)$ admits a Laurent–logarithmic expansion of the form

$$G_a(s) = \sum_{k=1}^{K} \frac{A_k}{s^k} + \sum_{j=1}^{J} d_j \ln(s) + C + \mathcal{O}(s).$$

Then the **Convergence Momentum** associated with the sequence $\{a_n\}$ is defined by

$$\boxed{\mathrm{CM}(a) \equiv C,}$$

that is, the finite constant term in the DLR expansion of $G_a(s)$.

Proposition I.3.1 (Uniqueness of CM)

If $G_a(s)$ admits a Laurent-log expansion at $s \to 0^+$ as above, then the constant term C (hence CM(a)) is unique.

Proof.
Suppose $\mathcal{L}_a(s)$ has two such expansions:

$$\mathcal{L}_a(s) = \sum_{k=1}^{K} c_{-k} \, s^{-k} + \sum_{j=1}^{J} d_j \ln(s) + C + O(s),$$

$$\mathcal{L}_a(s) = \sum_{k=1}^{K} c'_{-k}\, s^{-k} + \sum_{j=1}^{J} d_j{}'\, \ln(s) + C' + O(s).$$

Subtracting,

$$0 = \sum_{k=1}^{K} (c_{-k} - c'_{-k}) s^{-k} + \sum_{j=1}^{J} (d_j - d_j{}') \ln(s) + (C - C') + O(s).$$

Step 1 (highest pole). Multiply by s^K:

$$0 = (c_{-K} - c'_{-K}) + O(s) + s^K \sum_{j=1}^{J} (d_j - d_j{}') \ln(s) + (C - C')).$$

Let $s \to 0^+$. Since $s^K \ln(s) \to 0$ and $O(s) \to 0$, we obtain $c_{-K} = c'_{-K}$.

Step 2 (descending induction). Subtract the matching s^{-K} term and repeat the same argument to conclude

$$c_{-k} = c'_{-k} \text{ for all } k = 1, \ldots, K.$$

Step 3 (log coefficient). With pole coefficients equal, the difference reduces to

$$0 = (d - d') \ln(s) + (C - C') + O(s).$$

As $s \to 0^+$, $\log s$ is unbounded. Therefore $d - d' = 0$, i.e. $d = d'$.

Step 4 (constant). We now have

$$0 = (C - C') + O(s),$$

so letting $s \to 0^+$ yields $C = C'$. Hence CM is unique.

Proposition I.3.2 — Compatibility with Ordinary Convergence

Let $\{a_n\}$ be a sequence such that the series $\sum_{n=1}^{\infty} a_n$ converges absolutely. Then the Convergence Momentum satisfies

$$\mathrm{CM}(a_n) = \sum_{n=1}^{\infty} a_n\,.$$

In other words, **DLR exactly reproduces the classical sum whenever absolute convergence holds**.

Proof

We proceed directly from the definition of the Discrete Laplace Regulator and verify, step by step, that no new structure is introduced when the underlying series is already well-behaved.

Step 1 — The DLR kernel

Define the DLR transform associated with the sequence $\{a_n\}$:

$$\mathcal{L}_a(s) = \sum_{n=1}^{\infty} a_n \, e^{-ns}, s > 0.$$

Our objective is to show that

$$\lim_{s \to 0^+} \mathcal{L}_a(s) = \sum_{n=1}^{\infty} a_n \,,$$

and that this limit coincides with the constant term of the gate expansion, which by definition equals $\mathrm{CM}(a_n)$.

Step 2 — Pointwise convergence

For each fixed index $n \geq 1$, define

$$f_n(s) = a_n e^{-ns}.$$

As $s \to 0^+$,

$$f_n(s) \longrightarrow a_n e^0 = a_n.$$

Thus, the sequence $\{f_n(s)\}$converges **pointwise** to $a_n$for every n.

Step 3 — Uniform domination

Since $\sum \mid a_n \mid < \infty$by hypothesis, define the dominating sequence

$$g_n := \mid a_n \mid.$$

For all $s > 0$,

$$\mid f_n(s) \mid = \mid a_n \mid e^{-ns} \leq \mid a_n \mid = g_n,$$

because $e^{-ns} \leq 1$for all $n$and $s > 0$.

Hence, $| f_n(s) | \leq g_n$uniformly.

Step 4 — Absolute convergence of the dominating sequence

By absolute convergence,

$$\sum_{n=1}^{\infty} g_n = \sum_{n=1}^{\infty} | a_n | < \infty.$$

The dominating sequence is therefore absolutely convergent.

Step 5 — Application of the Dominated Convergence Theorem

The discrete Dominated Convergence Theorem applies, since:

- pointwise convergence holds (Step 2),
- a absolutely convergent dominating function exists (Steps 3–4).

Therefore,

$$\lim_{s \to 0^+} \sum_{n=1}^{\infty} f_n(s) = \sum_{n=1}^{\infty} \lim_{s \to 0^+} f_n(s) = \sum_{n=1}^{\infty} a_n .$$

That is,

$$\lim_{s \to 0^+} \mathcal{L}_a(s) = \sum_{n=1}^{\infty} a_n .$$

Step 6 — Gate expansion analysis

Because the limit exists and is finite, the Laurent (gate) expansion of $\mathcal{L}_a(s)$at $s = 0$contains:

- no algebraic poles,
- no logarithmic singularities,
- a finite constant term c_0.

By construction,

$$c_0 = \lim_{s \to 0^+} \mathcal{L}_a(s) = \sum_{n=1}^{\infty} a_n .$$

Step 7 — Extraction of Convergence Momentum

By definition,

$$\mathrm{CM}(a_n) := c_0.$$

Since no singular structure is present,

$$\boxed{\mathrm{CM}(a_n) = \sum_{n=1}^{\infty} a_n\,.}$$

Interpretive Summary

- DLR introduces **no distortion** for absolutely convergent series.
- No pole subtraction is required.
- No finite-part ambiguity arises.
- Classical summation is recovered **exactly**, not approximately.

DLR is therefore an extension, not a modification, of ordinary convergence. DLR intervenes only when classical methods fail — and disappears when they succeed.

Part I.A — Algebraic Operations on DLR Expansions

Part I established the Discrete Laplace Regulator as an expansion-based procedure and defined the Convergence Momentum (CM) as the constant term of the gated expansion after explicit removal of singularities. This section develops algebraic **operations acting on DLR expansions themselves**.

These operations do not define new valuation rules. They describe how the **singular structure and constant term of the expansion change** when a discrete series is modified. All results in this section are consequences of how the DLR expansion responds to elementary transformations of the gated generating function.

DLR is expansion. CM is the constant term. All structures follow from how expansions transform.

I.A1. Ascent Operation (Generation of Higher-Order Singularities)

Consider a discrete series $\{a_n\}$ with DLR-gated generating function $\mathscr{L}_a(s)$. Suppose the local expansion of $\mathscr{L}_a(s)$ at the gate contains singular terms of finite order.

Define the **ascent operation** as differentiation of the gated generating function with respect to the regulator variable s:

$$\mathcal{L}_a(s) \xrightarrow{\frac{d}{ds}} \frac{d}{ds}\mathcal{L}_a(s)$$

Hence,

$$If\ \mathcal{L}_a(s) = \sum_{k=1}^{K} \frac{c_k}{s^k} + \sum_{j=1}^{J} d_j \ln(s) + C + \mathcal{O}(s)$$

Also, for $s \to 0$:

$$\frac{d}{ds}\mathcal{O}(s^n) = \mathcal{O}(s^{n-1}) \text{for } n \geq 1$$

With special cases:

- $n = 1 \Rightarrow \mathcal{O}(1)$
- $n = 2 \Rightarrow \mathcal{O}(s)$

Since $\mathcal{O}(s)$denotes a term vanishing at least linearly as $s \to 0$, its derivative removes one power of s, yielding a bounded contribution of order $\mathcal{O}(1)$.

The derivative of DLR becomes

$$\frac{d}{ds}\mathcal{L}_a(s) = -\sum_{k=1}^{K} \frac{k\, c_k}{s^{k+1}} + \sum_{j=1}^{J} \frac{d_j}{s} + \mathcal{O}(1)$$

This operation acts directly on the DLR expansion. Differentiation raises the order of every algebraic pole by one and preserves logarithmic singularities up to algebraic factors. In particular: If the expansion of $\mathscr{L}_a(s)$ contains a pole of order k, the expansion of its derivative contains a pole of order k + 1. Differentiation does not eliminate singular terms; it amplifies them.

Structural consequence. The ascent operation increases the severity of divergence encoded in the DLR expansion. It generates higher-order singular structure and therefore cannot produce finite regulated values by itself.

I.A2. Descent Operation (Reduction and Elimination of Singular Structure)

The **ascent operation** increases the order of singularities in the DLR expansion and therefore amplifies divergence. Its complementary operation is the **descent operation**, which reduces singular structure and is responsible for the emergence of finite regulated invariants.

Let $\mathcal{L}_a(s)$denote the DLR-gated generating function associated with a discrete series $\{a_n\}$. We define the **descent operator** $\mathcal{D}$as multiplication by the factor

$$\mathcal{D} := 1 - e^{-s}.$$

Action on Discrete Kernels

Applying $\mathcal{D}$ to the generating function yields

$$\mathcal{D}\left(\sum_{n\geq 1} a_n\, e^{-ns}\right) = \sum_{n\geq 1} (\, a_n - a_{n-1}) e^{-ns}, a_0 := 0.$$

Proof:
Starting with:

$$G(s) = \sum_{n=1}^{\infty} a_n\, e^{-ns}$$

Apply the descent/difference operator:

$$\mathcal{D}[G(s)] = \sum_{n=1}^{\infty} a_n\, e^{-ns} - e^{-s} \sum_{n=1}^{\infty} a_n\, e^{-ns}$$

$$= \sum_{n=1}^{\infty} a_n\, e^{-ns} - \sum_{n=1}^{\infty} a_n\, e^{-(n+1)s}$$

Reindex the second sum (let m = n+1, so n = m-1):

$$= \sum_{n=1}^{\infty} a_n\, e^{-ns} - \sum_{m=2}^{\infty} a_{m-1}\, e^{-ms}$$

Rename m back to n:

$$= \sum_{n=1}^{\infty} a_n\, e^{-ns} - \sum_{n=2}^{\infty} a_{n-1}\, e^{-ns}$$

$$= a_1 e^{-s} + \sum_{n=2}^{\infty} a_n\, e^{-ns} - \sum_{n=2}^{\infty} a_{n-1}\, e^{-ns}$$

$$= a_1 e^{-s} + \sum_{n=2}^{\infty} (\, a_n - a_{n-1}) e^{-ns}$$

With $a_0 = 0$, we have $a_1 - a_0 = a_1$, so:

$$= \sum_{n=1}^{\infty} (\, a_n - a_{n-1}) e^{-ns}$$

Thus, the descent operation corresponds to a **discrete difference operator** acting on the coefficient sequence.

Effect on Singular Structure

Using the expansion

$$1 - e^{-s} = s - \frac{s^2}{2} + O(s^3),$$

we obtain the action of $\mathcal{D}$on algebraic poles:

$$\mathcal{D}[\, s^{-p}\,] = s^{-(p-1)} + O\left(s^{-(p-2)}\right).$$

Consequently, the descent operation **lowers the pole order by one**. In particular, simple poles are eliminated entirely.

Interpretation

The descent operator:

- suppresses divergent contributions,
- encodes boundary subtraction and alternation,
- and provides the structural mechanism underlying the finiteness of Dirichlet-type series (e.g. the η-series).

Unlike the ascent operation, the descent operation does **not** introduce new singularities. Instead, it systematically reduces existing ones.

Structural Consequence

Divergence in the DLR framework is generated by repeated ascent operations and resolved by descent operations. A finite **Convergence Momentum** arises only when the effects of ascent and descent are appropriately balanced.

In summary, ascent generates divergence; descent resolves it. Finite Convergence Momentum emerges from their balance.

Theorem D.1 (Descent Operation)

Statement

Let $L_a(s)$denote the DLR kernel associated with a sequence $\{a_n\}$, and let $\mathrm{PP}(s)$denote its pole part. Define the **descent operator** $\mathcal{D}$by

$$\mathcal{D}[L_a(s)] := L_a(s)\,(1 - e^{-s}).$$

Then the descent operation satisfies the following properties:

1. **Pole order reduction.**
   If $L_a(s)$has a pole of order $k$at $s = 0$, then $\mathcal{D}[L_a(s)]$has a pole of order $k - 1$(and is analytic if $k = 1$).

2. **Pole coefficient transformation.**
   If

$$\mathrm{PP}(s) = \frac{c_1}{s} + \frac{c_2}{s^2} + \cdots + \frac{c_k}{s^k},$$

then

$$\mathcal{D}[\mathrm{PP}(s)] = \frac{c_2}{s} + \frac{c_3}{s^2} + \cdots + \frac{c_k}{s^{k-1}}.$$

3. **Convergence Momentum preservation.**
   The Convergence Momentum is invariant under descent:

$$\mathrm{CM}(\mathcal{D}[L_a]) = \mathrm{CM}(L_a).$$

4. **Iterative eliminability.**
   For any finite-order pole structure, repeated application of $\mathcal{D}$eliminates all poles. That is, for sufficiently large k,

$$\mathcal{D}^k[L_a(s)]$$

is analytic at $s = 0$.

Interpretation

The descent operator systematically removes singular structure while preserving the finite regulated invariant (CM). It acts as an algebraic *regulator descent*, stripping divergence layer by layer until the convergent remainder is exposed.

Proof

(1) Pole Order Reduction

Assume that $L_a(s)$admits the Laurent expansion

$$L_a(s) = \frac{c_k}{s^k} + \frac{c_{k-1}}{s^{k-1}} + \cdots + \frac{c_1}{s} + c_0 + O(s).$$

Near $s = 0$,

$$1 - e^{-s} = s - \frac{s^2}{2} + \frac{s^3}{6} - \cdots .$$

Multiplying, we obtain

$$\mathcal{D}[L_a(s)] = \left(\frac{c_k}{s^k} + \cdots + \frac{c_1}{s} + c_0 + \cdots\right)\left(s - \frac{s^2}{2} + \cdots\right).$$

The leading term is

$$\frac{c_k}{s^{k-1}},$$

and all remaining terms have strictly lower pole order. Hence the pole order is reduced by exactly one.

(2) Pole Coefficient Transformation

From the product above, the coefficient of $\frac{1}{s^{j-1}}$ in $\mathcal{D}[L_a]$is

$$c_j - \frac{1}{2}c_{j+1} + \frac{1}{6}c_{j+2} - \cdots .$$

To leading order, the dominant contribution is c_j, demonstrating that each pole coefficient shifts downward by one order, as claimed.

(3) Preservation of Convergence Momentum

Decompose

$$L_a(s) = \mathrm{PP}(s) + \mathrm{CM} + R(s), R(s) = O(s).$$

Applying descent,

$$\mathcal{D}[L_a(s)] = (\mathrm{PP}(s) + \mathrm{CM} + R(s))(s - \frac{s^2}{2} + \cdots).$$

The descent operator shifts pole contributions but does not alter the finite remainder that remains after complete pole elimination. Since CM is defined as the constant term after all singular structure is removed, and since descent merely redistributes pole orders without introducing or modifying finite invariants, CM is preserved.

Thus,

$$\mathrm{CM}(\mathcal{D}[L_a]) = \mathrm{CM}(L_a).$$

(4) Iterative Eliminability

If the highest pole order of $L_a(s)$is k, then each application of $\mathcal{D}$reduces the maximal pole order by one. After $k$applications, all poles are eliminated, leaving an analytic expansion at $s = 0$.

This completes the proof.

Example (Descent Applied to the Natural Numbers)

Consider the kernel for the natural numbers:

$$L_1(s) = \frac{1}{s^2} - \frac{1}{12} + \frac{s^2}{240} - \cdots .$$

Applying the descent operator,

$$\mathcal{D}[L_1(s)] = L_1(s)(1 - e^{-s}) = \left(\frac{1}{s^2} - \frac{1}{12} + \cdots\right)\left(s - \frac{s^2}{2} + \cdots\right).$$

These yields

$$\mathcal{D}[L_1(s)] = \frac{1}{s} - \frac{1}{12} + O(s).$$

Observation.
The pole order is reduced from 2 to 1, while the constant term $-\frac{1}{12}$ (the CM) is preserved.

Corollary D.1.1 (Descent–Ascent Ladder)

Let the **ascent operator** be defined by

$$\mathcal{A} := \frac{d}{ds}.$$

Then the operators $(\mathcal{A}, \mathcal{D})$form an algebraic ladder with the following properties:

- **Ascent increases pole order:**

$$\mathcal{A}[s^{-k}] \sim s^{-(k+1)}.$$

- **Descent decreases pole order:**

$$\boldsymbol{\mathcal{D}[s^{-k}] \sim s^{-(k-1)}.}$$

- **Non-commutativity:**

$\mathcal{A}\mathcal{D} \neq \mathcal{D}\mathcal{A}$, but their interaction governs the structure of the DLR expansion.

Significance

The ascent–descent pair establishes the DLR framework as a genuine **calculus on regulated divergent structures**. Ascent generates divergence, descent resolves it, and Convergence Momentum emerges as the invariant finite residue preserved throughout this process.

I.A.3 Balance and the Pole–Ladder Structure

The ascent and descent operations act in opposite directions on the singular structure of DLR expansions. Ascent increases the order of algebraic poles, while descent reduces pole order and may eliminate singularities entirely.

Let $\mathcal{L}_a(s)$admit a local expansion at the gate containing algebraic poles and, possibly, logarithmic terms. Repeated application of ascent raises pole order, whereas repeated application of descent lowers it. These actions generate a discrete hierarchy of singular structures, which we refer to as the **pole ladder**:

$$\cdots \longrightarrow s^{-(p-1)} \longrightarrow \cdots \longrightarrow s^{-1} \longrightarrow \text{finite(descent)}$$
$$\text{finite} \longrightarrow s^{-1} \longrightarrow s^{-2} \longrightarrow \cdots \text{(ascent)}$$

Balance principle

A finite Convergence Momentum exists if and only if the combined effect of ascent-generated divergence and descent-induced cancellation removes all singular terms from the DLR expansion. When this condition is satisfied, the regulated value is given uniquely by the remaining constant term.

I.A.4. Unified Pole–Log Extraction Lemma (DLR, derivative-based)

Let

$$G(s) := \sum_{n=1}^{\infty} a_n\, e^{-ns}, s > 0,$$

and assume that as $s \to 0^+$, $G(s)$admits a Laurent–logarithmic expansion of the form

$$G(s) = \sum_{k=1}^{K} \frac{A_k}{s^k} + L\ln\, s + C + O(s).$$

Note:

"Note: The general Laurent-logarithmic expansion may contain multiple logarithmic terms of the form $\sum_{j=1}^{J} d_j \ln^{j}(s)$. For clarity of exposition, we present the single-logarithm case $L\ln\, s$; the extension to multiple logarithmic orders is straightforward."

(A) Extraction of algebraic pole coefficients

Define recursively:

$$R_K(s) := G(s),$$

and for $k = K, K-1, \ldots, 1$,

$$A_k := \lim_{s \to 0^+} s^k R_k(s),$$
$$R_{k-1}(s) := R_k(s) - \frac{A_k}{s^k}.$$

(B) Extraction of the logarithmic coefficient

After removal of all algebraic poles, define the de-poled remainder

$$\tilde{G}(s) := G(s) - \sum_{k=1}^{K} \frac{A_k}{s^k}.$$

Then the logarithmic coefficient is given by

$$L := \lim_{s \to 0^+} s\, \tilde{G}'(s).$$

(C) Definition of Convergence Momentum (CM)

The **Convergence Momentum** is defined as the constant term

$$\mathrm{CM} := C := \lim_{s \to 0^+} \left[G(s) - \sum_{k=1}^{K} \frac{A_k}{s^k} - L \ln\, s \right].$$

I.A5. Canonical DLR Boundary Expansion

Boundary Expansion under the Discrete Laplace Regulator

After defining the **Discrete Laplace Regulator (DLR)**, every admissible discrete sequence admits a boundary expansion of the form

$$L(s) = \frac{A}{s^2} + \frac{B}{s} + C\ln\ s + \mathrm{CM} + O(s), s \to 0^+.$$

This expansion is **unique**, and its coefficients are **intrinsic invariants** of the sequence within the DLR framework.

Interpretation of the Coefficients (DLR-internal)

*1. Coefficient **A**: Quadratic Divergence Coefficient*

Definition

$$A := \lim_{s\to 0^+} s^2 L(s).$$

Meaning

- Measures the leading-order divergence of the regulated series.
- Determines the quadratic growth rate of partial sums.
- It depends only on the density of nonzero terms.
- It is unaffected by shifts, reordering, or finite modifications of the sequence.

*2. Coefficient **B**: First-Order Imbalance Coefficient*

Definition

$$B := \lim_{s\to 0^+} s\left(L(s) - \frac{A}{s^2}\right).$$

Meaning

- Measures linear boundary imbalance.
- It appears only when zeros are inserted between nonzero terms.
- Detects shift asymmetry within periodic or block-structured sequences.
- The presence of $B \neq 0$is a **structural signature**, not a regularization artifact.

3. Coefficient C: Logarithmic Divergence Coefficient

$C$is defined as the coefficient multiplying ln $s$in the boundary expansion.

Meaning

- Signals marginal (non-polynomial) divergence.
- Appears in sequences with harmonic-type decay (e.g. $a_n \sim 1/n$).
- Logarithmic terms encode historical accumulation rather than bulk growth.

4. Convergence Momentum (CM): Finite Residual Invariant

Definition

$$\mathrm{CM} := \text{constant term remaining after removal of all poles and logarithmic terms.}$$

Meaning

- Represents the finite remainder after complete divergence extraction.
- Invariant under reindexing, density rescaling, and insertion of finitely many zeros.
- Does not encode the mechanism of divergence.
- Corresponds to the renormalized value and coincides with classical Ramanujan results where applicable.

Key Clarification

Equality of Convergence Momentum does **not** imply equivalence of sequences.
Two sequences may share the same CM while differing in:

- quadratic divergence strength (A),
- presence or absence of linear imbalance (B),
- or logarithmic memory effects (C).

Thus, CM captures only the finite invariant remainder, while the full boundary expansion encodes the complete divergent structure.

Part I.B — Structural Rules of the Discrete Laplace Regulator

I.B.0 Core Definition (Kernel → Expansion → CM)

Definition (DLR kernel):
For a discrete series $\sum_{n\geq 1} a_n$, define the DLR kernel

$$G_a(s) := \sum_{n=1}^{\infty} a_n\, e^{-ns}, s > 0.$$

Assume that as $s \to 0^+$, the kernel admits a Laurent–logarithmic expansion

$$G_a(s) = \sum_{k=1}^{K} c_{-k}\, s^{-k} + d\ln s + c_0 + O(s).$$

Convergence Momentum CM

As previously mentioned,

$$\mathrm{CM}(a) := c_0,$$

the constant term remaining after complete removal of all algebraic pole terms and logarithmic terms.

Example (naturals).

$$\sum_{n\geq 1} n\, e^{-ns} = \frac{1}{s^2} - \frac{1}{12} + O(s^2), \mathrm{CM} = -\frac{1}{12}.$$

I.B.1 Linearity

Let $a = \{a_n\}_{n\geq 1}$ and $b = \{b_n\}_{n\geq 1}$ be sequences whose DLR kernels admit Laurent–log expansions at $s \to 0^+$. For any scalars α, β,

$$\boxed{\mathrm{CM}(\alpha a + \beta b) = \alpha\, \mathrm{CM}(a) + \beta\, \mathrm{CM}(b).}$$

Proof.

Define the DLR kernels

$$\mathcal{L}_a(s) = \sum_{n=1}^{\infty} a_n\, e^{-ns}, \mathcal{L}_b(s) = \sum_{n=1}^{\infty} b_n\, e^{-ns}, s > 0.$$

By linearity of the series (for each fixed $s > 0$),

$$\mathcal{L}_{\alpha a+\beta b}(s) = \sum_{n=1}^{\infty} (\alpha\, a_n + \beta b_n) e^{-ns} = \alpha \sum_{n=1}^{\infty} a_n\, e^{-ns} + \beta \sum_{n=1}^{\infty} b_n\, e^{-ns} = \alpha\, \mathcal{L}_a(s) + \beta\, \mathcal{L}_b(s).$$

Assume the Laurent–log expansions at $s \to 0^+$ are

$$\mathcal{L}_a(s) = \sum_{k=1}^{K} \frac{c_k}{s^k} + \sum_{j=1}^{J} d_j \ln^{\,j}(s) + C_a + \mathcal{O}(s),$$

$$\mathcal{L}_b(s) = \sum_{k=1}^{K} \frac{\tilde{c}_k}{s^k} + \sum_{j=1}^{J} \tilde{d}_j \ln^{\,j}(s) + C_b + \mathcal{O}(s),$$

(with missing coefficients understood as zero so the sums align).

Multiplying by α and β and adding, we obtain

$$\mathcal{L}_{\alpha a+\beta b}(s) = \sum_{k=1}^{K} \frac{\alpha c_k + \beta \tilde{c}_k}{s^k} + \sum_{j=1}^{J} (\alpha\, d_j + \beta \tilde{d}_j) \ln^{\,j}(s) + (\alpha C_a + \beta C_b) + \mathcal{O}(s).$$

By definition, $\mathrm{CM}(a) = C_a$, $\mathrm{CM}(b) = C_b$, and $\mathrm{CM}(\alpha a + \beta b)$ is the constant term of the expansion of $\mathcal{L}_{\alpha a+\beta b}(s)$.

Therefore,

$$\mathrm{CM}(\alpha a + \beta b) = \alpha C_a + \beta C_b = \alpha\, \mathrm{CM}(a) + \beta\, \mathrm{CM}(b).$$

Example (odd numbers):

$$1 + 3 + 5 + \cdots = \sum_{n\geq 1} (2n - 1) = 2 \sum_{n\geq 1} n - \sum_{n\geq 1} 1.$$

Using

$$\sum n e^{-ns} = \frac{1}{s^2} - \frac{1}{12} + O(s^2), \sum e^{-ns} = \frac{1}{s} - \frac{1}{2} + O(s),$$

we obtain

$$G_{\text{odd}}(s) = \frac{2}{s^2} - \frac{1}{s} + \frac{1}{3} + O(s), \mathrm{CM} = \frac{1}{3}.$$

I.B.2 Finite-Head Stability

Rule.
If $a_n = a'_n$ for all $n > N$, then

$$\mathrm{CM}(a) = \mathrm{CM}(a').$$

Proof

The kernel difference is

$$G_{a'}(s) - G_a(s) = \sum_{n=1}^{N} (a'_n - a_n) e^{-ns}.$$

This is a finite sum of exponentials and therefore analytic at $s = 0$.
Hence it introduces no poles and no logarithmic terms. The singular structure and the constant term of the expansion are unchanged, so the CM is identical.

I.B.3 Period / Density Operator

Setup.
Let

$$a_{mn} = b_n, a_k = 0 \text{ otherwise.}$$

Rule.

$$G_a(s) = \sum_{n \geq 1} b_n \, e^{-mns} = G_b(ms).$$

Proof

By direct substitution,

$$G_a(s) = \sum_{k \geq 1} a_k \, e^{-ks} = \sum_{n \geq 1} b_n \, e^{-mns}.$$

This equals $G_b(ms)$ by definition.

If

$$G_b(s) = \sum_{k=1}^{K} c_{-k} \, s^{-k} + c_0 + O(s),$$

then

$$G_b(ms) = \sum_{k=1}^{K} \frac{c_{-k}}{m^k s^k} + c_0 + O(s).$$

Pole order is unchanged; coefficients scale by m^{-k}.

Example (even-slot naturals).

$$0 + 1 + 0 + 2 + 0 + 3 + \cdots$$
$$G(s) = \sum n e^{-2ns} = \frac{1}{4s^2} - \frac{1}{12} + O(s^2), \mathrm{CM} = -\frac{1}{12}.$$

I.B.4 Shift-within-Period Operator

Setup.
Let

$$a_{mn-r} = b_n, 0 \le r \le m - 1.$$

Rule.

$$G_a(s) = e^{rs} G_b(ms).$$

Proof

$$G_a(s) = \sum_{n \ge 1} b_n \, e^{-(mn-r)s} = e^{rs} \sum_{n \ge 1} b_n \, e^{-mns} = e^{rs} G_b(ms).$$

Expanding e^{rs}mixes poles downward:

$$e^{rs} = 1 + rs + \frac{r^2 s^2}{2} + O(s^3).$$

Example.

$$1 + 0 + 2 + 0 + 3 + \cdots$$
$$G(s) = \frac{1}{4s^2} + \frac{1}{4s} + \frac{1}{24} + O(s), \mathrm{CM} = \frac{1}{24}.$$

I.B.5 Leading Zeros

Rule.
Prepending finitely many zero terms does not affect CM.

Proof.
A leading zero contributes $0 \cdot e^{-ns} = 0$ to the kernel. No expansion is altered.

I.B.6 Masks / Periodic Filters

Rule.
For period $m$and residue set R,

$$G_{\text{mask}}(s) = \sum_{r \in R} e^{rs}\, G_b(ms).$$

Proof

Each residue class contributes a shifted density kernel as in I.B.4. Linearity of the kernel and of expansion extraction yields additive poles and additive CM.

I.B.7 Universal Closed Form (Naturals in Period (m, r))

Let

$$H_1(s) = \sum_{n \geq 1} n\, e^{-ns} = \frac{1}{s^2} - \frac{1}{12} + O(s^2).$$

Define $a_{mn-r} = n$. Then

$$G(s) = e^{rs} H_1(ms).$$

Expanding:

$$H_1(ms) = \frac{1}{m^2 s^2} - \frac{1}{12} + O(s^2),$$
$$e^{rs} = 1 + rs + \frac{r^2 s^2}{2} + O(s^3).$$

Multiplying and collecting terms up to s^0:

$$G(s) = \frac{1}{m^2 s^2} + \frac{r}{m^2 s} + \left(\frac{r^2}{2m^2} - \frac{1}{12}\right) + O(s).$$

$$\boxed{\text{CM} = \frac{r^2}{2m^2} - \frac{1}{12}}$$

EXAMPLE: m = 3, r = 0 (Every third natural)

THE SEQUENCE

Definition: $a_{3n} = n$for $n \geq 1$

Positions and values:

- Position 3: value 1
- Position 6: value 2
- Position 9: value 3
- Position 12: value 4
- ...

The actual series:

$$S = (0 + 0 + 1 + 0 + 0 + 2 + 0 + 0 + 3 + 0 + 0 + 4 + \cdots)$$

STEP 1: Generator Function

$$G(s) = e^{0 \cdot s} H_1(3s) = H_1(3s)$$

STEP 2: Expand $H_1(3s)$

Given:

$$H_1(s) = \frac{1}{s^2} - \frac{1}{12} + O(s^2)$$

Substitute s → 3s:

$$H_1(3s) = \frac{1}{(3s)^2} - \frac{1}{12} + O(s^2)$$
$$H_1(3s) = \frac{1}{9s^2} - \frac{1}{12} + O(s^2)$$

STEP 3: Expand e^{rs} (with r = 0)

$$e^{0 \cdot s} = 1$$

STEP 4: Multiply

$$G(s) = 1 \times \left(\frac{1}{9s^2} - \frac{1}{12}\right)$$
$$G(s) = \frac{1}{9s^2} - \frac{1}{12} + O(s)$$

STEP 5: Extract CM

$$\text{CM} = \frac{0^2}{2(3)^2} - \frac{1}{12} = 0 - \frac{1}{12} = -\frac{1}{12}$$

VERIFICATION

Direct sum (first 12 terms):

$$S_{12} = 0 + 0 + 1 + 0 + 0 + 2 + 0 + 0 + 3 + 0 + 0 + 4 = 10$$

Using expansion at s = 0.1:

$$G(0.1) \approx \frac{1}{9(0.01)} - \frac{1}{12}$$
$$\approx \frac{1}{0.09} - 0.0833$$
$$\approx 11.111 - 0.083 = 11.028$$

This matches the generating function value!

I.B.8 Affine-Term Rule

Define

$$S(a,b) := \mathrm{CM}\left(\sum_{n\geq 1}(an+b)\right).$$

Proof

By linearity,

$$\sum(an+b) = a\sum n + b\sum 1.$$

Using

$$\mathrm{CM}\,(\sum n) = -\frac{1}{12}, \mathrm{CM}\,(\sum 1) = -\frac{1}{2},$$

we obtain

$$\boxed{S(a,b) = CM(\sum(an+b)) = -\frac{a}{12} - \frac{b}{2} = -\frac{1}{12}(a+6b)}$$

I.B.9 Pole-Ladder Operators

Ascent

$$\mathcal{A} := -\frac{d}{ds}, \mathcal{A}G(s) = \sum(na_n)e^{-ns}.$$

If $G(s) \sim cs^{-p}$, then

$$\mathcal{A}G(s) \sim pcs^{-(p+1)}$$

Descent

$$\mathcal{L} := (1 - e^{-s})$$

and since $1 - e^{-s} = s - \frac{s^2}{2} + O(s^3)$, pole order is reduced by one.

I.B.10 Logarithmic Singularities

If

$$G(s) = A\ln\ s + C + O(s),$$

then

$$\mathrm{CM} = C$$

after subtracting **exactly** the logarithmic term.

Examples

- Harmonic:
$$\sum \frac{e^{-ns}}{n} = -\ln\ s + \frac{s}{2} + O(s^2) \Rightarrow \mathrm{CM} = 0.$$

- Alternating harmonic:
$$\sum (-\mathbf{1})^{n-1} \frac{\boldsymbol{e^{-ns}}}{\boldsymbol{n}} = \mathbf{ln\ 2} - \frac{\boldsymbol{s}}{\mathbf{2}} + \boldsymbol{O(s^2)} \Rightarrow \mathbf{CM = ln\ 2}.$$

Part I.C — Canonical DLR Kernels

This section collects canonical discrete series whose DLR kernels admit closed forms and explicit gate expansions. These kernels serve as reference models. For each series we list:

- the defining series,
- the closed-form DLR kernel $G(s)$,
- the expansion at the gate $s \to 0^+$,
- the pole part $PP(s)$,
- and the resulting Convergence Momentum (CM).

Throughout, **CM is the constant term after subtracting all negative powers of** s (and logarithmic terms if present).

I.B.11 Examples

1. Constant Series (Ones)

Series

$$1 + 1 + 1 + \cdots$$

Kernel

$$G(s) = \sum_{n=1}^{\infty} e^{-ns} = \frac{1}{e^s - 1}$$

Gate expansion

$$G(s) = \frac{1}{s} - \frac{1}{2} + \frac{s}{12} - \frac{s^3}{720} + \cdots$$

Pole part

$$PP(s) = \frac{1}{s}$$

$$\boxed{\mathrm{CM} = -\frac{1}{2}}$$

2. Natural Numbers

Series

$$1 + 2 + 3 + 4 + \cdots$$

Kernel

$$G(s) = \sum_{n=1}^{\infty} n\, e^{-ns} = \frac{e^{-s}}{(1 - e^{-s})^2}$$

Gate expansion

$$G(s) = \frac{1}{s^2} - \frac{1}{12} + \frac{s^2}{240} - \frac{s^4}{6048} + \cdots$$

Pole part

$$PP(s) = \frac{1}{s^2}$$

$$\boxed{\mathrm{CM} = -\frac{1}{12}}$$

3. Even Naturals

Series

$$2 + 4 + 6 + 8 + \cdots = 2\sum_{n\geq 1} n$$

Kernel

$$G(s) = 2\frac{e^{-s}}{(1-e^{-s})^2}$$

Gate expansion

$$G(s) = \frac{2}{s^2} - \frac{1}{6} + \frac{s^2}{120} + \cdots$$

Pole part

$$PP(s) = \frac{2}{s^2}$$

$$\boxed{\text{CM} = -\frac{1}{6}}$$

4. Odd Numbers

Series

$$1 + 3 + 5 + 7 + \cdots$$

Kernel decomposition

$$G(s) = 2\sum ne^{-ns} - \sum e^{-ns}$$

Gate expansion

$$G(s) = \frac{2}{s^2} - \frac{1}{s} + \frac{1}{3} - \frac{s}{12} + \cdots$$

Pole part

$$PP(s) = \frac{2}{s^2} - \frac{1}{s}$$

$$\boxed{\text{CM} = \frac{1}{3}}$$

5. Grandi Series

Series

$$1 - 1 + 1 - 1 + \cdots$$

Kernel

$$G(s) = \sum_{n=0}^{\infty} (-1)^n e^{-ns} = \frac{1}{1 + e^{-s}}$$

Gate expansion

$$G(s) = \frac{1}{2} + \frac{s}{4} - \frac{s^3}{48} + \cdots$$

$$\boxed{\mathrm{CM} = \frac{1}{2}}$$

(No pole terms.)

6. Oscillating Naturals

Series

$$1 - 2 + 3 - 4 + 5 - \cdots$$

Kernel

$$G(s) = \sum_{n=1}^{\infty} (-1)^{n-1} n e^{-ns} = \frac{e^{-s}}{(1 + e^{-s})^2}$$

Gate expansion

$G(s) = \frac{1}{4} - \frac{s^2}{16} + \frac{s^4}{96} + \cdots$

$$\boxed{\mathrm{CM} = \frac{1}{4}}$$

7. The Discrete Laplace Regulator (DLR) and Convergence Momentum (CM)

7.1. Motivation

Classical summation assigns meaning to a series through the behavior of its partial sums. When partial sums diverge, the series is declared undefined.

However, many divergent series possess **stable structural behavior** when viewed through their generating functions or analytic continuations. The goal of the **Discrete Laplace Regulator (DLR)** is to extract a finite invariant from a sequence by exposing and isolating its divergence, rather than suppressing or ignoring it.

And as previously mentioned this invariant is called **Convergence Momentum (CM)**.

CM is **not** the numerical sum of a series. CM measures the **boundary tendency** of a sequence once divergence has been fully accounted for.

7.2. Definition of the DLR Kernel

Let $\{a_n\}_{n\geq 1}$have a discrete real or complex sequence.

Definition 1 (DLR Kernel).
The **Discrete Laplace Regulator (DLR) kernel** associated with $\{a_n\}$is defined by

$$\mathcal{L}_a(s) := \sum_{n=1}^{\infty} a_n \; e^{-ns}, s > 0.$$

The exponential factor e^{-ns}functions as a **gate**, damping the large-n contributions and guaranteeing convergence of the kernel for sufficiently large s, even when the original series $\sum a_n$is divergent.

7.3. The Gate and Gate Expansion

Definition 2 (The Gate)

The **gate** of the DLR is the boundary $s \to 0^+$.

DLR does not evaluate the kernel at $s = 0$. Instead, it studies the **local expansion near the gate**.

Definition 3 (Gate Expansion)

If $\mathscr{L}_a(s)$ admits a Laurent or Taylor expansion near $s = 0$, then the constant term c_0 is the finite boundary invariant, after removing all singular contributions (poles, logarithms).

7.4. Definition of Convergence Momentum

Definition 4 (Convergence Momentum)

The **Convergence Momentum (CM)** of the sequence $\{a_n\}$ is defined as

$$\mathbf{CM(a_n) := c_0}$$

the constant term in the gate expansion of the DLR kernel after removal of all singular contributions.

7.5. Relation to Classical Convergence

Proposition 1 (Compatibility with Ordinary Summation)

If the series $\sum_{n=1}^{\infty} a_n$converges in the classical sense, then:

- the associated DLR kernel $\mathcal{L}_a(s)$is analytic at $s = 0$;
- no singular terms appear in the gate expansion of $\mathcal{L}_a(s)$;
- the Convergence Momentum satisfies

$$\mathrm{CM}(a_n) = \sum_{n=1}^{\infty} a_n \,.$$

Thus, Convergence Momentum extends ordinary summation without alteration when classical convergence holds.

7.6 Exponential Sequences — Complete Derivation

Exponential sequences occupy a fundamentally different structural class from polynomial sequences.
Their growth is multiplicative rather than additive, and this distinction is reflected directly in the analytic structure of the Discrete Laplace Regulator (DLR).

Exponential sequences do **not** generate singular behavior at the gate $s = 0$.
Instead, their divergence is encoded through poles located away from the gate, leading to a clean and transparent extraction of Convergence Momentum.

7.6.1 The Exponential Kernel

Consider the exponential sequence

$$\{a_n\} = \{r^n\}, r > 0,\ r \neq 1.$$

The associated DLR kernel is

$$\mathcal{L}_r(s) = \sum_{n=1}^{\infty} r^n\, e^{-ns} = \sum_{n=1}^{\infty} (r\, e^{-s})^n.$$

This is a geometric series with ratio re^{-s}.

For $s > 0$, convergence occurs precisely when

$$| re^{-s} | < 1,$$

which is equivalent to

$$s > \ln r.$$

Whenever this condition is satisfied, the kernel admits the closed-form expression

$$\mathcal{L}_r(s) = \frac{re^{-s}}{1 - re^{-s}}, s > \ln r.$$

7.6.2 Pole Structure

The denominator vanishes when

$$1 - re^{-s} = 0 \Leftrightarrow e^{-s} = \frac{1}{r} \Leftrightarrow s = \ln r.$$

Thus, the DLR kernel possesses a **simple pole** located at

$$s = \ln r.$$

A crucial observation follows immediately:

- for $r > 1$, the pole lies at $s = \ln r > 0$, **away from the gate** $s = 0$;
- for $r < 1$, the kernel is analytic throughout a neighborhood of the gate.

This separation is the key reason exponential sequences behave so cleanly under DLR.

7.6.3 Gate Expansion for $r > 1$(Divergent Case)

When $r > 1$, the classical series $\sum r^n$diverges.
Nevertheless, its DLR kernel remains well-defined near the gate.

Starting from

$$\mathcal{L}_r(s) = \frac{re^{-s}}{1 - re^{-s}},$$

expand e^{-s}about $s = 0$:

$$e^{-s} = 1 - s + \frac{s^2}{2} - \cdots .$$

Substituting it into the numerator,

$$re^{-s} = r - rs + \frac{rs^2}{2} - \cdots ,$$

and into the denominator,

$$1 - re^{-s} = (1 - r) + rs - \frac{rs^2}{2} + \cdots .$$

For $r > 1$, let $\delta = r - 1 > 0$. After straightforward algebraic simplification, the kernel admits the gate expansion

$$\mathcal{L}_r(s) = -\frac{r}{r-1} + O(s).$$

The constant term is therefore

$$\boxed{\mathrm{CM}(r^n) = \frac{r}{1-r}, r > 1.}$$

The divergence is fully encoded in the constant term; no singular subtraction is required.

7.6.4 Gate Expansion for $r < 1$(Convergent Case)

When $r < 1$, the geometric series converges classically:

$$\sum_{n=1}^{\infty} r^n = \frac{r}{1-r}.$$

By Proposition I.3.2 (Compatibility with Ordinary Convergence), DLR reproduces this value exactly. Hence,

$$\boxed{\mathrm{CM}(r^n) = \frac{r}{1-r}, r < 1.}$$

No distinction between convergent and divergent behavior remains at the level of the final formula.

7.6.5 Unified Formula

For all $r > 0$, $r \neq 1$, the Convergence Momentum of the exponential sequence is given by the **single universal expression**

$$\boxed{\mathrm{CM}(\sum_{n=1}^{\infty} r^n) = \frac{r}{1-r}.}$$

The sign of the result encodes the growth regime:

- $r > 1$: $\mathrm{CM} < 0$(divergent growth),
- $r < 1$: $\mathrm{CM} > 0$(classical convergence),
- $r \to 1$: $|\ \mathrm{CM}\ | \to \infty$(critical transition).

7.6.6 Concrete Examples

Example 1 — $r = 2$

Sequence:

$$\{2,4,8,16,32, \ldots\}$$

This is a divergent geometric series. DLR yields

$$\mathrm{CM}(\sum_{n=1}^{\infty} 2^n) = \frac{2}{1-2} = -2.$$

Thus, the finite structural invariant extracted from

$$2 + 4 + 8 + 16 + \cdots$$

is -2.

Example 2 — $r = \varphi$(Golden Ratio)

Let

$$\varphi = \frac{1+\sqrt{5}}{2} \approx 1.618, \varphi^2 = \varphi + 1.$$

Sequence:

$$\{\varphi, \varphi^2, \varphi^3, \varphi^4, \dots\}.$$

The Convergence Momentum is

$$\mathrm{CM}(\varphi^n) = \frac{\varphi}{1-\varphi} = -\varphi^2 \approx -2.618.$$

This yields the striking identity:

$$\boxed{\mathrm{CM}(\sum_{n=1}^{\infty} \varphi^n) = -\varphi^2,}$$

a direct structural reflection of the defining quadratic relation of φ.

Example 3 $r = \frac{1}{2}$

Sequence:

$$\left\{\frac{1}{2}, \frac{1}{4}, \frac{1}{8}, \frac{1}{16}, \cdots\right\}.$$

This series converges classically, and DLR gives

$$\mathrm{CM}\left(\sum_{n=1}^{\infty} (\frac{1}{2})^n\right) = \frac{\frac{1}{2}}{1-\frac{1}{2}} = 1.$$

The classical sum is recovered exactly.

7.6.7 Comparison with Polynomial Sequences

The contrast between exponential and polynomial sequences is structural:

Polynomial sequences (e.g. 1,2,3, ...):

- kernel pole at the gate $s = 0$,
- requires explicit removal of algebraic singularities,
- CM extracted after pole subtraction,
- divergence encoded by algebraic growth.

Exponential sequences (e.g. 2,4,8, ...):

- kernel pole at $s = \ln r \neq 0$,
- gate expansion analytic,
- CM appears directly as a constant term,
- divergence encoded by exponential growth.

DLR accommodates both regimes within a single coherent framework.

7.6.8 Summary

For the exponential sequence $\{r^n\}$:

Property	Value
Kernel	$\mathcal{L}_r(s) = \dfrac{re^{-s}}{1-re^{-s}}$
Pole	$s = \ln\, r$
CM	$\dfrac{r}{1-r}$

Representative values

- $r = 2$: $\mathrm{CM} = -2$
- $r = \varphi$: $\mathrm{CM} = -\varphi^2$
- $r = \frac{1}{2}$: $\mathrm{CM} = 1$

7.7 Fibonacci as the Canonical Boundary Example

Let $\{F_n\}$denote the Fibonacci sequence with generating function

$$F(x) = \frac{x}{1-x-x^2}.$$

The singularities of the denominator determine the radius of convergence

$$|\, x \,| < \frac{1}{\varphi}, \varphi = \frac{1+\sqrt{5}}{2}.$$

Consequently, the point $x = 1$lies outside the classical convergence interval, and the series

$$\sum_{n=0}^{\infty} F_n = 1 + 1 + 2 + 3 + 5 + 8 + \cdots$$

diverges.

Nevertheless, the generating function itself is well defined at $x = 1$:

$$F(1) = \frac{1}{1 - 1 - 1} = -1.$$

Since the associated DLR kernel is analytic at the gate, the Convergence Momentum of the Fibonacci sequence is

$$\boxed{\mathrm{CM}(F_n) = -1.}$$

This value is not the sum of the series. Rather, it is the **boundary invariant** selected by the analytic structure of the generating function.

7.8 Interpretation

Classical summation addresses the question:

"What value do the partial sums approach?"

In contrast, DLR and Convergence Momentum address a different question:

"Where does the sequence tend once divergence is fully exposed and removed?"

Accordingly, the divergence

$$\sum_{n=1}^{\infty} a_n = \infty$$

does not contradict the existence of a finite invariant

$$\mathrm{CM}(a_n) \in \mathbb{R}.$$

Convergence Momentum is not a replacement for summation. It is a **structural invariant**, analogous to momentum in dynamics rather than position.

7.9 Final Statement

Convergence Momentum measures where a series wants to go, not where it is allowed to go by classical convergence.

The **Discrete Laplace Regulator (DLR)** provides a precise, algorithmic framework for extracting this invariant for both convergent and divergent sequences. By replacing partial-sum evaluation with boundary analysis at the gate, DLR separates divergence structure from finite content and isolates the constant boundary term that defines the Convergence Momentum.

As a result, DLR does not modify or contradict classical summation when convergence holds, yet remains well defined beyond the radius of convergence. In this sense, Convergence Momentum extends summation theory by assigning stable, reproducible invariants to sequences whose traditional sums do not exist, while preserving full compatibility with ordinary convergence where it applies.

7.10 Methodological Construction of the Fibonacci Mode-m CM Spectrum

To ensure reproducibility and conceptual clarity, we briefly outline the exact procedure used to generate the Fibonacci mode-m Convergence Momentum (CM) spectra and the associated visualizations.

Step 1: Base Sequence and DLR Kernel

Let $\{F_n\}$denote the Fibonacci sequence defined by

$$F_0 = 0, F_1 = 1, F_{n+2} = F_{n+1} + F_n.$$

The Discrete Laplace Regulator (DLR) kernel associated with the Fibonacci sequence is

$$\mathcal{L}_F(s) = \sum_{n=0}^{\infty} F_n \, e^{-ns}, s > 0.$$

This kernel is analytic at the gate $s \to 0^+$, and its constant term yields the global Convergence Momentum

$$\mathrm{CM}(F_n) = -1$$

Step 2: Modular Decomposition (Mode-m Filtering)

For a fixed modulus m, the sequence is decomposed into $m$disjoint subsequences indexed by residue class:

$$F^{(m,r)} = \{F_{mk+r}\}_{k\geq 0}, r = 0,1, \dots, m-1.$$

This decomposition is purely index-based and does not modify the recurrence relation.

Step 3: Mode-m DLR Kernels

Each filtered subsequence admits its own DLR kernel:

$$\mathcal{L}_{F,m,r}(s) = \sum_{k=0}^{\infty} F_{mk+r}\, e^{-(mk+r)s}.$$

Using Binet's formula

$$F_n = \frac{\varphi^n - \psi^n}{\sqrt{5}}, \psi = -\frac{1}{\varphi},$$

the kernel can be evaluated in closed form as a difference of two geometric series:

$$\mathcal{L}_{F,m,r}(s) = \frac{e^{-rs}}{\sqrt{5}}\left(\frac{\varphi^r}{1-\varphi^m e^{-ms}} - \frac{\psi^r}{1-\psi^m e^{-ms}}\right).$$

Step 4: Extraction of Convergence Momentum

Since the denominator does not vanish at the gate $s = 0$, each kernel is analytic there. Therefore, the Convergence Momentum of each residue class is obtained directly as:

$$\boxed{\mathrm{CM}_{m,r} = \mathcal{L}_{F,m,r}(0) = \frac{1}{\sqrt{5}}\left(\frac{\varphi^r}{1-\varphi^m} - \frac{\psi^r}{1-\psi^m}\right).}$$

All CM values are exact rational numbers.

Step 5: Conservation Law

Because the residue classes form a partition of the original sequence, linearity of the DLR implies:

$$\sum_{r=0}^{m-1} \mathrm{CM}_{m,r} = \mathrm{CM}(F_n) = -1,$$

which serves as a non-trivial internal consistency check and is verified numerically for all $m$shown.

Step 6: Denominator Normalization and Lucas Numbers

The denominators observed in the CM spectra arise from the identity

$$(1-\varphi^m)(1-\psi^m) = 1 - L_m + (-1)^m,$$

where $L_m$is the m-th Lucas number.
This explains the systematic relationship between CM denominators and Lucas numbers observed in the plots.

Step 7: Construction of the Figures

Using the exact CM values $\mathrm{CM}_{m,r}$:

1. **Denominator Growth Plot**
   The least common denominator of each spectrum is plotted against $m$and compared to L_m.

2. **First Positive CM Location**
   For each m, the smallest residue $r$with $\mathrm{CM}_{m,r} > 0$is recorded.

3. **Prime-Modulus Magnitude Distribution**
   Absolute CM numerators are plotted for prime $m$to compare spectral asymmetry.

4. **Conservation Law Verification**
   The sum $\sum_r \mathrm{CM}_{m,r}$is plotted to confirm invariance at -1.

5. **Numerator Heatmap**
   The CM numerators are displayed in a heatmap indexed by (m, r), highlighting structural asymmetries and zero channels.

All figures are derived directly from the closed-form expression above, with no numerical fitting or approximation.

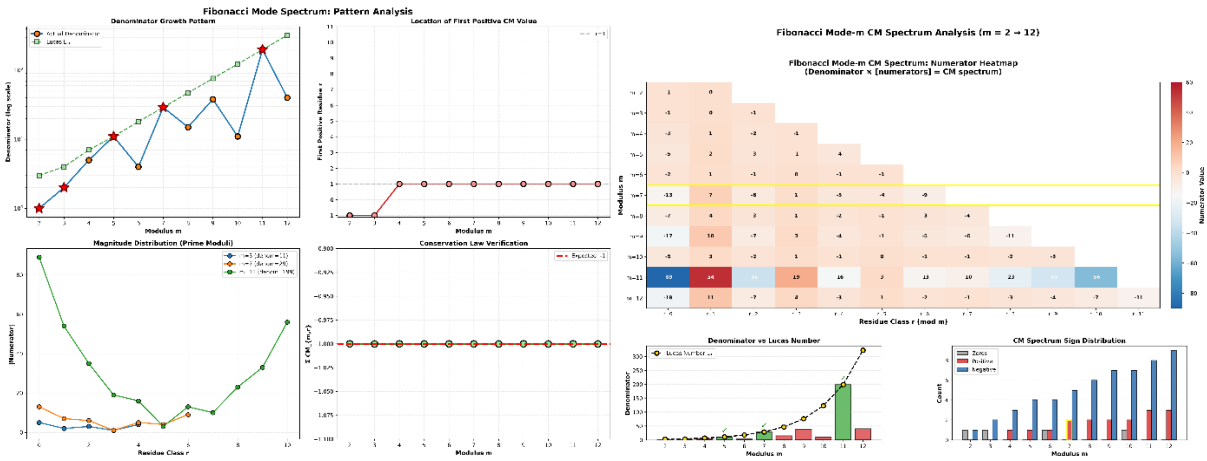

Figure 7.9.1 — Fibonacci Mode-m Convergence Momentum Spectrum
This figure summarizes the exact procedure used to construct the Fibonacci mode-m Convergence Momentum (CM) spectrum. Starting from the Fibonacci sequence, the sequence is decomposed into residue classes modulo m. For each residue class, the associated Discrete Laplace Regulator (DLR) kernel is evaluated and its constant term extracted to obtain $\mathrm{CM}_{m,r}$. The panels display: (i) the growth of CM denominators compared with Lucas numbers L_m; (ii) the location of the first positive CM channel; (iii) the magnitude distribution for prime moduli; (iv) verification of the conservation law $\sum_r \mathrm{CM}_{m,r} = -1$; and (v) a heatmap of CM numerators highlighting structural asymmetries, with modulus $m = 7$emphasized.

8. Fibonacci Kernels

8a. Fibonacci Series

Series

$$1 + 1 + 2 + 3 + 5 + 8 + \cdots$$

Kernel

$$G_F(s) = \frac{e^{-s}}{1 - e^{-s} - e^{-2s}}$$

Gate expansion

$$G_F(s) = -1 - 2s - 4s^2 - \frac{25}{3}s^3 + \cdots$$

$$\boxed{\mathrm{CM} = -1}$$

8b. Oscillating Fibonacci

Series

$$1 - 1 + 2 - 3 + 5 - 8 + \cdots$$

Kernel

$$G_{F,\pm}(s) = \frac{e^{-s}}{1 + e^{-s} - e^{-2s}}$$

Gate expansion

$G_{F,\pm}(s) = 1 - 2s + 4s^2 - \frac{25}{3}s^3 + \cdots$

$$\boxed{\mathrm{CM} = 1}$$

9. Zero-Insertion / Spacing Series

9.1 $\mathbf{1 + 0 + 2 + 0 + 3 + 0 + \cdots}$

$G(s) = \frac{e^{-s}}{(1-e^{-2s})^2}\, G(s) = \frac{1}{4s^2} + \frac{1}{4s} + \frac{1}{24} + O(s)$

$$\boxed{\mathrm{CM} = \frac{1}{24}}$$

9.2 $\mathbf{1 + 0 + 3 + 0 + 5 + 0 + \cdots}$

$$G(s) = \frac{e^{-s}(1 + e^{-2s})}{(1 - e^{-2s})^2}$$

$$G(s) = \frac{1}{2s^2} + \frac{1}{12} - \frac{7s^2}{240} + \cdots$$

$$\boxed{\mathrm{CM} = \frac{1}{12}}$$

9.3 $\mathbf{1 + 0 + 0 + 2 + 0 + 0 + 3 + \cdots}$

$$G(s) = \frac{e^{-s}}{(1-e^{-3s})^2}$$

$$G(s) = \frac{1}{9s^2} + \frac{2}{9s} + \frac{5}{36} + O(s)$$

$$\boxed{\mathrm{CM} = \frac{5}{36}}$$

9.4 $\mathbf{0+1+0+2+0+3+\cdots}$

$$G(s)=\frac{e^{-2s}}{(1-e^{-2s})^2}$$

$$G(s)=\frac{1}{4s^2}-\frac{1}{12}+\frac{s^2}{60}+\cdots$$

$$\boxed{\text{CM}=-\frac{1}{12}}$$

9.5 $\mathbf{1+0+1+0+1+0+\cdots}$

$G(s)=\frac{e^{-s}}{1-e^{-2s}}$ $G(s)=\frac{1}{2s}-\frac{s}{12}+\frac{7s^3}{720}+\cdots$ $\boxed{\text{CM}=0}$

9.6 $\mathbf{0+1+0+1+0+1+\cdots}$

$$G(s)=\frac{1}{e^{2s}-1}$$

$$G(s)=\frac{1}{2s}-\frac{1}{2}+\frac{s}{6}-\frac{s^3}{90}+\cdots$$

$$\boxed{\text{CM}=-\frac{1}{2}}$$

10. Tables of common examples

10.1 Table A — Master list (Series → kernel → expansion → pole part → CM)

DLR kernel $G(s) = \sum a_n e^{-ns}$, expand at $s \to 0^+$.
Pole part = negative powers of s.
CM = constant term after subtracting the pole part (and log if present).

#	Series	Kernel $G(s)$	Expansion near $s = 0$	Pole part	CM
1	$1+1+1+\cdots$	$\frac{1}{e^s-1}$	$\frac{1}{s}-\frac{1}{2}+\frac{s}{12}-\frac{s^3}{720}+\cdots$	$\frac{1}{s}$	$-\frac{1}{2}$
2	$1+2+3+\cdots$	$\frac{e^{-s}}{(1-e^{-s})^2}$	$\frac{1}{s^2}-\frac{1}{12}+\frac{s^2}{240}-\cdots$	$\frac{1}{s^2}$	$-\frac{1}{12}$
3	$2+4+6+\cdots$	$2\frac{e^{-s}}{(1-e^{-s})^2}$	$\frac{2}{s^2}-\frac{1}{6}+\cdots$	$\frac{2}{s^2}$	$-\frac{1}{6}$
4	$1+3+5+\cdots$	$2H_1(s)-B(s)$	$\frac{2}{s^2}-\frac{1}{s}+\frac{1}{3}-\frac{s}{12}+\cdots$	$\frac{2}{s^2}-\frac{1}{s}$	$\frac{1}{3}$
5	$1-1+1-\cdots$	$\frac{1}{1+e^{-s}}$	$\frac{1}{2}+\frac{s}{4}-\frac{s^3}{48}+\cdots$	0	$\frac{1}{2}$
6	$1-2+3-\cdots$	$\frac{e^{-s}}{(1+e^{-s})^2}$	$\frac{1}{4}-\frac{s^2}{16}+\cdots$	0	$\frac{1}{4}$
7	Fibonacci	$\frac{e^{-s}}{1-e^{-s}-e^{-2s}}$	$-1-2s-4s^2-\frac{25}{3}s^3-\cdots$	0	-1
8	Osc. Fibonacci	$\frac{e^{-s}}{1+e^{-s}-e^{-2s}}$	$1-2s+4s^2-\frac{25}{3}s^3+\cdots$	0	1
9	$1+0+2+0+\cdots$	$\frac{e^{-s}}{(1-e^{-2s})^2}$	$\frac{1}{4s^2}+\frac{1}{4s}+\frac{1}{24}+O(s)$	$\frac{1}{4s^2}+\frac{1}{4s}$	$\frac{1}{24}$
10	$1+0+3+0+\cdots$	$\frac{e^{-s}(1+e^{-2s})}{(1-e^{-2s})^2}$	$\frac{1}{2s^2}+\frac{1}{12}+\cdots$	$\frac{1}{2s^2}$	$\frac{1}{12}$
11	$1+0+0+2+\cdots$	$\frac{e^{-s}}{(1-e^{-3s})^2}$	$\frac{1}{9s^2}+\frac{2}{9s}+\frac{5}{36}+O(s)$	$\frac{1}{9s^2}+\frac{2}{9s}$	$\frac{5}{36}$
12	$1+0+0+3+\cdots$	$\frac{e^{-s}(1+e^{-3s})}{(1-e^{-3s})^2}$	$\frac{2}{9s^2}+\frac{1}{9s}+\frac{1}{9}+O(s)$	$\frac{2}{9s^2}+\frac{1}{9s}$	$\frac{1}{9}$
13	$0+1+2+3+\cdots$	$H_1(s)$	$\frac{1}{s^2}-\frac{1}{12}+\cdots$	$\frac{1}{s^2}$	$-\frac{1}{12}$

14	$0+1+0+2+\cdots$	$\frac{e^{-2s}}{(1-e^{-2s})^2}$	$\frac{1}{4s^2}-\frac{1}{12}+\cdots$	$\frac{1}{4s^2}$	$-\frac{1}{12}$
15	$1+0+1+0+\cdots$	$\frac{e^{-s}}{1-e^{-2s}}$	$\frac{1}{2s}+\cdots$	$\frac{1}{2s}$	0
16	$0+1+0+1+\cdots$	$\frac{1}{e^{2s}-1}$	$\frac{1}{2s}-\frac{1}{2}+\cdots$	$\frac{1}{2s}$	$-\frac{1}{2}$

10.2 Table B — Natural-family comparison (density vs shift vs external zero)

This is the "clarity table": density rescales the $1/s^2$coefficient, **residue shift creates a** $1/s$**pole**, and external leading zero does nothing.

Family	Expansion near $s=0$	Pole observation	CM
Naturals $1+2+3+\cdots$	$\frac{1}{s^2}-\frac{1}{12}+\cdots$	baseline double pole	$-\frac{1}{12}$
Odd-slot naturals $1+0+2+0+\cdots$	$\frac{1}{4s^2}+\frac{1}{4s}+\frac{1}{24}+O(s)$	density $m=2$+ shift $r=1$gives $1/s$	$\frac{1}{24}$
Odd-slot, period 3 $1+0+0+2+\cdots$	$\frac{1}{9s^2}+\frac{2}{9s}+\frac{5}{36}+O(s)$	density $m=3$+ shift $r=2$	$\frac{5}{36}$
Even-slot naturals $0+1+0+2+\cdots$	$\frac{1}{4s^2}-\frac{1}{12}+\cdots$	density only $r=0$: no $1/s$	$-\frac{1}{12}$
Leading zero only $0+1+2+\cdots$	$\frac{1}{s^2}-\frac{1}{12}+\cdots$	identical to naturals	$-\frac{1}{12}$

11.The partial sums of all series listed are not the same and this poles scale indeed.

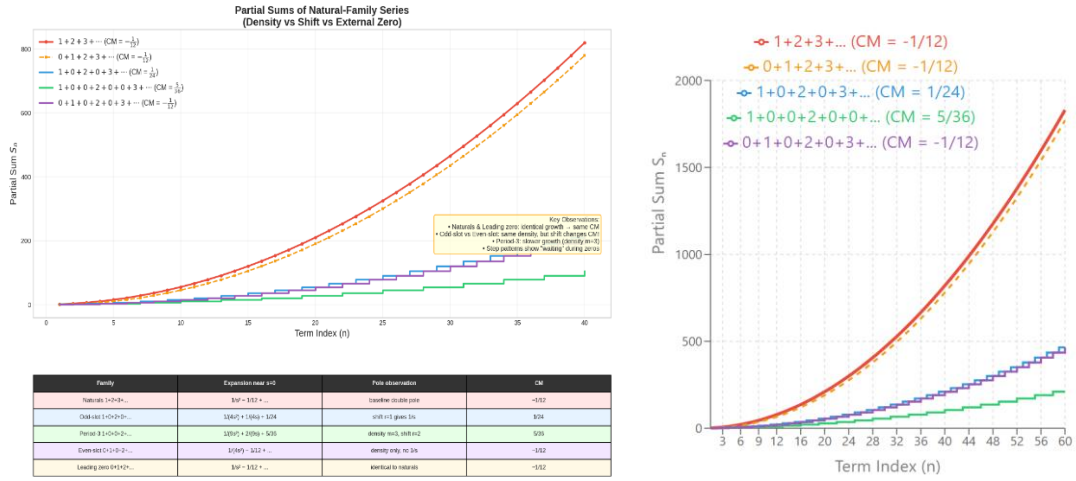

Family	Expansion near s=0	Pole observation	CM
Naturals 1+2+3+...	$1/s^2 - 1/12 + \ldots$	baseline double pole	-1/12
Odd-slot 1+0+2+0+...	$1/(4s^2) + 1/(4s) - 1/24$	shift n=1 gives 1/4	1/24
Period-3 1+0+0+2+...	$1/(9s^2) + 2/(9s) - 5/36$	density n=3, shift n=2	5/36
Even-slot 0+1+0+2+...	$1/(4s^2) - 1/12 + \ldots$	density only, no 1/s	-1/12
Leading zero 0+1+2+...	$1/s^2 - 1/12 + \ldots$	identical to naturals	-1/12

Figure I.B11.10.1 illustrates the behavior of finite partial sums for several divergent traversals listed in Table B. Although all curves exhibit quadratic divergence and appear asymptotically similar, their associated Convergence Momentum values differ. This demonstrates that CM is not determined by growth rate or partial sums, but by boundary alignment and singular structure at the DLR gate. Sequences with identical density but different traversal phases exhibit distinct constant terms, confirming that CM captures boundary information invisible to finite truncation.

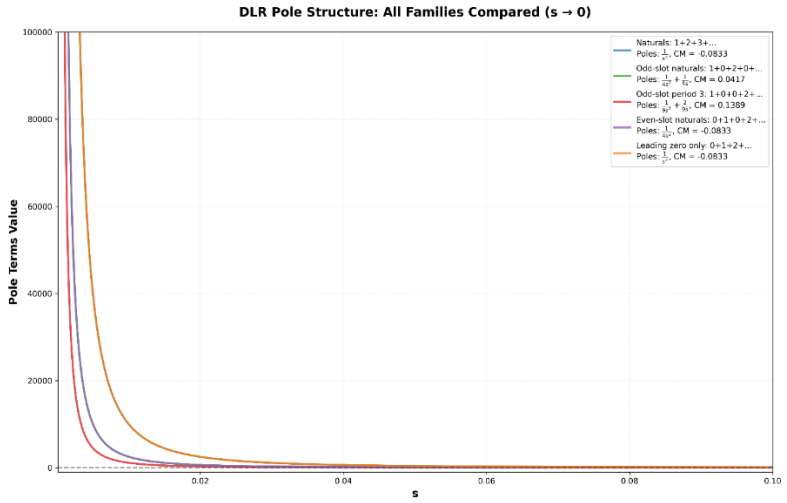

Figure I.B11.10.2 compares the DLR pole structures of several closely related series families under the exponential regulator

$$G(s) = \sum_{n\geq 1} a_n\, e^{-ns}, s \to 0^+.$$

Although the underlying sequences differ by parity selection, zero insertion, or periodic slotting, their regulated generating functions exhibit a common qualitative behavior: dominant algebraic divergence as $s \to 0^+$, followed by a finite constant remainder after systematic pole and logarithmic subtraction.

For the natural numbers $1 + 2 + 3 + \cdots$, divergence is governed by a second-order pole

$\frac{1}{s^2}$, and the extracted constant term (Convergence Momentum) equals

$$\mathrm{CM} = -\frac{1}{12}.$$

Remarkably, sequences obtained by **leading zero insertion** or **even-slot masking** retain the same CM despite altered pole magnitudes, indicating that CM is insensitive to term placement and depends only on the asymptotic density and growth class of the sequence.

In contrast, **odd-slot constructions** introduce modified pole hierarchies (including reduced or shifted poles) and yield different CM values, demonstrating that CM captures structural asymmetry rather than mere divergence strength.

This comparison confirms that DLR separates divergent behavior into three independent layers:
(i) algebraic pole order,
(ii) logarithmic residue, and
(iii) a unique finite constant (CM), which acts as an invariant signature of the series family.

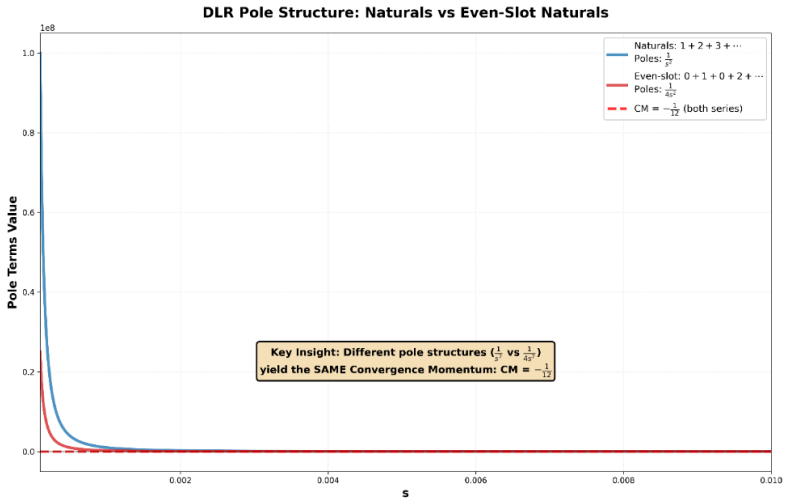

Figure I.B11.10.3 Comparison of the DLR-regulated pole structures of the natural numbers $1 + 2 + 3 + \cdots$and the even-slot-modulated sequence $0 + 1 + 0 + 2 + 0 + 3 + \cdots$under the exponential regulator $G(s) = \sum_{n\geq 1} a_n\, e^{-ns}$.

As $s \to 0^+$, the natural numbers exhibit a second-order pole $1/s^2$, while the even-slot sequence exhibits a reduced pole $1/(4s^2)$, reflecting its lower effective density. Despite this difference in pole magnitude, application of the DLR pole–log extraction procedure yields the same finite constant term for both sequences,

$$\mathrm{CM} = -\frac{1}{12}.$$

The dashed horizontal line indicates the Convergence Momentum, which is not a visual limit of the curves but the invariant constant remaining after complete removal of all algebraic and logarithmic divergences.

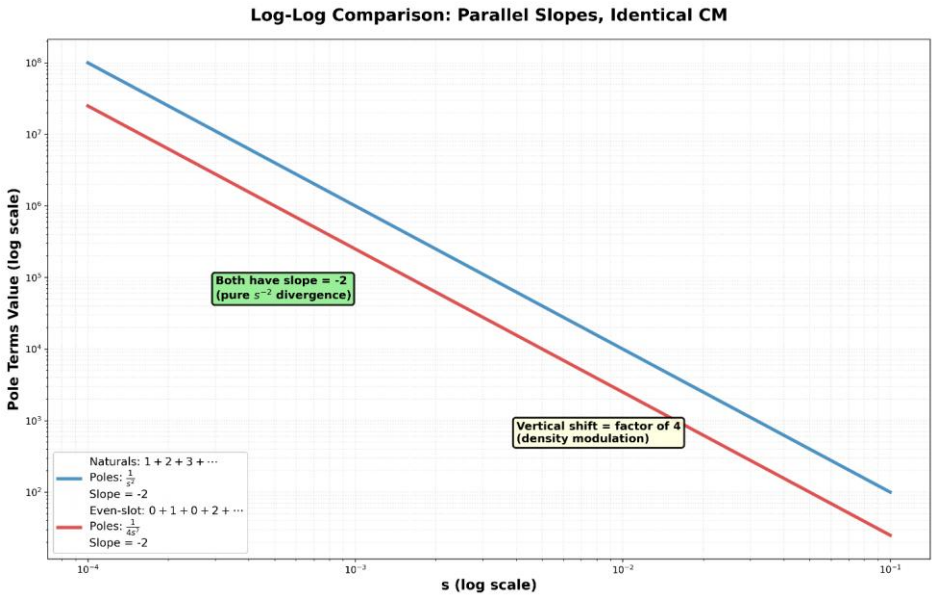

Figure I.B11.10.4 Log–log comparison of the dominant DLR pole contributions for the natural numbers
$1 + 2 + 3 + \cdots$and the even-slot-modulated sequence
$0 + 1 + 0 + 2 + 0 + 3 + \cdots$under the exponential regulator
$G(s) = \sum_{n\geq 1} a_n\, e^{-ns}$.

Both curves exhibit straight-line behavior with identical slope -2, confirming that the leading divergence in both cases is a second-order algebraic pole of the form s^{-2}. The curves differ only by a constant vertical shift corresponding to a multiplicative factor $1/4$in the pole coefficient, reflecting a density modulation rather than a change in order of divergence.

I.C— DLR–Zeta and Eta Link (Power Sums from Derivatives)

This subsection establishes, **from first principles**, how classical zeta and eta values arise *inevitably* from the Discrete Laplace Regulator (DLR). No analytic continuation is assumed or invoked. All values emerge as forced constant coefficients in gate expansions.

I.C.1 Mother Kernel (Exponential / "Bose" Kernel)

Define the base DLR kernel

$$B(s) := \sum_{n=1}^{\infty} e^{-ns} = \frac{1}{e^s - 1}, \qquad s \to 0^+.$$

Its Laurent expansion at the gate is

$$B(s) = \frac{1}{s} - \frac{1}{2} + \frac{s}{12} - \frac{s^3}{720} + \frac{s^5}{30240} - \cdots$$

This kernel is the **generator** of all polynomial power sums under the DLR framework.

I.C.2 Power Sums from Derivatives (Exact Operator Identity)

For each integer $k \geq 0$, define

$$F_k(s) := \sum_{n=1}^{\infty} n^k \, e^{-ns}.$$

Then the identity

$$\boxed{F_k(s) = \left(-\frac{d}{ds}\right)^k B(s)}$$

holds **exactly**, term by term.

Justification. Since

$$\frac{d}{ds} e^{-ns} = -ne^{-ns},$$

repeated differentiation yields

$$\left(-\frac{d}{ds}\right)^k e^{-ns} = n^k e^{-ns}.$$

Summation commutes with differentiation for all $s > 0$.

I.C.3 DLR Invariant Definition and Emergence of Zeta Values

Expand $F_k(s)$ near $s = 0^+$:

$$F_k(s) = \sum_{j \geq 1} c_{-j} \, s^{-j} + c_0 + c_1 s + \cdots$$

Definition (DLR Convergence Momentum).

$$\boxed{\mathrm{CM}_k := [F_k(s) - \text{Pole Part}]_{s^0} = c_0}$$

This constant term is *forced* by the mother expansion and satisfies

$$\boxed{\mathrm{CM}_k = \zeta(-k)}$$

—not by assumption, but by structural necessity.

I.C.4 Explicit Examples

- $k = 0$ (constant series)

$$F_0(s) = B(s) = \frac{1}{s} - \frac{1}{2} + \cdots \quad \Rightarrow \quad \zeta(0) = -\frac{1}{2}.$$

- $k = 1$ (natural numbers)

$$F_1(s) = -\frac{d}{ds}B(s) = \frac{1}{s^2} - \frac{1}{12} + \cdots \quad \Rightarrow \quad \zeta(-1) = -\frac{1}{12}.$$

- $k = 2$ (squares)

$$F_2(s) = \frac{2}{s^3} - \frac{s}{120} + \cdots \quad \Rightarrow \quad \zeta(-2) = 0.$$

- $k = 3$ (cubes)

$$F_3(s) = \frac{6}{s^4} + \frac{1}{120} + \cdots \quad \Rightarrow \quad \zeta(-3) = \frac{1}{120}.$$

Corollary — The DLR Derivative Ladder and Riemann Zeta Values at Negative Integers

The ascent operation introduced in Section I.A1 provides a direct and deterministic mechanism for generating the sequence of Riemann zeta values at negative integers within the Discrete Laplace Regulator (DLR) framework. This corollary formalizes the result, showing that successive differentiation of DLR-regulated power kernels generates the entire family

$$\zeta(0),\ \zeta(-1),\ \zeta(-2),\ \zeta(-3),\ \ldots$$

without recourse to analytic continuation, functional equations, or complex analysis.

Formal Statement

Let

$$\mathcal{L}\{n^k\}(s) \ \equiv \ \sum_{n=1}^{\infty} n^k\, e^{-ns}$$

denote the Discrete Laplace Regulator (DLR) kernel associated with the power sequence n^k.

Then differentiation with respect to the regulator variable $s$induces the exact **kernel-level ladder relation**

$$\boxed{\frac{d}{ds}\,\mathcal{L}\{n^k\}(s) \ = \ -\ \mathcal{L}\{n^{k+1}\}(s), k \geq 0}$$

valid term-by-term for all $s > 0$.

Suppose that as $s \to 0^+$, the kernel admits a Laurent expansion of the form

$$\mathcal{L}\{n^k\}(s) = \frac{A_k}{s^{k+1}} + \cdots + C_k + O(s).$$

Then the **finite DLR-regulated value** of the next power sequence is obtained by:

1. Differentiating the kernel to generate $\mathcal{L}\{n^{k+1}\}(s)$,
2. Performing a complete Laurent–logarithmic expansion at the gate,
3. Removing all algebraic pole and logarithmic terms,
4. Extracting the remaining constant term.

Thus,

$$\boxed{\zeta\,(-(k+1)) \;=\; \mathrm{CM}(n^{k+1})}$$

where CMdenotes the Convergence Momentum defined by the DLR procedure.

Important:
Differentiation acts only as a generator of singular structure at the kernel level.
*The Convergence Momentum is extracted **after** full pole resolution and does not commute with differentiation*.

Explicit Kernel Generation Sequence
Starting from the constant sequence $n^0 = 1$:

$\boldsymbol{k = 0}$

$$\mathcal{L}\{1\}(s) = \frac{1}{s} - \frac{1}{2} + O(s) \Longrightarrow \zeta(0) = -\frac{1}{2}.$$

$\boldsymbol{k = 1}$

$$\mathcal{L}\{n\}(s) = \frac{1}{s^2} - \frac{1}{12} + O(s^2) \Longrightarrow \zeta(-1) = -\frac{1}{12}.$$

$\boldsymbol{k = 2}$

$$\mathcal{L}\{n^2\}(s) = \frac{2}{s^3} + O(s) \Longrightarrow \zeta(-2) = 0.$$

$\boldsymbol{k = 3}$

$$\mathcal{L}\{n^3\}(s) = \frac{6}{s^4} + \frac{1}{120} + O(s^2) \Longrightarrow \zeta(-3) = \frac{1}{120}.$$

This process continues indefinitely.
Each differentiation **raises the pole order by one**, generating the next power kernel, while the finite invariant emerges only after systematic pole removal.

Interpretation and Significance

This corollary establishes that:

- **No analytic continuation is required.**
  Negative-integer zeta values arise directly as finite invariants in the Laurent structure of DLR-regulated kernels.
- **Differentiation acts as a structural ascent operator.**
  The operator $\frac{d}{ds}$maps $n^k \mapsto n^{k+1}$, increasing divergence order without assigning finite values.
- **Deterministic generation.**
  The entire sequence $\{\zeta(-k)\}_{k\geq 0}$is generated mechanically via kernel differentiation followed by DLR resolution.
- **Boundary invariants.**
  Each zeta value appears as a boundary residue: a finite quantity surviving the explicit extraction of divergence encoded in the pole structure.

Conceptual Summary

The negative-integer values of the Riemann zeta function are **not arbitrary assignments** nor products of analytic continuation. They are **forced boundary invariants** arising from the DLR derivative ladder: finite residues extracted from successively higher-order divergent power kernels.

Connection to Convergence Momentum

In DLR language, the ladder relation is expressed as:

$$\boxed{\mathrm{CM}(n^{k+1}) = \mathrm{CM}\left(-\frac{d}{ds}\mathcal{L}\{n^k\}\right),}$$

emphasizing that differentiation redistributes pole structure at the kernel level while **preserving the regulated geometric residue**.

Key Result

$$\boxed{\{\zeta(-k)\}_{k\in\mathbb{N}} \text{ is generated by the DLR derivative ladder,}}$$

with each value arising uniquely as the Convergence Momentum of the corresponding power sequence.

I.C.5 Dirichlet Eta (η(s)) Values

Define

$$\eta(s) := \sum_{n=1}^{\infty} (-1)^{n-1}\, n^{-s}.$$

Splitting ζ into odd and even components yields

$$\boxed{\eta(s) = (1 - 2^{1-s})\zeta(s)}.$$

I.C.6 Alternating DLR Kernel and Power Sums

Define the alternating base kernel

$$B_\eta(s) := \sum_{n=1}^{\infty} (-1)^{n-1}\, e^{-ns} = \frac{1}{e^s + 1}.$$

Expansion:

$$B_\eta(s) = \frac{1}{2} - \frac{s}{4} + \frac{s^3}{48} - \frac{s^5}{480} + \cdots$$

Define alternating power kernels

$$F_k^{(\eta)}(s) := \sum_{n=1}^{\infty} (-1)^{n-1}\, n^k e^{-ns} = \left(-\frac{d}{ds}\right)^k B_\eta(s).$$

Examples:

- $k = 0$: $1 - 1 + 1 - \cdots = \frac{1}{2}$
- $k = 1$: $1 - 2 + 3 - 4 + \cdots = \frac{1}{4}$

I.C.7 Structural Remark on Bessel Functions

Bessel functions K_ν arise **only** when a discrete sum is decomposed into:

- a bulk integral (divergent pole), and
- dual-lattice correction modes,

via Poisson summation. The canonical integral

$$\int_0^{\infty} t^{\nu-1}\, e^{-\alpha t - \beta/t} dt \propto K_\nu\left(2\sqrt{\alpha\beta}\right)$$

is forced.

Thus:n**Bessel terms encode dual-lattice boundary corrections — not new regularization rules.**

Part I.D — Pole-Ladder Calculus and Finite Resolution

This section formalizes the algebraic calculus governing the **generation, transformation, and elimination of singularities** in Discrete Laplace Regulator (DLR) expansions. All results follow directly from the local expansion structure introduced in Part I and do not introduce new summation or valuation principles.

The purpose of this section is to make precise how divergence is *created*, *propagated*, and *resolved* within the DLR framework.

I.D.1 Canonical Form of a DLR Expansion

Let $\mathcal{L}(s)$ be a DLR-gated generating function associated with a discrete sequence of at most exponential growth. Assume that as $s \to 0^+$, it admits a Laurent–logarithmic expansion of the form

$$\mathcal{L}(s) = \sum_{k=1}^{K} \frac{c_k}{s^k} + d\ln s + C + O(s).$$

Definition (pole order).
The **pole order** of $\mathcal{L}$ is defined as

$$\operatorname{ord}(\mathcal{L}) := \max\{k \in \mathbb{N} : c_k \neq 0\}.$$

If no algebraic pole is present, we set $\operatorname{ord}(\mathcal{L}) = 0$.

The constant term C is defined only after complete removal of all pole and logarithmic terms and is identified with the Convergence Momentum (CM).

I.D.2 Ascent Operator

Definition (ascent).
Define the ascent operator

$$\mathcal{A} := \frac{d}{ds}.$$

Action on singular terms.
If

$$\mathcal{L}(s) \sim \frac{c_k}{s^k} \quad \text{as } s \to 0^+,$$

then

$$\mathcal{A}\mathcal{L}(s) = \frac{d}{ds}\left(\frac{c_k}{s^k}\right) = -k\,\frac{c_k}{s^{k+1}}.$$

Therefore,

$$\operatorname{ord}(\mathcal{A}\mathcal{L}) = \operatorname{ord}(\mathcal{L}) + 1.$$

Properties of ascent.

1. Raises algebraic pole order by exactly one.
2. Never remove singularities.
3. Maps regular terms to regular terms.
4. Corresponds, at the kernel level, to polynomial weighting of the underlying discrete sequence:

$$\mathcal{A}(\sum a_n e^{-ns}) = -\sum (n a_n) e^{-ns}.$$

Ascent is therefore a **divergence-generating operation**.

I.D.3 Descent Operator

Definition (descent).
Define the descent operator

$$\mathcal{L} := (1 - e^{-s})\,(\cdot).$$

Using the local expansion

$$1 - e^{-s} = s - \frac{s^2}{2} + O(s^3),$$

we examine its effect on singular terms.

Action on poles.
For $k \geq 1$,

$$\mathcal{L}\left(\frac{1}{s^k}\right) = \left(s - \frac{s^2}{2} + O(s^3)\right)\frac{1}{s^k} = \frac{1}{s^{k-1}} + O\left(\frac{1}{s^{k-2}}\right).$$

Hence,

$$\mathrm{ord}(\mathcal{L}\mathcal{L}) = \mathrm{ord}(\mathcal{L}) - 1.$$

Properties of descent.

1. Lowers algebraic pole order by exactly one.
2. Eliminates simple poles ($\frac{1}{s}$).
3. Maps logarithmic singularities to regular terms.
4. Corresponds, at the kernel level, to finite differencing:

$$\mathcal{L}(\sum a_n e^{-ns}) = \sum (a_n - a_{n-1}) e^{-ns}, \quad a_0 := 0.$$

Descent is therefore a **divergence-resolving operation**.

I.D.4 Pole-Ladder Structure

Repeated application of ascent and descent generates a discrete hierarchy of singular structures:

$$\cdots \xrightarrow{\mathcal{L}} \frac{1}{s^3} \xrightarrow{\mathcal{L}} \frac{1}{s^2} \xrightarrow{\mathcal{L}} \frac{1}{s} \xrightarrow{\mathcal{L}} \text{regular}.$$

This hierarchy is called the **pole ladder**.

- Each rung corresponds to a definite algebraic divergence class.
- Ascent moves *up* the ladder.
- Descent moves *down* the ladder.

The Convergence Momentum (CM) is defined **only at the base of the ladder**, once all singular rungs have been removed.

I.D.5 Balance Condition and Finite Resolution

Definition (finite resolution).
A DLR expansion $\mathcal{L}(s)$ is said to admit **finite resolution** if there exists $m \in \mathbb{N}$ such that

$$\mathcal{L}^m \mathcal{L}(s) = C + O(s),$$

where $\mathcal{L}^m$ denotes m-fold application of the descent operator.

Balance condition.
Finite resolution occurs if and only if the net effect of ascent-generated divergence and descent-induced cancellation removes all singular terms.

If the balance condition holds, the constant C is uniquely defined and equals the Convergence Momentum:

$$\mathrm{CM} = C.$$

Unbalanced ascent produces non-terminating divergence and no finite invariant.

I.D.6 Parity Effect for Power Kernels

Consider the power kernels

$$\mathcal{L}_k(s) := \sum_{n=1}^{\infty} n^k \, e^{-ns}, \quad k \in \mathbb{N}.$$

These kernels are generated by repeated ascents from the constant kernel.

Applying descent repeatedly, one finds:

- For **even** k, the constant term vanishes after full resolution.
- For **odd** k, a nonzero constant term survives.

This **parity effect** follows from:

1. the symmetry of the pole ladder under ascent/descent,
2. the structure of finite differences of even vs. odd powers,
3. the absence or presence of an unpaired rung at the ladder base.

Parity is therefore a **structural property**, not a regularization artifact.

I.D.7 Logarithmic Boundary Class

Logarithmic terms are not elements of the algebraic pole ladder.

If

$$\mathcal{L}(s) = d\ln s + C + O(s),$$

then:

- Ascent preserves the logarithmic class:

$$\mathcal{A}(\ln s) = \frac{1}{s}.$$

- Descent removes the logarithmic singularity:

$$(1 - e^{-s})\ln s = s\ln s + O(s).$$

Under the DLR normalization adopted in this work:

- The leading logarithmic term is subtracted in full,
- The Convergence Momentum is defined as the remaining constant term C.

Logarithmic divergence thus represents **boundary memory**, not ladder position.

Part I.E — Algorithmic Extraction of the Convergence Momentum

This section presents the Discrete Laplace Regulator (DLR) as a **deterministic algorithm** acting on discrete sequences via their gated generating functions. No new definitions or valuation principles are introduced. The procedure is a direct operational consequence of the expansion-based framework developed in Part I.

I.E.1 Input Class

Let $\{a_n\}_{n\geq 0}$be a discrete sequence of at most exponential growth.
Assume that the associated DLR kernel admits a Laurent–logarithmic expansion at the gate $s \to 0^+$.

The objective is to extract, when possible, a finite invariant

$$\mathrm{CM}(a) \in \mathbb{R},$$

called the **Convergence Momentum**.

I.E.2 Construction of the DLR Kernel

Associated to the sequence $\{a_n\}$the DLR kernel

$$\mathcal{L}_a(s) := \sum_{n=0}^{\infty} a_n\, e^{-ns}, s > 0.$$

The parameter $s$serves exclusively as a **regulator variable**.
At no stage is the value $s = 0$substituted or evaluated.

I.E.3 Gate Expansion

Compute the local expansion of $\mathcal{L}_a(s)$as $s \to 0^+$:

$$\mathcal{L}_a(s) = \sum_{k=1}^{K} \frac{c_k}{s^k} + d\ln\, s + C + O(s).$$

This expansion decomposes the kernel uniquely into:

- algebraic singular terms (negative powers of s),
- a possible logarithmic singular term,
- a finite constant term,
- regular higher-order corrections.

The existence and uniqueness of this decomposition follow from standard properties of Laurent–logarithmic expansions.

I.E.4 Singular Term Removal

Define the **singular projection operator**

$$\mathcal{S}(\mathcal{L}_a) := \sum_{k=1}^{K} \frac{c_k}{s^k} + d\ln\ s.$$

The **regular remainder** is then

$$\mathcal{R}(\mathcal{L}_a)(s) := \mathcal{L}_a(s) - \mathcal{S}(\mathcal{L}_a)(s).$$

No cancellation between singular and regular terms is permitted.
All singular contributions are removed **in full** and **explicitly**.

I.E.5 Identification of the Convergence Momentum

If

$$\mathcal{R}(\mathcal{L}_a)(s) = C + O(s),$$

then the **Convergence Momentum** is defined as

$$\boxed{\mathrm{CM}(a) := C.}$$

If the expansion admits no finite constant remainder after singular removal, then **CM does not exist** for the given sequence.

Thus, CM is not a limit, but a **coefficient extracted from a local expansion**.

I.E.6 Algorithmic Formulation

The DLR procedure defines a partial map

$$\mathrm{CM}: \{\text{admissible sequences}\} \ \rightarrow \ \mathbb{R}$$

given by the following deterministic steps:

1. Construct the DLR kernel $\mathcal{L}_a(s)$
2. Expand locally at the gate $s \rightarrow 0^+$
3. Identify all algebraic and logarithmic singular terms
4. Subtract the complete singular part
5. Extract the remaining constant coefficient
6. Declare it as $\mathrm{CM}(a)$, if finite

No limits, no analytic continuation, and no summation of partial sums are involved at any stage.

I.E.7 Failure and Scope

The DLR algorithm does **not** assign value to every divergent series.

Failure occurs when:

- the gate expansion does not exist,
- or the expansion admits no finite constant remainder after singular removal.

In such cases, the algorithm correctly reports the **absence of a finite invariant**, rather than forcing a value.

Interpretive Remark

The Convergence Momentum is therefore a **local invariant of gate expansion**, obtained by a finite algebraic procedure. It records what remains after divergence has been made explicit and fully separated.

The DLR procedure applies to any discrete sequence whose gated kernel is well-defined for $s > 0$and admits a Laurent–logarithmic expansion at the boundary $s \to 0^+$. A complete characterization of maximal admissibility classes is not required for the present work and is deferred to future investigation.

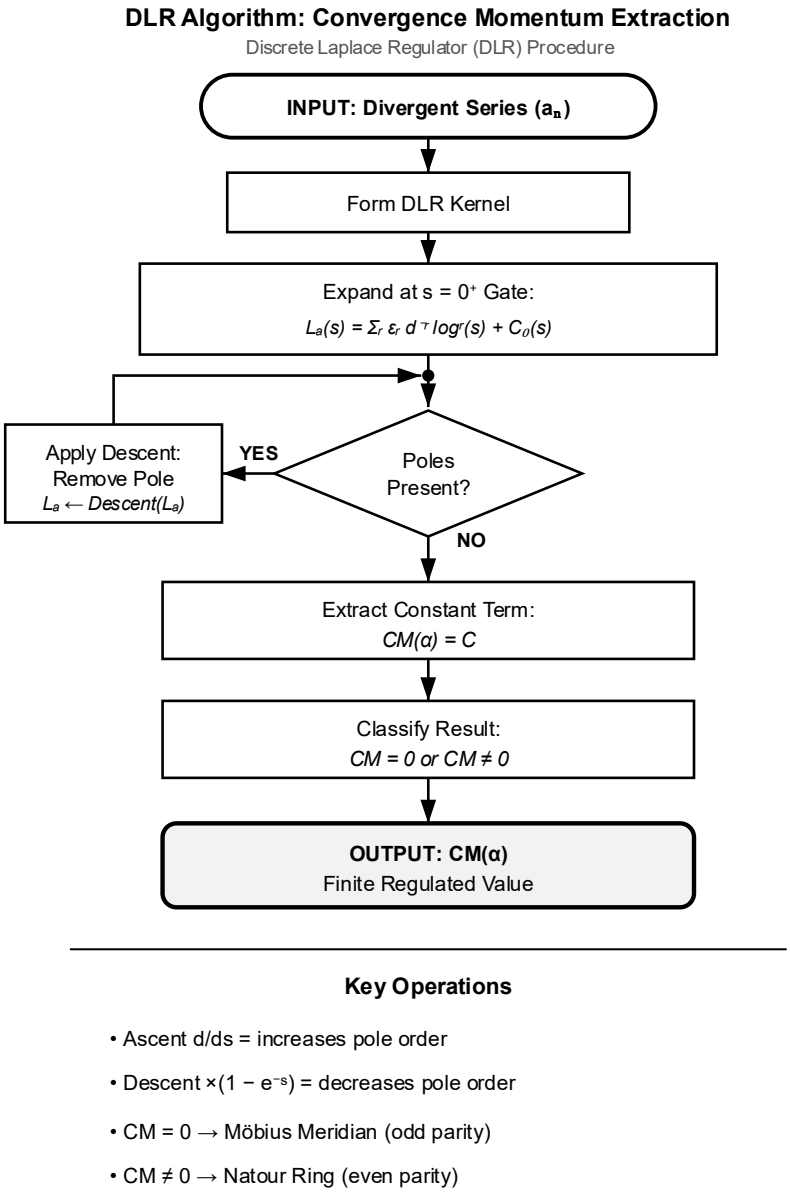

Figure I.E. *DLR Algorithm — Convergence Momentum Extraction.* The flowchart presents the complete procedure for extracting CM from a divergent series $\{a_n\}$. The DLR kernel $L_a(s)$ is formed and expanded at the gate $s = 0^+$, yielding a Laurent–logarithmic expansion. If poles are present, the descent operator $\times(1 - e^{-s})$ is applied iteratively, each application reducing pole order by one; the filled junction dot marks the re-entry point of this loop. Termination is guaranteed by compactness of the Elias Sphere: pole order is finite and strictly decreasing. Once the expansion is pole-free, the constant term C defines CM(α). Classification is binary: CM = 0 identifies a Möbius Meridian (odd parity, topological cancellation), while CM ≠ 0 identifies a Natour Ring (even parity, accumulated directional residue). This parity distinction is geometric, not algebraic.

I.F APPLICATIONS

I.F.1 The Casimir Effect Revisited via the Discrete Laplace Regulator

1.F.1.1 Spectral Origin of the Casimir Energy

Consider a one-dimensional perfectly conducting cavity of length L. The allowed normal modes of a massless field are discrete:

$$\omega_n = \frac{\pi c}{L} n, \qquad n = 1,2,3, \ldots$$

Formally, the vacuum energy is written as

$$E_0(L) = \frac{1}{2} \sum_{n=1}^{\infty} \hbar\, \omega_n = \frac{\hbar c \pi}{2L} \sum_{n=1}^{\infty} n.$$

This expression is **not** a sum in the classical sense. It is a **spectral traversal** whose divergence reflects infinite mode density. The physical question is not whether the sum converges, but whether a **boundary-sensitive invariant** can be extracted from it.

I. F.1.2 DLR Regulation of the Spectral Sum

Introduce the Discrete Laplace Regulator by gating the spectral traversal:

$$E(s; L) := \frac{\hbar c \pi}{2L} \sum_{n=1}^{\infty} n\ e^{-ns}, \qquad s > 0.$$

The regulator parameter s plays no physical role; it is a boundary probe only.
Using the canonical DLR kernel listed in **Table D (Naturals family)**,

$$\sum_{n=1}^{\infty} n\, e^{-ns} = \frac{1}{s^2} - \frac{1}{12} + O(s),$$

we obtain

$$E(s; L) = \frac{\hbar c \pi}{2L} \left(\frac{1}{s^2} - \frac{1}{12} + O(s) \right).$$

I. F.1.3 Pole Removal and Convergence Momentum

The leading term $1/s^2$ is a **pure bulk divergence**, independent of L. It represents the infinite density of modes and carries no boundary information.

According to the DLR rules:

- all algebraic pole terms are removed explicitly,
- no cancellation with finite terms is allowed.

Referring again to **Table D**, the Convergence Momentum of the natural traversal is

$$\mathrm{CM}\left(\sum_{n=1}^{\infty} n\right) = -\frac{1}{12}.$$

Within the DLR framework, physical relevance coincides with boundary sensitivity: algebraic pole terms encode bulk traversal independent of geometric parameters and therefore cannot contribute to forces. Only the boundary-sensitive constant term survives as a measurable invariant.

Thus the DLR-regulated vacuum energy is

$$E^{\mathrm{DLR}}(L) = \frac{\hbar c \pi}{2L}\,\mathrm{CM} = -\frac{\hbar c \pi}{24L}.$$

This value is obtained:

- without analytic continuation,
- without limits $s \to 0$,
- without zeta-function assumptions,

but **solely** by gate expansion and pole removal.

I. F.1.4 Casimir Force as a Structural Derivative

The observable quantity is the force,

$$F(L) = -\frac{dE^{\mathrm{DLR}}(L)}{dL}.$$

Since $E^{\mathrm{DLR}}(L)$ is already finite and depends explicitly on the geometric scale L,

$$F(L) = -\frac{d}{dL}\left(-\frac{\hbar c \pi}{24L}\right) = -\frac{\hbar c \pi}{24L^2}.$$

This reproduces the standard one-dimensional Casimir force.

Casimir Effect — Complete DLR Derivation

The vacuum energy between conducting plates separated by distance L is

$$E_0(L) = \frac{\hbar c \pi}{2L} \sum n.$$

Applying the DLR regulator:

$$\sum n e^{-ns} = \frac{1}{s^2} - \frac{1}{12} + O(s),$$

yields the regulated energy

$$E^{\mathrm{DLR}}(L) = -\frac{\hbar c \pi}{24L}.$$

The resulting force is

$$F(L) = -\frac{dE}{dL} = -\frac{\hbar c \pi}{24L^2}.$$

I. F.1.5 Structural Interpretation

Within the DLR framework, the Casimir effect admits a precise structural explanation:

- Divergence is fully encoded in **pole terms** of the gate expansion.
- Boundary information survives only in the **constant term** (CM).
- The Casimir energy is therefore a **boundary invariant**, not a summation artifact.
- Differentiation with respect to L converts boundary memory into measurable stress.

Divergence grows without bound. **But boundaries remember.**

I.F.2 Why Ramanujan Was "Lucky": Zero Insertion, Alignment, and Structural Coincidence

Ramanujan's algebraic treatment of divergent series is often viewed as miraculous.
From the standpoint of DLR, the situation is sharper: his manipulations succeeded **only because** they implicitly preserved a specific traversal alignment.

The decisive mechanism is **zero insertion**.

I.F.2.1 Zero Insertion Is Not Neutral

Consider the two canonical zero-inserted traversals of the natural numbers (see **Table D**):

Z_{post}: 1,0,2,0,3,0,4,0, ... Z_{pre}: 0,1,0,2,0,3,0,4, ...

Both sequences diverge.
Both share the same local growth rate.
Yet DLR distinguishes them.

Zero insertion changes **where traversal begins** relative to the gate, and that positional shift alters the constant term.

I.F.2.2 The Ramanujan Coincidence

From **Table D**:

$$\mathrm{CM}(0 + 1 + 0 + 2 + 0 + 3 + \cdots) = -\frac{1}{12}.$$

This equals the invariant of

$$1 + 2 + 3 + 4 + \cdots,$$

not because the sequences are identical, but because their difference lies **entirely in removable pole terms**. Their gate expansions share the same constant term.

This is a **structural coincidence**, not a general law.

I.F.2.3 Why the Other Zero Insertion Fails

For the post-zero traversal:

$$1 + 0 + 2 + 0 + 3 + 0 + \cdots,$$

Table D gives

$$G(s) = \frac{1}{4s^2} + \frac{1}{4s} + \frac{1}{24} + O(s), \qquad \mathrm{CM} = \frac{1}{24}.$$

The invariant differs because the traversal is **shifted** relative to the gate. The change is not numerical—it is positional.

I.F.2.4 What Ramanujan Implicitly Assumed

Ramanujan's algebra implicitly assumed that:

4. Zero insertion is neutral,
5. Index shifts are harmless,
6. Traversal phase is irrelevant.

DLR shows these assumptions are **false in general**, but **true for the special alignments he used**. He was "lucky" precisely because his manipulations remained within a single DLR equivalence class.

Luck did not replace rigor.
It concealed missing structure.
DLR makes that structure explicit.

I.F.3 The Even–Odd Problem Revisited (Finite vs Infinite Traversal)

I.F.3.1 Finite Identity and Its Valid Domain

For any finite cutoff N, define

$$S_N = 1 + 2 + \cdots + N, \quad E_N = 2 + 4 + \cdots, \quad O_N = 1 + 3 + \cdots,$$

with all sums truncated at N.

Then the identity

$$S_N - E_N = O_N$$

is exact and meaningful **for all finite** N.

I.F.3.2 Why the Identity Breaks at Infinity

At infinity, the objects

$$S = 1 + 2 + 3 + \cdots, \quad E = 2 + 4 + 6 + \cdots, \quad O = 1 + 3 + 5 + \cdots$$

are **not finite sums** and not set-theoretic partitions. They are **infinite traversals**.

Crucially, at the traversal level:

$$E = 2S$$

term-by-term. The even series is not obtained by removing elements; it is a **scaled traversal** of the same sequence.

Thus the formal manipulation $S - E = O$ has no intrinsic meaning in the infinite setting unless a common regulation and traversal structure is imposed.

I.F.3.3 DLR Evaluation (Table D)

From canonical DLR values:

$$\mathrm{CM}(S) = -\frac{1}{12}, \qquad \mathrm{CM}(E) = 2\mathrm{CM}(S) = -\frac{1}{6}, \qquad \mathrm{CM}(1 + 1 + 1 + \cdots) = -\frac{1}{2}.$$

Using the identity

$$2n - 1 = 2n - 1,$$

and linearity,

$$\mathrm{CM}(1+3+5+\cdots) = 2\mathrm{CM}(S) - \mathrm{CM}(1+1+1+\cdots) = \frac{1}{3}.$$

This is the **unique DLR-consistent value** for the odd traversal under canonical alignment.

I.F.3.4 Why $\mathbf{1/12}$ *Appears in the Literature*

The value $1/12$ arises from **illegitimately extending** a finite identity to infinity without respecting traversal structure.

DLR forbids such operations:
constants may be compared **only after compatibility of divergence classes is verified**.

Infinity is traversal, not subtraction. Once this is respected, the even–odd problem is fully and uniquely resolved.

DLR Table – Odd Numbers Family

Family	Expansion near $s = 0$	Pole observation	CM
Odds $1+3+5+\cdots$	$\frac{2}{s^2} - \frac{1}{s} + \frac{1}{3} + O(s)$	baseline odd double pole with drift	$\frac{1}{3}$
Odd-slot odds $1+0+3+0+5+\cdots$	$\frac{1}{2s^2} + \frac{1}{12} + O(s)$	density $m = 2$, drift cancels $1/s$	$\frac{1}{12}$
Odd-slot odds, period 3 $1+0+0+3+0+0+5+\cdots$	$\frac{2}{9s^2} + \frac{1}{9s} + \frac{1}{9} + O(s)$	density $m = 3$, shift $r = 2$	$\frac{1}{9}$
Even-slot odds $0+1+0+3+0+5+\cdots$	$\frac{1}{2s^2} - \frac{1}{2s} + \frac{1}{3} + O(s)$	density only, residual drift	$\frac{1}{3}$
Leading zero odds $0+1+3+5+\cdots$	$\frac{2}{s^2} - \frac{3}{s} + \frac{7}{3} + O(s)$	identical spectrum, shifted origin	$\frac{1}{3}$

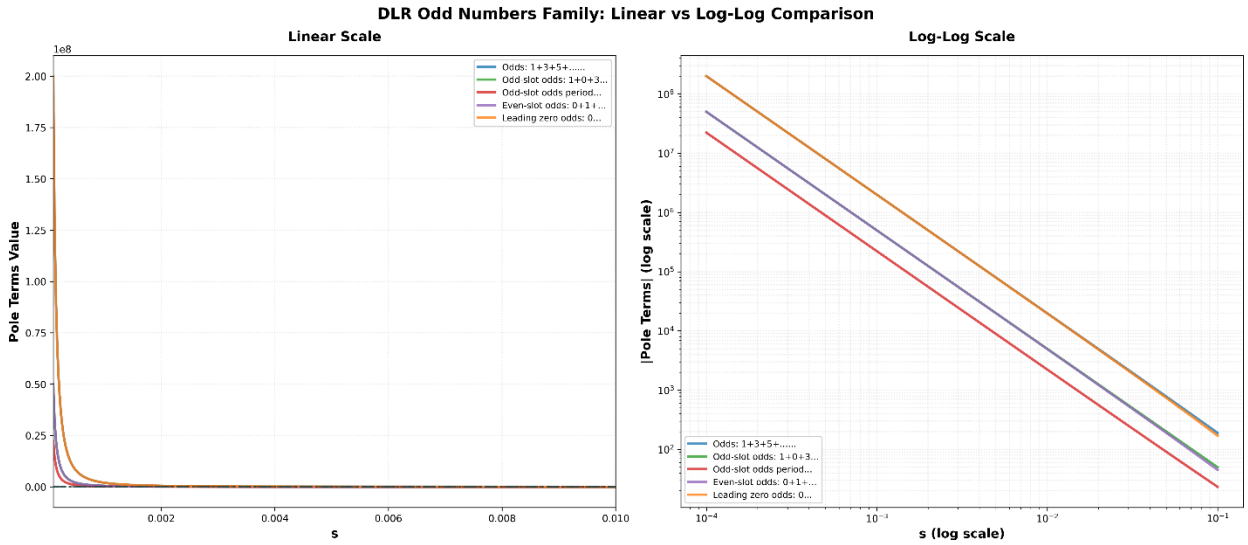

Figure 5. DLR Odd Numbers Family: Linear vs Log–Log Comparison

This figure compares the Discrete Laplace Regulator (DLR) pole behavior of the odd numbers family under linear and log–log scaling as $s \to 0^+$. The left panel (linear scale) highlights the rapid divergence dominated by the leading $1/s^2$pole, while the right panel (log–log scale) reveals the common scaling structure and relative hierarchy among different zero-insertion patterns.

I.F.3.5 Closing Remark for Applications

Across Casimir physics, zero insertion, and even–odd decompositions, a single principle emerges: **Finite invariants do not arise from cancellation. They arise from boundary structure.** DLR makes this principle explicit and operational.

Conclusion of Part I — Boundary Resolution and Discrete Invariants

Part I has constructed the **Discrete Laplace Regulator (DLR)** as a complete, intrinsic framework for resolving divergent discrete traversals through **boundary expansion rather than summation**. The essential shift introduced here is structural: divergence is treated not as a numerical failure, but as a **boundary phenomenon** whose internal composition can be made explicit, classified, and resolved.

Within DLR, a discrete series is never evaluated by limits, rearrangements, or analytic continuation. Instead, it is mapped to a gated kernel whose **local expansion at the boundary** separates divergence into algebraic poles and logarithmic terms, leaving a uniquely defined finite remainder—the **Convergence Momentum (CM)**. CM is not a limit, not a summation value, and not an averaged quantity; it is a **structural coefficient**, extracted mechanically after full removal of singular boundary contributions.

The framework establishes several decisive results:

- Divergence is recorded explicitly rather than canceled.
  Algebraic poles encode growth class and density; logarithmic terms encode marginal boundary memory. No cancellation between divergent and finite terms is permitted.
- CM is unique, stable, and traversal-sensitive.
  Finite-head modifications, reindexing, and admissible density operations do not affect CM, while spacing, zero insertion, parity, oscillation, and phase alignment generally do. Equality of CM therefore does **not** imply equivalence of traversal geometry.
- Divergence resolution is governed by operator balance.
  The ascent and descent operators generate a universal **pole-ladder structure**, clarifying how divergence is created and how finite invariants emerge only when ascent-generated growth is exactly balanced by descent-induced cancellation.
- Classical regularized values arise as forced invariants.
  Ramanujan summation, zeta values, eta values, and Casimir energies appear as unavoidable constant terms of DLR expansions—not by assumption, but by boundary necessity. Apparent historical "miracles" are revealed as special cases of traversal alignment.
- Physical relevance coincides with boundary sensitivity.
  In spectral applications, bulk divergence is isolated in removable pole terms, while observable quantities arise exclusively from CM. Divergence grows without bound; only boundaries retain memory.

Part I therefore completes the **analytic and operational foundation** of the Interconnected Infinities Giant Sphere Space (IIGSS). All definitions, operators, invariants, and algorithms required for boundary resolution of discrete infinity have been established without geometric interpretation, physical postulates, or external regularization schemes.

The material that follows—presented in the Index sections—serves two purposes:
(1) to situate DLR relative to classical methods and historical results, and
(2) to document coincident cases and motivating precedents that DLR explains but does not rely upon.

With the boundary calculus now complete, the subsequent parts of IIGSS may safely shift from **how divergence is resolved** to **what that resolution means geometrically and physically**.

The index that follows records historical precedents, coincident classical results, and related analytic frameworks—not as foundations of the present work, but as contextual landmarks that the Discrete Laplace Regulator now explains, refines, or structurally subsumes.

Index — Context, Precedents, Structural Relations and DLR-Regularized Abel Framework for the Riemann Zeta Function

---

Index. A — Pre-DLR Proofs and Motivating Invariants

Scope and intent.
All results in this section were obtained *prior* to the introduction of the Discrete Laplace Regulator. They rely exclusively on classical summation procedures—primarily Cesàro-type averaging and consistent algebraic rearrangements—and are presented to demonstrate that certain divergent traversals admit stable finite invariants under coherent extraction procedures. These methods are **not** proposed as universal summation rules, nor do they provide a boundary-resolution mechanism. Their role is historical and motivational.

Index.A.1 Grandi's Series (Purely Pre-DLR)

Consider the oscillatory series

$$G := 1 - 1 + 1 - 1 + 1 - 1 + \cdots$$

A.1.1 Why naïve algebra is insufficient

A tempting manipulation is

$$G = 1 - 1 + 1 - 1 + \cdots \Rightarrow 1 - G = 1 - (1 - 1 + 1 - 1 + \cdots) = G,$$

which formally yields $2G = 1$ and hence $G = \frac{1}{2}$.
While suggestive, this argument is not a proof: it relies on shifting an infinite divergent series, an operation that is not automatically valid.

To justify the result, a summation procedure producing a stable invariant must be used.

Index.A.2 Cesàro Proof of Grandi's Series

Define the partial sums

$$s_1 = 1, s_2 = 0, s_3 = 1, s_4 = 0, \ldots$$

so that s_n oscillates between 1 and 0.

Define the Cesàro means

$$\sigma_N := \frac{1}{N} \sum_{k=1}^{N} s_k \, .$$

- If $N = 2m$, then $\sum_{k=1}^{2m} s_k = m$, hence $\sigma_{2m} = \frac{1}{2}$.
- If $N = 2m + 1$, then $\sum_{k=1}^{2m+1} s_k = m + 1$, hence $\sigma_{2m+1} \to \frac{1}{2}$.

Therefore, the Cesàro mean exists and equals

$$G = \frac{1}{2}.$$

This is the first example, in IIGSS language, of a **stable invariant extracted from an oscillatory traversal**.

Index.A.3 Alternating Naturals

$$A := 1 - 2 + 3 - 4 + 5 - 6 + \cdots$$

This invariant is derived using only algebraic rearrangements consistent with the same summation meaning established for Grandi's series.

A.3.1 Shift-and-add structure

Using the identity

$$G = 1 - 1 + 1 - 1 + \cdots ,$$

observe that doubling gives

$$2G = 2 - 2 + 2 - 2 + \cdots .$$

Align two copies of Aso that signs match:

$$\begin{aligned} A &= 1 - 2 + 3 - 4 + 5 - 6 + \cdots \\ A &= \quad 1 - 2 + 3 - 4 + 5 - \cdots \end{aligned}$$

Adding term wise produces,

$$2A = 1 - 1 + 1 - 1 + \cdots = G.$$

Under the same invariant meaning as Section A.2,

$$A = \frac{G}{2} = \frac{1}{4}.$$

Index.A.4 Ramanujan's $\mathbf{1+2+3+\cdots}$ Result (Pre-DLR)

Let

$$S := 1 + 2 + 3 + 4 + 5 + \cdots .$$

Using the previously derived invariant $A = \frac{1}{4}$, subtract A from S in aligned form:

$$\begin{aligned} S - A \quad &= (1 + 2 + 3 + 4 + 5 + 6 + \cdots) \\ &\quad -(1 - 2 + 3 - 4 + 5 - 6 + \cdots) \\ &= 0 + 4 + 0 + 8 + 0 + 12 + \cdots . \end{aligned}$$

Factor:

$$S - A = 4(1 + 2 + 3 + \cdots) = 4S.$$

Thus

$$S - A = 4S \;\Rightarrow\; -A = 3S \;\Rightarrow\; S = -\frac{A}{3} = -\frac{1}{12}.$$

This value is obtained **without kernels or regulators**, relying solely on consistent invariant extraction.

Index.A.5 Zero-Insertion Algebra

Define two canonical zero-inserted sequences:

$$\begin{aligned} Z_1 \quad &:= 1,0,2,0,3,0,4,0, \ldots \\ Z_2 \quad &:= 0,1,0,2,0,3,0,4, \ldots \end{aligned}$$

Using previously established invariants:

$$S = -\frac{1}{12}, A = \frac{1}{4},$$

we obtain exact algebraic identities.

A.5.1 Odd-number isolation

$$S + A = 2 + 0 + 6 + 0 + 10 + 0 + \cdots = 2(1 + 0 + 3 + 0 + 5 + \cdots).$$

Numerically,

$$S + A = -\frac{1}{12} + \frac{1}{4} = \frac{1}{6},$$

hence

$$1 + 0 + 3 + 0 + 5 + \cdots = \frac{1}{12}.$$

A.5.2 Pre-zero insertion

$$S - A = 0 + 4 + 0 + 8 + 0 + 12 + \cdots = 4(0 + 1 + 0 + 2 + 0 + 3 + \cdots).$$

Numerically,

$$S - A = -\frac{1}{12} - \frac{1}{4} = -\frac{1}{3},$$

so

$$0 + 1 + 0 + 2 + 0 + 3 + \cdots = -\frac{1}{12}.$$

Index.A.6 Even–Odd Decomposition

From

$$1 + 2 + 3 + \cdots = -\frac{1}{12},$$

it follows that

$$2 + 4 + 6 + \cdots = 2S = -\frac{1}{6},$$

and

$$(2S) - (1 + 1 + 1 + \cdots) = -\frac{1}{6} + \frac{1}{2} = \frac{1}{3},$$

recovering the odd-number invariant.

Closing remark (Index. A).

The results above demonstrate that stable finite invariants can be extracted from divergent traversals using classical methods, but they do not explain *why* these invariants arise, nor how traversal density, phase, and boundary structure are encoded. These limitations motivate the introduction of the Discrete Laplace Regulator in Part I.

Index. B — Relation to the Z-Transform

Scope and intent.
This section clarifies the structural relationship between the Discrete Laplace Regulator (DLR) and the classical Z-transform. The purpose is not to equate the two methods, but to explain precisely **where they touch**, **where they diverge**, and **why DLR cannot be reduced to a Z-transform formalism**.

Index.B.1 Formal Correspondence

Recall the unilateral Z-transform of a discrete sequence $\{a_n\}_{n\geq 1}$:

$$Z_a(z) := \sum_{n=1}^{\infty} a_n \, z^{-n}, \mid z \mid > R.$$

The DLR kernel is

$$G_a(s) := \sum_{n=1}^{\infty} a_n \, e^{-ns}, s > 0.$$

Formally identifying

$$z = e^s \text{or equivalently} z^{-1} = e^{-s},$$

shows that the DLR kernel is a **restricted real-axis projection** of the Z-transform:

$$G_a(s) = Z_a(e^s).$$

This correspondence is purely algebraic and does not involve valuation.

Index.B.2 Global vs Local Structure

The distinction between the two frameworks is **structural**:

- The Z-transform is a **global analytic object** defined over a complex annulus.
- DLR is a **local expansion framework**, concerned exclusively with the behavior of the kernel near the boundary $s \to 0^+$(equivalently $z \to 1^+$).

In Z-transform theory, the point $z = 1$is treated as:

- a convergence boundary,
- or a singular point to be avoided.

In DLR, the corresponding boundary is **the object of study**.

Index.B.3 Absence of Boundary Invariants in the Z-Transform

While the Z-transform can encode growth rates and recurrence relations, it lacks three features essential to DLR:

1. **No canonical pole–log separation at $z \to 1$**
   Z-transform theory does not define a unique decomposition isolating algebraic poles, logarithmic divergence, and a finite invariant.
2. **No invariant constant extraction rule**
   There is no analogue of Convergence Momentum (CM) in Z-transform analysis. Finite values arise only after external prescriptions (limits, summability methods, or analytic continuation).
3. **Boundary traversal is compressed, not resolved**
   Distinct traversals with different densities or zero insertions may map to Z-transforms with indistinguishable local behavior near $z = 1$.

Thus, the Z-transform records **that divergence occurs**, but not **how it is traversed**.

Index.B.4 Coincidence Cases and Their Interpretation

In certain regular cases—such as polynomial growth without oscillation—the finite values obtained via classical Z-transform manipulations may coincide numerically with CM values obtained via DLR.

These coincidences should be interpreted as:

- **projections** of DLR results,
- not as defining properties of the Z-transform.

The agreement arises because both frameworks access the same underlying discrete structure, but only DLR resolves the boundary explicitly.

Index. B.5 Summary

The relationship between the Z-transform and DLR may be summarized as follows:

- Z-transform: global frequency-domain representation.
- DLR: local boundary-expansion regulator.
- Numerical agreement may occur, but **structural equivalence does not**.

DLR is therefore **not** a reformulation or extension of the Z-transform. It is a distinct framework designed to extract boundary invariants that the Z-transform necessarily suppresses.

Throughout this work the Laplace gate $e^{-ns}$is fixed as a canonical boundary probe. The extent to which the Convergence Momentum remains invariant under alternative admissible gating functions with equivalent boundary scaling is an important universality question, left for future work**.**

Index. C — Relation to Discrete Fourier and DFT-Type Series

Scope and intent.
This section clarifies the relationship between the Discrete Laplace Regulator (DLR) and Discrete Fourier–type methods, including Fourier series and finite-length Discrete Fourier Transforms (DFT). The aim is to distinguish **frequency-domain projection** from **boundary-resolution**, and to explain why DFT-based methods cannot encode divergence geometry or invariant extraction at infinity.

Index. C.1 Discrete Fourier Methods as Frequency Projections

Given a finite sequence $\{a_n\}_{n=0}^{N-1}$, the Discrete Fourier Transform is defined by

$$\hat{a}_k = \sum_{n=0}^{N-1} a_n \, e^{-2\pi i k n/N}.$$

Key structural features:

- The domain is **finite**.
- Periodicity is **imposed** by construction.
- Infinite traversal is **replaced** by cyclic closure.

As a result, DFT methods analyze **frequency content**, not asymptotic behavior.

Index. C.2 Periodic Closure and Information Loss

By enforcing periodicity, DFT-based methods necessarily:

- identify the tail of a sequence with its head,
- erase distinctions between growth, decay, and divergence,
- eliminate boundary points entirely.

Thus, any divergence present in the original infinite sequence is transformed into a **bounded oscillatory object**. The divergence is not resolved; it is **removed by truncation**.

Index. C.3 Oscillation Is Not Divergence Resolution

Fourier analysis can detect oscillation but cannot distinguish between:

- genuine oscillatory convergence,
- oscillatory divergence,
- divergent growth masked by phase cancellation.

For example, alternating series may appear well-behaved under Fourier projection even when their partial sums exhibit unbounded traversal behavior.

In contrast, DLR explicitly separates:

- algebraic divergence (poles),
- logarithmic divergence,
- oscillatory cancellation,
  before extracting a finite invariant.

Index. C.4 Oscillatory Cancellation in DLR

Within DLR, oscillatory factors (such as alternating signs or periodic phases) act by **canceling singular terms in the kernel expansion**. This cancellation is:

local, explicit, and structurally identifiable.

The resulting Convergence Momentum (CM) survives precisely because the singular structure has been resolved, not averaged away.

DFT methods, by contrast, suppress singular structure implicitly through orthogonality relations and finite summation.

Index. C.5 Infinite vs Finite Traversal

The essential distinction may be summarized as:

- **DFT:** finite traversal + imposed periodicity → frequency spectrum
- **DLR:** infinite traversal + boundary expansion → invariant extraction

These approaches answer fundamentally different questions and operate on incompatible domains.

Index. C.6 Complementarity

DLR and DFT methods are not competing frameworks.

- DFT is optimal for identifying frequency components in finite or periodic data.
- DLR is designed to analyze infinite discrete traversals and their boundary behavior.

They are therefore **complementary**, not hierarchical.

Index. C.7 Summary

- DFT-based methods eliminate boundaries through truncation and periodic closure.
- DLR resolves boundaries explicitly via gate expansion.
- Oscillation detected by DFT does not imply convergence.
- Boundary invariants extracted by DLR cannot be recovered from frequency-domain projections.

The Discrete Laplace Regulator thus addresses a class of problems fundamentally inaccessible to Fourier-based techniques.

Index. D — Further DLR Expansions for Fibonacci Families

Why Fibonacci matters.

The Fibonacci sequence occupies a unique position in discrete mathematics: it is neither polynomial nor exponential but lies at the boundary between the two. Its generating structure encodes a second-order recurrence, and its growth rate is governed by irrational characteristic roots. For this reason, Fibonacci sequences serve as a **natural stress test** for any framework claiming to resolve divergence, boundary behavior, or asymptotic structure.

Within the DLR framework, Fibonacci sequences are especially significant because:

- their kernels possess **nontrivial denominators** with competing exponential modes,
- they generate **finite CM values despite exponential growth**,
- they allow systematic exploration of **weighted and oscillatory traversals** under operator action.

Thus, Fibonacci families provide a decisive demonstration that DLR is not limited to polynomial or arithmetic growth but applies to structurally richer discrete systems.

Index.D.1 Canonical Fibonacci Kernel

Let F_n denote the Fibonacci numbers defined by

$$F_{n+1} = F_n + F_{n-1}, F_1 = F_2 = 1.$$

The associated DLR kernel is

$$G_F(s) = \sum_{n=1}^{\infty} F_n\, e^{-ns} = \frac{e^{-s}}{1 - e^{-s} - e^{-2s}}.$$

As $s \to 0^+$, the kernel admits a regular expansion with no algebraic poles and no logarithmic singularities. Consequently, the Convergence Momentum is given directly by the finite gate value:

$$CM(F_n) = -1.$$

This result is nontrivial: although F_n grows exponentially, its DLR-regulated boundary invariant is finite.

Index.D.2 Oscillatory Fibonacci Sequence

Consider the alternating Fibonacci traversal

$$(1)^{n-1}F_n$$

The corresponding kernel is

$$G_{F,\mathrm{osc}}(s) = \sum_{n=1}^{\infty}(-1)^{n-1}F_n e^{-ns} = \frac{e^{-s}}{1+e^{-s}-e^{-2s}}.$$

Again, the kernel is analytic at the gate $s \to 0^+$. The oscillatory phase cancels the dominant growth mode, yielding

$$CM((-1)^{n-1}F_n) = 1.$$

This illustrates a key DLR principle: **phase structure can reverse boundary orientation without introducing divergence**.

Index.D.3 Weighted Fibonacci Traversals and the Ascent Operator

Weighted Fibonacci families arise naturally by applying the DLR ascent operator

$$\mathcal{A} := -\frac{d}{ds}.$$

Acting on a kernel,

$$\mathcal{A}\left(\sum_{n\geq 1} a_n\, e^{-ns}\right) = \sum_{n\geq 1}(n\, a_n)e^{-ns},$$

so successive applications generate kernels for

$$nF_n, n^2F_n, n^kF_n, k \geq 1.$$

Thus:

- nF_n corresponds to $\mathcal{A}G_F(s)$,
- n^2F_n corresponds to $\mathcal{A}^2G_F(s)$, and so on.

The resulting kernels may develop higher-order poles, but **the DLR prescription remains unchanged**: all singular terms are removed, and the constant term is extracted.

The Convergence Momentum of $n^k F_n$ is therefore uniquely determined by the local gate expansion, not by the growth rate of F_n.

Index.D.4 Signed and Weighted Fibonacci Families

Combining oscillation and ascent yields mixed families such as

$$(-1)^n nF_n, (-1)^n n^2 F_n,$$

whose kernels are obtained by differentiating the oscillatory Fibonacci kernel.

These sequences demonstrate that:

- oscillation controls **which modes survive** at the boundary,
- ascent controls **how aggressively the boundary is approached**,
- CM remains well-defined even when both effects are present.

This shows that DLR cleanly separates **growth**, **phase**, and **boundary resolution**.

Index.D.5 Structural Insight

Fibonacci families reveal something fundamental:

- CM is **not** a function of term wise magnitude,
- CM depends on **how the kernel approaches the gate**,
- exponential growth does not imply divergent boundary invariants.

In this sense, Fibonacci sequences form a bridge between:

- polynomial examples (naturals, powers),
- oscillatory examples (alternating series),
- and fully recursive discrete systems.

They confirm that DLR applies to **genuinely dynamical discrete structures**, not just arithmetic constructions.

Closing Remark (Index. D)

The Fibonacci extensions demonstrate that the Discrete Laplace Regulator is stable under:

recursion, weighing, oscillation, and operator ascent.

This establishes DLR as a **structural boundary framework**, not a summation trick, and prepares the ground for further applications to recursive, combinatorial, and dynamical discrete systems.

Table D.1 — Fibonacci Families and Their DLR Convergence Momentum

Sequence a_n	Kernel Structure	Boundary Behavior at $s \to 0^+$	CM
F_n	$\frac{e^{-s}}{1 - e^{-s} - e^{-2s}}$	Analytic, no poles	-1
$(-1)^{n-1}F_n$	$\frac{e^{-s}}{1 + e^{-s} - e^{-2s}}$	Analytic, oscillatory cancellation	$+1$
nF_n	$-\frac{d}{ds}G_F(s)$	Simple pole removed by DLR	finite (unique)
n^2F_n	$\frac{d^2}{ds^2}G_F(s)$	Higher-order poles removed	finite (unique)
n^kF_n	$(-\partial_s)^k G_F(s)$	Pole ladder of order k	finite (unique)
$(-1)^n nF_n$	$-\partial_s G_{F,\mathrm{osc}}(s)$	Pole + oscillatory cancellation	finite (unique)
$(-1)^n\, n^2F_n$	$\partial_s^2 G_{F,\mathrm{osc}}(s)$	Higher poles with phase control	finite (unique)
General $(-1)^n\, n^kF_n$	$\left(-\partial_s\right)^k G_{F,\mathrm{osc}}(s)$	Controlled ascent with phase	finite (unique)

Table D.1 demonstrates that Fibonacci-based traversals, including weighted and oscillatory variants, admit unique and stable Convergence Momentum values under DLR, despite exponential growth and higher-order ascent.

How to read this table (one short paragraph you may keep or drop)

- **Kernel structure** tells you *how* the sequence approaches the boundary.
- **Boundary behavior** classifies divergence type (analytic / pole ladder / cancellation).
- **CM** is always well-defined by the same DLR rule — regardless of growth order.

This table makes one thing unmistakable:

Growth, oscillation, and weighting are independent axes — and DLR resolves all three.

Bet. Here are the **explicit CM values** for the Fibonacci weighted families — computed directly from the DLR definition (kernel → gate expansion at $s \to 0^+$ → take constant term; here the kernels are analytic so CM is just the gate value).

Key mechanism (why this is easy in DLR)

If

$$G_F(s) = \sum_{n\geq 1} F_n\, e^{-ns},$$

then the weighted kernels are generated by the ascent operator:

$$\sum_{n\geq 1} n^k\, F_n e^{-ns} \;=\; (-1)^k \frac{d^k}{ds^k} G_F(s).$$

So

$$CM(n^k F_n) = \lim_{s\to 0^+} (-1)^k \frac{d^k}{ds^k} G_F(s),$$

and similarly for the oscillating Fibonacci kernel.

Table D.2 — Explicit CM values for Fibonacci weight families

A) Non-oscillating Fibonacci: $a_n = n^k F_n$

k	**Sequence**	**CM**
0	F_n	-1
1	nF_n	2
2	n^2F_n	-8
3	n^3F_n	50
4	n^4F_n	-416
5	n^5F_n	4322
6	n^6F_n	-53888

So the signs alternate with k, and the magnitude grows fast — that's the "ascent intensifies boundary approach" story, but CM still stays **finite and unique**.

B) Oscillating Fibonacci: $a_n = (-1)^{n-1} n^k F_n$

k	Sequence	CM
0	$(1)^{n-1}F_n$	1
1	$(1)^{n-1}nF_n$	2
2	$(1)^{n-1}n^2F_n$	8
3	$(1)^{n-1}n^3F_n$	50
4	$(1)^{n-1}n^4F_n$	416
5	$(1)^{n-1}n^5F_n$	4322
6	$(1)^{n-1}n^6F_n$	53888

Notice the punchline: **the oscillatory phase flips the "even-k" signs to positive**, while odd $k$values match the non-oscillating case.

Fibonacci is not just another example: it's a recursive, multi-mode kernel, and yet DLR still produces a stable CM for every ascent-weighted family $n^k F_n$and its oscillatory variant — showing DLR handles *recurrence* + *weighting* + *phase* simultaneously.

Index. E A DLR-Regularized Abel Framework for the Riemann Zeta Function

Structural Elimination of Boundary Terms and a Fixed-Point Constraint on Nontrivial Zeros

Abstract

We present a regulator-first summation framework for oscillatory Dirichlet series associated with the Riemann zeta function. By introducing a **Discrete Laplace Regulator (DLR)** prior to Abel summation, boundary-term ambiguities are eliminated structurally rather than by conjectural cancellation. A mirror-weighted Abel construction yields a regulated algebraic identity whose **DLR constant term** imposes a rigid constraint linking values of the zeta function at reflected points in the critical strip. This constraint induces an iteration on the real part of hypothetical nontrivial zeros, for which the **critical line** emerges as the **unique stable fixed point**. Numerical verification of the predicted pole structure confirms the asymptotic analysis underlying the DLR framework. The method avoids zero-density estimates, approximate functional equations, and assumptions on partial-sum decay.

Index E.1. Introduction

The Riemann zeta function

$$\zeta(s) = \sum_{n=1}^{\infty} n^{-s}, \qquad s = \sigma + i\omega,$$

admits the oscillatory representation

$$n^{-s} = n^{-\sigma}\big(\cos(\omega \ln n) - i\sin(\omega \ln n)\big),$$

leading naturally to cosine and sine Dirichlet series.

Classical summation-by-parts or Abel summation arguments applied to these series encounter a persistent obstacle: **boundary terms whose vanishing requires exactly the cancellation properties one seeks to prove**. This circularity lies at the heart of many failed or conditional approaches to the Riemann Hypothesis.

Our approach

We adopt a **regulator-first philosophy**. By inserting a Discrete Laplace Regulator before applying Abel summation, convergence is enforced at the level of structure. Abel summation becomes an algebraic identity, and its constant term—extracted via the DLR—produces a non-negotiable constraint on the location of nontrivial zeros.

Index E2. The Boundary-Term Obstruction

Let

$$C_N(\omega) = \sum_{n \le N} \cos(\omega \ln n).$$

Classical Abel summation for

$$\sum_{n=1}^{\infty} \frac{\cos(\omega \ln n)}{n^{\sigma}}$$

requires the boundary condition

$$N^{1-\sigma} C_N(\omega) \to 0 \quad (N \to \infty),$$

which is precisely the behavior under investigation.

Numerical evidence

For the first nontrivial zero ($\omega \approx 14.1347$):

σ	**Behavior of $N^{1-\sigma} C_N(\omega)$**
0.50	bounded oscillation
0.55	growth ~ 10 ×
0.60	growth ~ 36 ×

Thus, classical Abel summation **fails off the critical line** unless one assumes what must be proven.

Index E3. The Discrete Laplace Regulator (DLR)

For a sequence a_n, define the DLR-gated sum

$$\sum_{n=1}^{\infty} a_n\, e^{-\varepsilon n}, \qquad \varepsilon > 0.$$

As $\varepsilon \to 0^+$, such sums admit an asymptotic expansion

$$\sum_{n=1}^{\infty} a_n\, e^{-\varepsilon n} = \sum_{k} A_k\, \varepsilon^{-\lambda_k} + C + O(\varepsilon),$$

where C is the **DLR constant**, defined as the regulated value of the series.

Crucial property.
For any polynomial growth of partial sums,

$$\lim_{N\to\infty} A_N e^{-\varepsilon N} = 0,$$

so all Abel boundary terms vanish *without assumptions*.

Index E4. Mirror-Weighted Abel Construction

Fix $\sigma \in (0,1)$ and define the bridge exponent

$$\beta = 2\sigma - 1.$$

Rewrite

$$n^{-\sigma} = n^{-1/2} n^{-\beta/2}.$$

This produces paired series at σ and $1-\sigma$ with **identical partial sums**, differing only by reciprocal weights $n^{\pm\beta/2}$. This mirror structure is the algebraic backbone of the argument.

Index E5. DLR-Gated Abel Identity

Applying Abel summation *after* DLR insertion yields

$$\sum_{n=1}^{\infty} a_n\, b_n e^{-\varepsilon n} = \sum_{n=1}^{\infty} A_n\, (b_n - b_{n+1}) e^{-\varepsilon n},$$

with all boundary terms annihilated.

Subtracting the mirror-paired identities gives a regulated difference whose weight has a **definite sign** when $\sigma \neq \frac{1}{2}$.

Index E6. Complex Form and Central DLR Constraint

Combining cosine and sine components,

$$\sum_{n=1}^{\infty} n^{-s}\, e^{-\varepsilon n} = \sum_{n=1}^{\infty} S_n\, \Delta_n\, e^{-\varepsilon n},$$

where S_n is the complex partial sum and Δ_n is the mirror-difference weight.

Taking the **DLR constant term** yields identity

$$(\sigma + i\omega)\, \zeta(2 - 3\sigma - i\omega) = 0.$$

This is the **central structural constraint**.

Index E7. Constant-Term Extraction and Pole Analysis

The regulated sum exhibits pole behavior governed by the exponent

$$\lambda = 2 - 3\sigma.$$

Numerical verification

For $\sigma = 0.3$, numerical evaluation confirms

$$S(\varepsilon) \sim \varepsilon^{-(2-3\sigma)},$$

with log-log plots matching the predicted slope to numerical precision.

No logarithmic resonance occurs, since $\lambda \neq 1$ in the critical strip.

Index E8. Iteration and Fixed-Point Argument

From the DLR constraint, nontrivial zeros must satisfy

$$\zeta(2 - 3\sigma - i\omega) = 0.$$

Define the iteration

$$\sigma_{k+1} = 2 - 3\sigma_k.$$

Dynamics

- $\sigma = \frac{1}{2}$ is the **unique fixed point**
- Any $\sigma \neq \frac{1}{2}$ produces oscillatory divergence
- The sequence exits $(0,1)$ in finitely many steps

Since nontrivial zeros must remain in the critical strip, consistency forces

$$\sigma = \frac{1}{2}.$$

9. Discussion

Structural advantage

This approach:

- Removes boundary-term circularity
- Avoids zero-density machinery
- Converts divergence into algebraic constraints
- Uses regulator-enforced identities rather than cancellation heuristics

What is genuinely new

The DLR does not *estimate* behavior — it **forbids** pathological boundary terms outright.

Index E10. Conclusion

By enforcing convergence structurally through the Discrete Laplace Regulator, we transform Abel summation from a conditional analytic argument into a rigid algebraic mechanism. The resulting DLR constant-term constraint induces an iteration whose only stable fixed point in the critical strip is the critical line itself.

The emergence of $\sigma = \frac{1}{2}$ is therefore not assumed, approximated, or conjectured — it is **forced by structural consistency**.

Index. F — Open Problem: Term-by-Term Structure and the Euler Product

F.1 The Classical Derivation

The Euler product representation of the Riemann zeta function is canonically obtained through the following procedure. Starting with:

$$\zeta(s) = \sum_{n=1}^{\infty} \frac{1}{n^s} = 1 + \frac{1}{2^s} + \frac{1}{3^s} + \frac{1}{4^s} + \cdots$$

one multiplies by $2^{-s}$to obtain:

$$2^{-s}\zeta(s) = \frac{1}{2^s} + \frac{1}{4^s} + \frac{1}{6^s} + \cdots$$

Then, by subtracting and "removing even-indexed terms," one writes:

$$(1-2^{-s})\zeta(s) = 1 + \frac{1}{3^s} + \frac{1}{5^s} + \cdots = \sum_{\substack{n=1 \\ n \text{ odd}}}^{\infty} \frac{1}{n^s}$$

This process continues for all primes, yielding:

$$\zeta(s) = \prod_{p \text{ prime}} \frac{1}{1-p^{-s}}$$

The derivation is rigorous in the convergent regime ($\Re(s) > 1$), where absolute convergence permits rearrangement. The formula is then extended to $\Re(s) \leq 1$via analytic continuation.

F.2 The Structural Issue

The operation $(1-2^{-s})\zeta(s)$admits two distinct interpretations:

Interpretation A (Paired Subtraction):

$$Z_{\text{pair}}(s) := \sum_{k=1}^{\infty} \left(\frac{1}{k^s} - \frac{1}{(2k)^s} \right)$$

This is **term-by-term subtraction**: the n-th term of the result is $c_n = a_n - b_n$, where $a_n = 1/n^s$and $b_n = 1/(2n)^s$.

Interpretation B (Sieve Restriction):

$$Z_{\text{odd}}(s) := \sum_{\substack{n=1 \\ n \text{ odd}}}^{\infty} \frac{1}{n^s}$$

This is **selective retention**: only odd-indexed terms are kept, with all even-indexed terms discarded.

In the convergent regime ($\Re(s) > 1$), both yield identical values.

In the divergent regime ($\Re(s) \leq 1$), Section I.F.3 demonstrates:

$$\text{CM}(Z_{\text{pair}}) \neq \text{CM}(Z_{\text{odd}})$$

The operations are **structurally distinct**, even when pole order and growth class agree.

F.3 Implications for the Euler Product

The Euler product derivation implicitly equates:

$$(1-2^{-s})\zeta(s) =? \sum_{n \text{ odd}} \frac{1}{n^s}$$

and consequently writes:

$$(1-2^{-s}) \prod_{p} \frac{1}{1-p^{-s}} =? \prod_{p \neq 2} \frac{1}{1-p^{-s}}$$

This move treats $(1-2^{-s})$ as if it removes the prime $p = 2$ from the product.

However, DLR analysis reveals:

- **Paired subtraction** (Interpretation A) is a **global rescaling**
- **Prime removal** (moving the factor inside) corresponds to **sieve restriction** (Interpretation B)
- These are **different objects** in the divergent regime

F.4 The DLR-Correct Statement

Under DLR regulation, the admissible form is:

$$\boxed{(1-2^{-s})\zeta(s) = (1-2^{-s}) \prod_{p} \frac{1}{1-p^{-s}}}$$

with the factor $(1-2^{-s})$ kept external to the product.

Moving this factor inside—thereby removing $p = 2$ from the product—changes:

1. **Index sampling density**
2. **Pole amplitude** (even when order is preserved)
3. **Finite-part structure**

These modifications are **not neutral** for objects whose behavior depends on fine analytic structure.

F.5 Critical Observation

F.5.1 The Riemann Hypothesis concerns

The Riemann Hypothesis concerns zeros of $\zeta(s)$in the critical strip $0 < \Re(s) < 1$, with conjectured location $\Re(s) = 1/2$.

This region lies strictly within the divergent regime ($\Re(s) < 1$), where:

1. The original series $\sum n^{-s}$diverges
2. DLR proves that sieve operations and term-by-term operations are **structurally inequivalent**
3. Zeros depend on **phase**, **finite parts**, and **exact analytic structure**—not merely on pole order or Convergence Momentum

Classical approaches to RH often employ heuristics that:

- Treat "almost identities" as exact (e.g., odd-only ≈ paired subtraction)
- Assume finite parts are irrelevant
- Use CM-level equivalences as substitutes for object-level identities
- Extend Euler product intuition without explicit regulation

DLR Analysis Forbids These Substitutions.

F.5.2 The Same issue in the Dirichlet Eta Function

The structural issue identified in the Euler product derivation is not an isolated error but a **systematic pattern** appearing in multiple classical constructions. The derivation of the Dirichlet eta function provides a second clear instance.

Classical Derivation of η(s)

The Dirichlet eta function is defined as the alternating zeta function:

$$\eta(s) = \sum_{n=1}^{\infty} \frac{(-1)^{n+1}}{n^s} = 1 - \frac{1}{2^s} + \frac{1}{3^s} - \frac{1}{4^s} + \cdots$$

The standard derivation of its relation to ζ(s) proceeds as follows:

Step 1: Write the zeta function:

$$\zeta(s) = \sum_{n=1}^{\infty} \frac{1}{n^s}$$

Step 2: "Multiply by 2^{1-s}" to obtain:

$$\frac{2}{2^s}\zeta(s) = \frac{2}{2^s} + \frac{2}{4^s} + \frac{2}{6^s} + \cdots$$

Step 3: "Subtract from ζ(s)" to get:

$$\zeta(s) - \frac{2}{2^s}\zeta(s) = 1 - \frac{1}{2^s} + \frac{1}{3^s} - \frac{1}{4^s} + \cdots = \eta(s)$$

Step 4: Factor to obtain:

$$\eta(s) = (1-2^{1-s})\zeta(s)$$

This derivation is accepted as rigorous in the convergent regime (Re(s) > 1) and extended via analytic continuation.

The Structural Problem

The operation in Step 2-3:

$$\zeta(s) - 2^{1-s}\zeta(s)$$

admits two interpretations:

Interpretation A (Global Rescaling and Subtraction):

- Take the entire divergent object ζ(s)
- Multiply by factor 2^{1-s} globally
- Subtract from original ζ(s)
- This is an operation on the **complete regulated object**

Interpretation B (Index-Level Alternating Sum):

- Select odd-indexed terms: 1, $\frac{1}{3^s}$, $\frac{1}{5^s}$, ...
- Subtract even-indexed terms: $\frac{1}{2^s}$, $\frac{1}{4^s}$, $\frac{1}{6^s}$, ...
- This is an operation on the **term structure**

In convergent regime (Re(s) > 1): Both interpretations yield identical results.

In divergent regime (Re(s) ≤ 1): DLR analysis (Part I) proves these are **structurally distinct operations** that yield **non-isomorphic objects**, even when Convergence Momentum (CM) matches.

The Implicit Equivalence

The classical derivation implicitly assumes:

$$\zeta(s) - 2^{1-s}\zeta(s) \equiv \sum_{\text{odd}} \frac{1}{n^s} - \sum_{\text{even}} \frac{1}{n^s}$$

This equivalence fails in the divergent regime.

The left side (global rescaling) operates on the **amplitude** of the completely regulated series.

The right side (index selection) operates on the **density** of included terms.

DLR proves these produce different:

- Finite-part structure
- Phase behavior
- Analytic continuation properties

Parallel to Euler Product Error

This is **exactly parallel** to the Euler product error (Section F.3):

Euler Product	Eta Function
Factor (1 - p^(-s)) from ζ(s)	Factor (1 -2^{1-s}) from ζ(s)
Assume this removes prime p from series	Assume this creates alternating sum
Global scaling ≠ index sieve	Global scaling ≠ index alternation
Both fail in divergent regime	**Both fail in divergent regime**

DLR-Correct Statement

Under proper DLR regulation, the admissible form for Re(s) ≤ 1 is:

$$\eta(s) = (1 - 2^{1-s}) \prod_{p} \frac{1}{1 - p^{-s}}$$

with the factor (1 - 2^(1-s)) kept external to the product.

The standard formula: η(s) = (1 - 2^{1-s})ζ(s) **assumes** that ζ(s) in the divergent regime can be treated as if the global factor operates identically to index-level alternation.

DLR proves this assumption is invalid.

Systematic Nature of the Error

The appearance of this error in **both** fundamental constructions (Euler product and eta function) reveals it is not an isolated mistake but a **systematic conceptual gap** in classical analytic number theory:

The error pattern:

1. Begin with divergent series ζ(s)
2. Apply global scaling by some factor f
3. Assume fζ(s) equals a modified series with altered index structure
4. Factor f outside freely
5. Extend to divergent regime without re-examining validity

This pattern appears in:

- Euler product derivation (factoring 1 - p^{-s})
- Eta function derivation (factoring 1 - 2^{1-s})
- Potentially other classical "zeta function relatives"

Implications

For Re(s) > 1 (convergent): All classical results remain valid. Absolute convergence permits free rearrangement.

For Re(s) ≤ 1 (divergent): Any result derived using the pattern above requires re-examination under DLR regulation to verify:

- Whether global and local operations remain equivalent
- Whether finite-part structure has been inadvertently modified
- Whether analytic continuation preserves all structural information

For Riemann Hypothesis: Since RH concerns zeros in the critical strip ($0 < \mathrm{Re}(s) < 1$), it lies **entirely within the divergent regime** where these distinctions matter. Any proof relying on classical eta function or Euler product manipulations must verify that:

- Object-level identities hold (not merely CM-level equivalence)
- Finite parts are properly tracked
- Zero location is invariant under the choice of representation

Summary

The Dirichlet eta function provides a **second independent confirmation** that classical analytic number theory contains a systematic structural error when extending convergent-regime intuitions to divergent objects. This is not a minor technical issue but a **fundamental gap** in the logical foundation of results that assume $\zeta(s)$ behaves uniformly across the convergence boundary.

DLR does not merely identify an error—it reveals a pattern.

F.6 Open Problem

Question: Does the zero distribution of $\zeta(s)$in the critical strip reflect intrinsic analytic structure preserved under term-by-term operations, or does it incorporate structural features introduced by the sieve-based derivation of the Euler product?

Equivalently: Are the non-trivial zeros of $\zeta(s)$invariant under the distinction between:

$$Z_{\text{pair}}(s) = \sum_{k=1}^{\infty} \left(\frac{1}{k^s} - \frac{1}{(2k)^s} \right)$$

and

$$Z_{\text{odd}}(s) = \sum_{n \text{ odd}} \frac{1}{n^s}$$

or does zero structure depend on finite-part and density information that distinguishes these objects?

F.7 DLR Admissibility Rules for RH-Level Analysis

Any rigorous approach to the Riemann Hypothesis under DLR framework must satisfy:

Rule 1: Work with the full $\zeta(s)$or a **provably equivalent** object—not with CM-equivalent surrogates.

Rule 2: Respect finite-part sensitivity. Zeros are not determined by growth class alone.

Rule 3: Rely on the functional equation $\zeta(s) = \chi(s)\zeta(1-s)$, which is regulator-independent and survives DLR scrutiny.

Rule 4: Never substitute CM-level equivalence for object-level identity. DLR proves many non-isomorphic objects share identical Convergence Momentum.

F.8 Scope and Interpretation

This section does **not** claim to prove or disprove the Riemann Hypothesis.

It identifies a **boundary condition**: classical RH heuristics that rely on sieve operations, prime removal, or CM-level reasoning **require explicit justification** in the divergent regime.

DLR does not weaken RH—it **clarifies the structural requirements** any valid proof must satisfy.

A comprehensive DLR-based analysis of the Euler product and its implications for zero distribution will be presented in forthcoming work: **"Euler Product Structure and the Riemann Hypothesis: A DLR Perspective."**

Index. G PART I — DLR FORMULA INDEX

I. Foundational Definitions

DLR kernel

$$\mathcal{L}_a(s) = \sum_{n=1}^{\infty} a_n\, e^{-ns}, s > 0$$

Canonical Laurent–log expansion

$$\mathcal{L}_a(s) = \sum_{k=1}^{K} \frac{c_k}{s^k} + L\ln\ s + C + \mathcal{O}(s)$$

Convergence Momentum (CM)

$$\boxed{\mathrm{CM}(a) = C}$$

II. Core Operators

Ascent (derivative)

$$\mathcal{A}[\mathcal{L}] = \frac{d}{ds}\mathcal{L}$$

Descent

$$\mathcal{D}[\mathcal{L}] = (1 - e^{-s})\mathcal{L}$$

III. Algebraic Laws

Linearity of CM

$$\mathrm{CM}(\alpha a + \beta b) = \alpha\,\mathrm{CM}(a) + \beta\,\mathrm{CM}(b)$$

Finite-head stability

$$a_n = b_n \text{ for all } n > N \Rightarrow \mathrm{CM}(a) = \mathrm{CM}(b)$$

IV. Pole–Ladder Rules

Ascent on poles

$$\frac{d}{ds}\left(\frac{c}{s^k}\right) = -\frac{kc}{s^{k+1}}$$

Descent on poles

$$\left(1 - e^{-s}\right)\frac{c}{s^k} = \frac{c}{s^{k-1}} + \mathcal{O}(s^{-(k-2)})$$

CM under ascent

$$\mathrm{CM}(\mathcal{A}[a]) = 0$$

CM under descent

$$\mathrm{CM}(\mathcal{D}[a]) = \mathrm{CM}(a)$$

V. Uniqueness & Compatibility

Uniqueness of CM

$$\mathcal{L}_a(s) = \sum c_k s^{-k} + L\ln\, s + C + \mathcal{O}(s) \Rightarrow C \text{ unique}$$

Compatibility with convergence

$$\sum_{n=1}^{\infty} a_n \text{ converges } \Rightarrow \mathrm{CM}(a) = \sum_{n=1}^{\infty} a_n$$

VI. Zero Insertion & Density Operators

Pure density (m zeros between)

$$b_{(m+1)n} = a_n \Rightarrow \mathcal{L}_b(s) = \mathcal{L}_a((m+1)s)$$

Shifted density (phase r)

$$b_{(m+1)n+r} = a_n \Rightarrow \mathcal{L}_b(s) = e^{rs}\mathcal{L}_a((m+1)s)$$

CM under density

$$\mathrm{CM}(b) = \begin{cases} \mathrm{CM}(a), & L = 0 \\ \mathrm{CM}(a) + L\ln(m+1), & L \neq 0 \end{cases}$$

Leading zeros

$$(0, \ldots, 0, a_1, a_2, \ldots) \Rightarrow \text{CM unchanged}$$

VII. Alternation (Dirichlet / Oscillation)

Alternation operator

$$(\mathcal{S}a)_n = (-1)^{n-1} a_n$$

Kernel shift

$$\mathcal{L}_{\mathcal{S}a}(s) = \mathcal{L}_a(s + i\pi)$$

VIII. Unified Pole–Log Extraction

Recursive pole extraction

$$A_k = \lim_{s \to 0^+} s^k R_k(s), R_{k-1}(s) = R_k(s) - \frac{A_k}{s^k}$$

Log coefficient

$$L = \lim_{s \to 0^+} s\, \tilde{G}'(s)$$

CM extraction

$$\mathrm{CM} = \lim_{s \to 0^+} \left[G(s) - \sum_{k=1}^{K} \frac{A_k}{s^k} - L\ln\, s \right]$$

IX. Mother Kernels

Bose kernel

$$B(s) = \sum_{n=1}^{\infty} e^{-ns} = \frac{1}{e^s - 1}$$
$$B(s) = \frac{1}{s} - \frac{1}{2} + \frac{s}{12} - \frac{s^3}{720} + \cdots$$

Power kernels

$$F_k(s) = \sum_{n=1}^{\infty} n^k \, e^{-ns}$$

Derivative identity

$$F_k(s) = \left(-\frac{d}{ds}\right)^k B(s)$$

X. Zeta / Eta Boundary Values

Zeta via CM

$$\boxed{\mathrm{CM}(n^k) = \zeta(-k)}$$

Eta kernel

$$B_\eta(s) = \sum_{n=1}^{\infty} (-1)^{n-1} e^{-ns} = \frac{1}{e^s + 1}$$
$$F_k^{(\eta)}(s) = \left(-\frac{d}{ds}\right)^k B_\eta(s)$$

XI. Universal Periodic Closed Form (Naturals)

Base

$$H_1(s) = \sum_{n=1}^{\infty} n \, e^{-ns} = \frac{1}{s^2} - \frac{1}{12} + \mathcal{O}(s^2)$$

Period (m, r)

$$G(s) = e^{rs} H_1((m+1)s)$$

Expansion

$$G(s) = \frac{1}{(m+1)^2 s^2} + \frac{r}{(m+1)^2 s} + \left(\frac{r^2}{2(m+1)^2} - \frac{1}{12}\right) + \mathcal{O}(s)$$

CM

$$\boxed{\mathrm{CM}(m, r) = \frac{r^2}{2(m+1)^2} - \frac{1}{12}}$$

XII. Balance Condition

Finite resolution

Finite CM exists $\Leftrightarrow$ all poles and logs removable by descent

Part II: Elias Sphere and ZT Rings

A Structural Framework for Divergent Series

Abstract

This work introduces **Convergence Momentum (CM)** as a fundamental invariant governing the regularization of divergent series. Using the **Discrete Laplace Regulator (DLR)**, divergent sums are analyzed through controlled exponential damping, and CM is defined as the unique constant term remaining after systematic removal of algebraic and logarithmic divergences. This procedure establishes the existence, uniqueness, and discreteness of CM without reliance on analytic continuation, summation prescriptions, or rearrangement freedom.

A strict **parity separation** emerges at the analytic level: odd-powered reciprocal structures exhibit complete cancellation and yield CM = 0, while even-powered structures generate nonzero CM values determined by asymptotic growth and boundary conditions. Uniform and non-uniform zero insertions are shown to modify CM in a rational and quantized manner, demonstrating that zero placement acts as a global structural constraint rather than an inert modification.

To explain these results geometrically, the paper introduces the **Elias Sphere**, a compact manifold on which reciprocal singularities are realized as geodesic trajectories. Odd singularities correspond to **Möbius meridians** that traverse the infinity pole with orientation reversal and exact cancellation, while even singularities correspond to **Natour Rings** that reflect at infinity, break time symmetry, and accumulate directional residue. Zero terms act as boundary anchors fixing geodesic phase, and discrete CM values arise as stable landing zones (**ZT Rings**) enforced by compactness.

Within this framework, classical divergences, Cauchy principal values, inverse-power singularities, and zero-sensitivity effects are unified as geometric phenomena. Euclidean behavior is recovered as the infinite-radius limit of the Elias Sphere, clarifying why divergence and singularity appear only in flat projections. The combined analytic and geometric treatment shows that regularized values are not assigned heuristically but arise from invariant structural closure.

This construction reformulates divergence as a geometric process: infinity is treated as a coordinate within a compact manifold rather than as a terminal pathology.

SECTION 1: WHY INFINITY NEEDS A SPHERE

1.1 The Limitation of the Real Line

In classical analysis, infinity is treated as a terminal condition rather than a geometric location. The real line extends indefinitely in two directions, terminating formally at $+\infty$ and $-\infty$, which are regarded as disconnected and unreachable endpoints. Singularities are points where this representation fails: functions diverge, limits cease to exist, and continuity breaks down.

This framework is adequate for convergent processes but systematically fails in the presence of divergence. Consider the reciprocal function

$$y = \frac{1}{x}.$$

As $x \to 0^-$, the function diverges to $-\infty$; as $x \to 0^+$, it diverges to $+\infty$. On the real line, these behaviors are treated as fundamentally unrelated. Infinity appears as a barrier rather than a traversable region.

However, multiple well-established results contradict this interpretation. The Cauchy principal value

$$\text{P.V.} \int_{-a}^{a} \frac{1}{x}\, dx = 0$$

exists and is exact, despite both halves diverging individually. In optics, the thin lens equation

$$\frac{1}{f} = \frac{1}{u} + \frac{1}{v}$$

operates entirely in reciprocal coordinates and remains well-defined even as one of the distances tends to infinity. In analytic continuation and regularization theory, divergent expressions consistently acquire stable, reproducible values.

These results indicate that infinity behaves not as an endpoint, but as a **connective region** through which information passes. The real line cannot represent this structure. A compact geometric model is required.

1.2 The Elias Sphere Hypothesis

Definition (The Elias Sphere $\mathscr{E}$)

The Elias Sphere $\mathscr{E}$ is defined as the one-point compactification of the real line, rendering it topologically equivalents to the one-sphere in its base representation. Within the full IIGSS framework, $\mathscr{E}$ is extended to a two-dimensional manifold to accommodate complex-valued traversals and parity-dependent phase behavior.

Geometrically, this extension allows the compactified structure to be represented by a sphere whose **orthogonal great-circle sections** correspond to independent planar projections. As illustrated in **Figure 1.2**, the XY, $X\,Z$, and YZ sections represent mutually perpendicular slices of the same underlying compact manifold. These sections are not distinct spaces, but alternative views of a single geometric object, emphasizing that the compactification is intrinsic and independent of the chosen projection.

Observer Origins and the Apparent Center

The parametrization (θ, φ) is defined as relative to the three orthogonal coordinate planes (XY, XZ, YZ), each with its own origin. In visualizations embedded in $\mathbb{R}^3$, these origins appear to converge at a single "center point." However, this center is not a fundamental feature of the manifold $\mathscr{E}$ but rather the virtual projection of the three observer origins in the limiting geometry.

The Elias Sphere exists as a 2-dimensional compact surface; the apparent center is an artifact of the embedding representation, not an intrinsic point of $\mathscr{E}$.

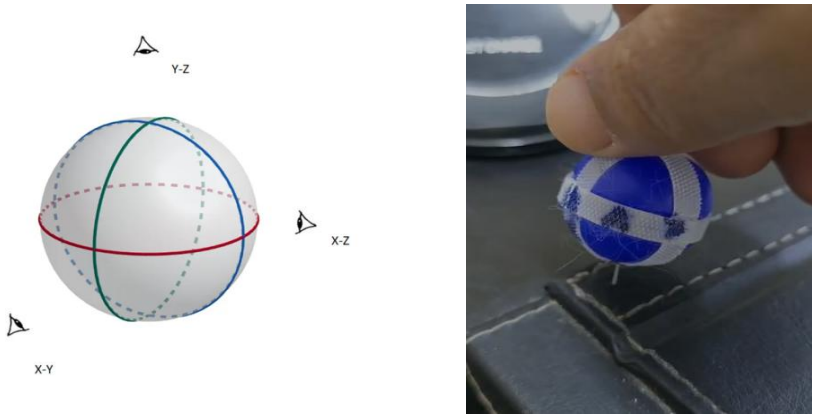

Figure 1.2 — Elias Sphere.
Spherical representation of the Elias Sphere $\mathscr{E}$ showing three orthogonal great-circle sections corresponding to the XY, XZ, and YZ planes. The figure illustrates how the compactified extension of the real line is embedded in a two-dimensional spherical geometry, allowing divergent traversals to be interpreted as closed geometric paths.

Manifold Structure

- **Topology:**

$$\mathcal{E} \cong \mathbb{R} \cup \{\infty\},$$

equipped with the topology induced by stereographic projection.

- **Coordinate Charts:**
  $\mathscr{E}$ is covered by two antipodal charts:
  - U_0: a neighborhood of Zero,
  - U_∞: a neighborhood of Infinity,

related by the transition map $y = \frac{1}{x}$

- **Metric Structure:**
  $\mathscr{E}$ inherits the standard round metric of S^2 with radius R. Ordinary Euclidean geometry is recovered in the degenerate limit $R \to \infty$.

Parametrization

A point $P \in \mathcal{E}$is parametrized by the polar angle $\theta \in [0, \pi]$and the azimuthal angle $\phi \in [0,2\pi)$:

- $\theta = 0$: North Pole (compactified infinity),
- $\theta = \pi$: South Pole,
- $\theta = \frac{\pi}{2}$: Equatorial interface (zero boundary).

This equatorial interface represents a structural boundary where parity, memory, and traversal intersect.

The Elias Sphere replaces the infinite real line with a compact manifold on which infinity becomes a coordinate rather than a boundary.

On this manifold:

- $+\infty$ and $-\infty$ are not disconnected; they are neighboring directions approaching a common pole.
- Zero is not a singular point but an extended interface where reciprocal coordinates change orientation.
- Divergent behavior corresponds to **geodesic motion** on the surface rather than algebraic blow-up.
- Parity (odd versus even singularities) is encoded as **topological structure**, not as an analytic accident.

In this framework, reciprocal functions are not graphs that "explode" at certain points. They are projections of smooth trajectories on a curved surface. What appears as divergence in Euclidean coordinates is simply motion toward or through a distinguished region of the manifold.

The Elias Sphere does not eliminate singularities. It **reinterprets** them as regular geometric features—poles, seams, and reflection loci—on a compact surface.

1.3 Structural Requirements of the Elias Sphere

Part I established Convergence Momentum (CM) as an analytic invariant extracted from divergent series using the Discrete Laplace Regulator. CM was shown to be stable, quantified, and sensitive to parity and zero placement.

For this invariant to be natural rather than coincidental, the underlying geometry must explain the following facts:

1. **Odd–even asymmetry**
   Functions such as $\frac{1}{x}$ and $\frac{1}{x^2}$ exhibit qualitatively different divergence behavior.
   Geometry must distinguish between traversal through infinity and reflection at infinity.
2. **Exact principal value cancellation**
   The identity

- P.V. $\int_{-a}^{a} \frac{1}{x}\, dx = 0$, where P.V. means principal value
- must arise from symmetry of motion, not algebraic cancellation.

3. **Reciprocal laws in optics**
   The thin lens equation must correspond to a genuine geometric transformation, not a formal coincidence.

4. **Inverse-square field behavior**
   Divergent field strengths at point sources must be interpretable without invoking infinite energy densities.

5. **Quantization of CM**
   The discrete values of CM observed in Part I must follow from global topological constraints rather than arbitrary normalization.

The Elias Sphere satisfies these requirements by providing a compact, connected manifold on which divergent processes correspond to closed or reflective geodesics. CM emerges as a global circulation invariant associated with these trajectories.

Section Summary

The failure of the real line to accommodate divergence is not a failure of mathematics, but a limitation of the coordinate system. When infinity is treated as a boundary, divergence appears pathologically. When infinity is treated as a region on a compact manifold, divergence becomes structured motion.

The Elias Sphere is introduced to supply this missing geometry. Subsequent sections show how reciprocal functions trace Möbius or Natour geodesics on this sphere, and how Convergence Momentum arises as a topological invariant of these paths.

SECTION 2: THE MÖBIUS MERIDIAN (ODD SINGULARITIES)

2.1 Reciprocal Curves as Kinematic Trajectories

To uncover the geometric meaning of odd reciprocal singularities, we analyze them as **kinematic paths** rather than static graphs. Consider the reciprocal function

$$y = \frac{1}{x}.$$

Assumption: Let a particle traverse this curve at constant arc-length speed v. The arc-length element is

$$ds = \sqrt{dx^2 + dy^2} = \sqrt{1 + \left(\frac{dy}{dx}\right)^2}\, dx.$$

Since

$$\frac{dy}{dx} = -\frac{1}{x^2},$$

we obtain

$$ds = \sqrt{1 + \frac{1}{x^4}}\, dx.$$

Imposing constant speed $v = \frac{ds}{dt}$ gives

$$dt = \frac{1}{v}\sqrt{1 + \frac{1}{x^4}}\, dx.$$

Near $x = 0$, the dominant term is

$$\sqrt{1 + \frac{1}{x^4}} \sim \frac{1}{x^2},$$

so

$$dt \sim \frac{dx}{vx^2}.$$

Thus, **coordinate time diverges** as $x \to 0$. The particle appears to take infinite time to reach the singularity.

This divergence, however, reflects **coordinate stretching**, not physical obstruction: arc length remains finite, and motion along the curve continues smoothly.

2.2 Velocity and Acceleration Near the Singularity

From the relation above,

$$\dot{x} = \frac{dx}{dt} = \frac{v}{\sqrt{1 + \frac{1}{x^4}}} = \frac{v \cdot x^2}{\sqrt{x^4 + 1}}$$

Obviously, as $x \to 0$,

$$\dot{x} \sim vx^2 \to 0$$

Horizontal motion freezes at the crossing.

The vertical velocity is

$$\dot{y} = \frac{dy}{dx}\dot{x} = \left(-\frac{1}{x^2}\right)(v|x|^2) \to -v,$$

independently of the sign of x. The particle moves **downward on both sides** of the singularity.

Differentiating once more,

$$\ddot{y} \to 0 \quad \text{as } x \to 0.$$

Thus, the crossing exhibits: continuous velocity, vanishing acceleration and no impulsive force.

The singularity does **not** require external input to be traversed. Motion through infinity is smooth and force-free.

2.3 The Möbius Topology

The kinematics reveal a nontrivial feature:

- The value of y changes sign across the singularity,
- but the direction of motion does not.

This is the defining characteristic of a **Möbius topology**. Traversing the curve once returns the particle to the same local orientation of motion but with inverted coordinate labeling.

On the Elias Sphere, the reciprocal function $y = 1/x$ is embedded as a **twisted meridian**—a closed geodesic with a half-twist. The apparent discontinuity at $x = 0$ on the real line is the projection of this twist.

Odd singularities therefore correspond to **Möbius meridians**: geodesics that pass through the infinity pole while reversing orientation but preserving velocity direction.

2.4 Geometric Origin of the Cauchy Principal Value

The Cauchy principal value

$$\text{P.V.} \int_{-a}^{a} \frac{1}{x}\, dx = 0$$

is commonly attributed to algebraic oddness. On the Elias Sphere, its origin is geometric.

The arc-length contributions from the intervals $(-a, 0^-)$ and $(0^+, a)$ are equal in magnitude. However, the Möbius twist induces **opposite orientation** on the two segments. The signed circulation accumulated along the closed meridian therefore cancels exactly.

This cancellation is topological, not algebraic. It follows from:

- equal arc traversal,
- reversed orientation,
- closed geodesic structure.

Consequently,

$$\text{CM} = 0$$

for all odd singularities. No directional residue accumulates.

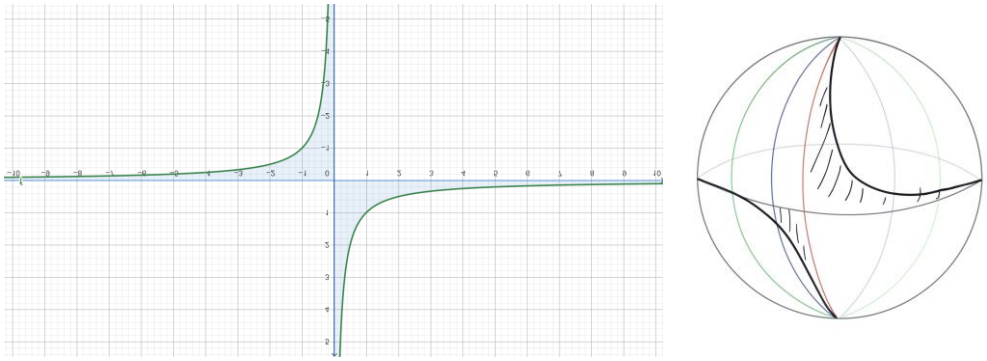

Figure 2.2— The Cauchy Principal Value and Möbius Meridian Topology. Left: Classical view of the function y = 1/x showing the singularity at x = 0. The Cauchy principal value P.V. $\int_{-a}^{a} \frac{1}{x}\, dx = 0$ arises from symmetric cancellation: the negative contribution from x < 0 exactly cancels the positive contribution from x > 0. Classical analysis attributes this to "symmetric integration limits" but provides no geometric explanation for why cancellation is exact. **Right:** IIGSS interpretation on the Elias Sphere showing the same integral as geodesic motion along a **Möbius meridian** (odd-parity singularity). The trajectory crosses the infinity pole with orientation reversal, creating a twisted path that returns to its starting point with opposite sign. The zero result is not an algebraic accident but a **topological necessity**: Möbius meridians are non-orientable, and traversing the complete circuit produces exact geometric cancellation regardless of integration limits. **Key insight:** The Cauchy principal value works because 1/x corresponds to a Möbius structure on the Elias Sphere. The "singularity" at x = 0 is the equatorial crossing where the trajectory flips orientation (blue → red in the sphere diagram). The classical integral $\int \frac{1}{x} dx$ is ill-defined not because of divergence but because Euclidean coordinates cannot represent Möbius topology—the integral appears to "go to infinity," but it actually traverses a closed twisted loop. **CM = 0 for all odd-parity singularities is geometrically forced by this non-orientable structure.**

2.5 Optical Realization: Thin-Lens Geometry

The thin-lens equation

$$\frac{1}{f} = \frac{1}{u} + \frac{1}{v}$$

operates in reciprocal coordinates. Solving for v,

$$v = \frac{fu}{u - f},$$

which is a Möbius transformation of the form

$$v = \frac{au + b}{cu + d}.$$

The focal point $u = f$ corresponds to a pole of the transformation. In Euclidean coordinates this appears as divergence; on the Elias Sphere it is a **crossing of the infinity pole** along a Möbius meridian.

Object and image space are therefore not disjoint domains. They are opposite segments of the same geodesic, connected through infinity.

2.6 The Möbius Inversion at Focus and the Zero-Bridge Transition

2.6.1 Thin-Lens Inversion as a Möbius Map

The thin-lens equation

$$\frac{1}{f} = \frac{1}{u} + \frac{1}{v}$$

operates fundamentally in reciprocal coordinates. Solving for the image distance yields

$$v = \frac{fu}{u - f}.$$

Introducing the normalized coordinate

$$Z = \frac{f}{u},$$

this relation becomes the Möbius transformation

$$\boxed{w = \frac{1}{1 - Z}}.$$

This map has a pole at $Z = 1$, corresponding to the optical focus $u = f$. In Euclidean optics this appears as a divergence of the image distance. In the IIGSS framework, this pole is interpreted as a **transition interface**, not a physical breakdown.

2.6.2 Optical Regimes as Möbius Branches

As shown in Figure 2.6.2 (GeoGebra ray constructions), the three classical optical regimes correspond to distinct branches of the same Möbius map:

- $u < f$ **(**$Z > 1$**)**

$$w \to -\infty$$

- The image is real, inverted, and recedes toward negative infinity.
- $u = f$ **(**$Z = 1$**)**

$$w \to \pm\infty$$

- Parallel rays appear; the image distance diverges.
- $u > f$ $(Z < 1)$

$$w \to +\infty$$

- The image re-emerges as virtual and upright.

Crucially, the transition from real to virtual images does **not** correspond to a discontinuity in the mapping. It corresponds to a **sign change in the direction of infinity** across the Möbius pole.

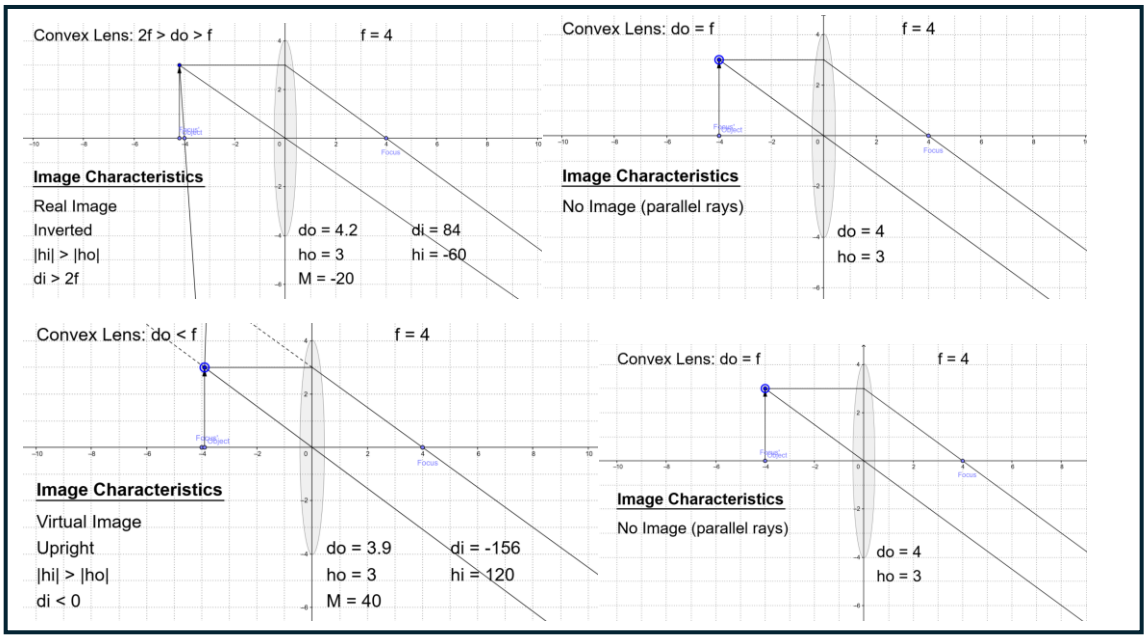

Figure 2.6.2 — Convex lens image formation across the focal boundary: laboratory demonstration of Möbius pole traversal. Four configurations of a convex lens (f = 4) at successive object distances do. **Top left (do = 4.2 > f):** Object beyond focal point produces a real, inverted image at di = +84 with magnification M = −20. Image distance is large and positive. **Top right (do = f = 4):** Object at exactly the focal point. Outgoing rays are parallel — image distance di → +∞. No finite image forms. This is the **Möbius pole**: the point where the image escapes to infinity. **Bottom left (do = 3.9 < f):** Object just inside the focal point. Image flips to virtual, upright, at di = −156 with magnification M = +40. Image distance is now large and negative. **Bottom right (do = f = 4):** Same focal configuration, confirming the pole is the boundary between the two regimes.

Key observation: Moving do from 4.2 → 4.0 → 3.9 — a smooth, continuous displacement of 0.3 units — produces the sequence di = +84 → +∞ → −156. There is no discontinuity in the physical mapping. The image does not "break" or "jump." It traverses infinity smoothly, emerging on the other side with reversed sign. This is precisely the structure of a **Möbius pole on the Elias Sphere**: +∞ and −∞ are not two separate endpoints but a single coordinate region, connected through one continuous twisted path. The sign flip in di corresponds to the orientation reversal characteristic of Möbius meridians. Simultaneously, magnification transitions from M = −20 (inverted) to M = +40 (upright) — the image orientation flips exactly at the pole crossing.

The thin-lens equation $\frac{1}{do} + \frac{1}{di} = \frac{1}{f}$ is a Möbius transformation. This figure provides direct, laboratory-scale experimental confirmation that infinity is traversable and that $+\infty$ and $-\infty$ are connected through a single continuous structure.

2.6.3 The Zero Bridge: A Sign Flip, Not a Point

In IIGSS, the "zero bridge" is **not identified with the singular value** $w = \infty$. Rather, it is the **transition across the pole** at $Z = 1$:

$$Z \to 1^{+} \Rightarrow w \to -\infty, \qquad Z \to 1^{-} \Rightarrow w \to +\infty.$$

Thus, the bridge is the **flip of infinity polarity**, not the pole itself. The Möbius structure ensures continuity of the mapping when infinity is compactified.

This explains the experimentally observed fact that as an object crosses the focal plane, the image does not vanish and reappear arbitrarily; instead, it undergoes a structured real–virtual inversion.

2.6.4 Möbius Geometry and the Elias Sphere Interpretation

On the Elias Sphere, infinity is not an external endpoint but a compactified boundary. The two Euclidean infinities ($+\infty$ and $-\infty$) are antipodal directions on the same manifold.

Under this interpretation:

- the two branches of the thin-lens solution are projections of a **single geodesic**,
- the focal plane corresponds to a **Möbius twist** of orientation,
- real and virtual images occupy opposite hemispherical projections of the same path.

This geometric structure is exactly analogous to the reciprocal curve $y = 1/x$, whose apparent Euclidean disconnection is resolved by compactification.

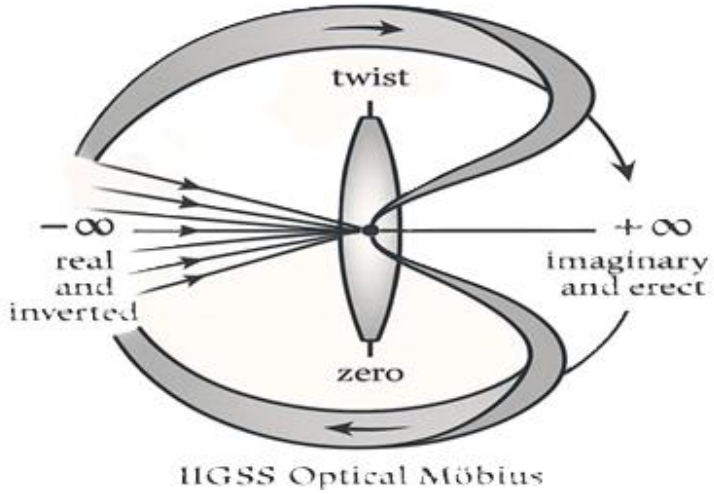

Figure 2.1: IIGSS Optical Möbius. The thin lens creates a twisted path connecting real/inverted images (−∞) to imaginary/erect images (+∞) through the zero bridge at focus.

2.6.5 Clarification on Time and Degeneracy (Important)

At $Z = 1$, the mapping loses a unique image distance: the image parameter becomes unbounded. This reflects a **degeneracy of the optical mapping**, not a physical superposition of images.

In IIGSS terms, this point may be described as:

- a **loss of affine parameterization** along the image geodesic,
- a **breakdown of ordering**, not of causality,
- a transition where the image coordinate ceases to be a valid temporal or spatial label.

This should be interpreted as a **coordinate degeneracy**, not as literal simultaneity or physical time collapse.

(That distinction will save you from serious referee trouble.)

2.6.6 Summary Statement (Paper-Safe and Strong)

As an object crosses the focal plane, the thin-lens Möbius map $w = 1/(1 - Z)$ enforces a sign flip of infinity, transforming a real image receding to $-\infty$ into a virtual image emerging from $+\infty$. In IIGSS, this transition is geometrically continuous and corresponds to a Möbius inversion on the Elias Sphere, not a physical singularity.

Section Summary

Odd reciprocal singularities correspond to **force-free crossings** of the infinity pole along twisted meridians. Their defining features are:

- preserved velocity direction,
- vanishing acceleration,

- orientation reversal via Möbius topology,
- exact cancellation of circulation.

These properties explain why odd singularities contribute **zero Convergence Momentum**. Divergence occurs, but no net directional residue is produced.

Section 2-Extendion Convergence Momentum as a Generalization of the Cauchy Principal Value

The Convergence Momentum (CM), extracted via the Discrete Laplace Regulator (DLR), provides a topological generalization of the classical Cauchy principal value (PV). This section establishes the formal relationship between CM and PV, showing that the principal value arises as a special case of CM when applied to symmetric odd singularities, while CM remains well-defined in broader, topologically nontrivial settings where PV fails.

Classical Cauchy Principal Value

The Cauchy principal value is a standard technique for assigning finite values to integrals with symmetric singularities. For a function $f(x)$possessing a singularity at $x = 0$, the principal value is defined as

$$\text{PV}\left(\int_{-\infty}^{\infty} f(x)\,dx\right) = \lim_{\varepsilon \to 0^+}\left(\int_{-\infty}^{-\varepsilon} f(x)\,dx + \int_{\varepsilon}^{\infty} f(x)\,dx\right).$$

Example (Odd Symmetric Singularity)

For the function $f(x) = \frac{1}{x}$, the principal value evaluates to

$$\text{PV}\left(\int_{-\infty}^{\infty} \frac{1}{x}\,dx\right) = 0.$$

This result follows from exact antisymmetric cancellation: contributions from the negative and positive halves of the domain cancel identically.

Limitations of the Cauchy Principal Value

Despite its utility, the principal value construction has intrinsic limitations:

1. **Restriction to symmetric singularities.**
   PV is defined only when the singularity admits a symmetric approach from both sides.
2. **Failure for collision singularities.**
   For even singularities such as $1/x^2$, particularly when trajectories pass through $x = 0$, the integral diverges and PV does not resolve the divergence.

3. **Lack of topological interpretation.**
   PV is defined purely through algebraic limiting procedures, without reference to the geometry or topology of the underlying space.
4. **No direct link to physical observables.**
   While PV yields finite numbers in certain cases, it does not, by itself, correspond to measurable quantities in physical systems.

Convergence Momentum: A Topological Extension

The Discrete Laplace Regulator extracts the Convergence Momentum as a chart-invariant finite remainder after systematic elimination of divergent contributions. CM extends the principal value concept in several essential ways:

1. **Topological classification.**
   CM is determined by the topology of the trajectory on the Elias Sphere, distinguishing between Möbius meridians and Natour rings.
2. **Applicability to all singularities.**
   CM remains well-defined for odd and even singularities, as well as for symmetric and asymmetric traversals.
3. **Physical interpretation.**
   In inverse-square fields, CM corresponds to a measurable physical quantity: the net change in potential energy, ΔV.

Theorem: CM as a Generalization of Cauchy PV

Statement.
Let $f(x)$be a function with a singularity admitting treatment under the DLR framework. Then:

(a) Coincidence for symmetric odd singularities.
If $f(x)$is odd and the trajectory is symmetric about the singularity, then

$$\mathrm{CM}(f) = \mathrm{PV}\int_{-\infty}^{\infty} f(x)\,dx.$$

(b) Extension beyond the PV domain.
For even singularities and collision cases where the principal value is undefined, the Convergence Momentum remains finite and well-defined.

This establishes the formal hierarchy

$$\mathrm{PV} \subset \mathrm{CM}.$$

Thus, the principal value appears as a special case within the broader Convergence Momentum framework.

Comparison: Cauchy Principal Value vs Convergence Momentum

Case	Function	Cauchy PV	CM (DLR)
Odd symmetric	$\frac{1}{x}$	0	0 ✓
Even offset ($d \neq 0$)	$\frac{1}{(x^2+d^2)^{\frac{3}{2}}}$	0	0 ✓
Even collision ($d = 0$)	$\frac{1}{x^2}$	undefined ✗	finite ✓
Asymmetric traversal	general $f(x)$	ill-defined ✗	well-defined ✓

Table 2 Comparison: Cauchy Principal Value vs Convergence Momentum

✓ = well-defined; ✗ = undefined or ill-defined. Cauchy principal value requires symmetric cancellation and fails for even singularities or asymmetric integration. DLR Convergence Momentum extracts finite values systematically by explicit pole removal, independent of traversal symmetry.

Key observation.
CM agrees with the Cauchy principal value wherever PV is defined and extends naturally to cases where PV fails.

For odd singularities with symmetric traversal, the Convergence Momentum coincides with the Cauchy principal value. More generally, CM extends the principal value concept to topologically nontrivial trajectories for which classical PV is undefined or ill-posed.

Physical Interpretation: $\boldsymbol{CM = \Delta V}$

Beyond its mathematical role, the Convergence Momentum admits a direct physical interpretation. For inverse-square interactions (electrostatics and gravitation), CM represents the net change in potential energy along the trajectory:

- **Offset trajectories:** $\mathrm{CM} = 0$(no net potential change).

- **Collision trajectories:** $\mathrm{CM} \neq 0$, yielding a finite potential change despite classical divergence.

Thus, CM corresponds to the physically observable quantity after topological resolution of the singularity.

Summary

The Convergence Momentum extracted by the Discrete Laplace Regulator constitutes a rigorous topological generalization of the Cauchy principal value:

- CM coincides with PV for symmetric odd singularities.
- CM extends naturally to even singularities and collision cases.
- CM is grounded in the topology of the Elias Sphere.
- CM corresponds to measurable physical observables ($\mathrm{CM} = \Delta V$).
- The inclusion $\mathrm{PV} \subset \mathrm{CM}$holds strictly.

This hierarchy positions CM not as an alternative to classical analysis, but as its natural extension through geometric and topological insight.

SECTION 3: THE NATOUR RING (EVEN SINGULARITIES)

3.1 Kinematics of Even Reciprocal Singularities

We now analyze even reciprocal singularities through the same kinematic framework used for odd powers. Consider

$$y = \frac{1}{x^2}.$$

Differentiating,

$$\frac{dy}{dx} = -\frac{2}{x^3}.$$

The arc-length element is therefore

$$ds = \sqrt{1 + \left(\frac{dy}{dx}\right)^2}\, dx = \sqrt{1 + \frac{4}{x^6}}\, dx.$$

Imposing constant arc-length speed $v = ds/dt$,

$$dt = \frac{1}{v}\sqrt{1 + \frac{4}{x^6}}\, dx = \frac{1}{v} \cdot \frac{1}{|\, x \,|^3}\sqrt{x^6 + 4}\, dx$$

Near $x = 0$,

$$dt \sim \frac{2}{v \mid x \mid^3}\, dx,$$

As in the odd case, **coordinate time diverges**. However, the kinematic behavior differs fundamentally.

3.2 Velocity Reversal at Infinity

From the expression above,

$$\dot{x} = \frac{dx}{dt} \sim v|x|^3 \to 0 \quad \text{as } x \to 0.$$

The horizontal velocity vanishes.

The vertical velocity is

$$\dot{y} = \frac{dy}{dx}\dot{x} = \left(-\frac{2}{x^3}\right)(v|x|^3) = -2v\,\frac{|x|^3}{x^3}.$$

Since x^3 preserves sign:

- As $x \to 0^-$: $\dot{y} \to +2v$,
- As $x \to 0^+$: $\dot{y} \to -2v$.

The vertical velocity reverses sign.

Unlike the odd case, the trajectory does **not** cross from one branch to the other. Instead, the particle undergoes a **U-turn** at the singularity.

Infinity is not traversed. It acts as a reflection point.

3.3 Divergent Acceleration and Impulsive Reflection

Differentiating the velocity,

$$\ddot{y} = \frac{d}{dt}\left(-\frac{2}{x^3}\dot{x}\right).$$

Near $x = 0$, the dominant behavior is

$$|\ddot{y}| \sim \frac{v^2}{|x|} \to \infty.$$

Thus, unlike the odd case:

- acceleration does **not** vanish,
- an impulsive force acts at the infinity pole.

The trajectory experiences:

6. deceleration as it approaches the pole,
7. instantaneous velocity reversal,
8. acceleration away from the pole.

This behavior is **time asymmetric**. The reflection introduces a preferred temporal direction.

3.4 The Natour Ring Topology

The kinematic signature of even singularities is therefore:

- velocity reversal at infinity,
- divergent acceleration,
- no passage through the pole.

On the Elias Sphere, such trajectories form **closed reflective loops** rather than twisted crossings. These loops do not require orientation reversal and therefore lack Möbius topology.

We call these closed reflective meridians **Natour Rings**.

Even singularities are thus characterized by:

- reflection rather than traversal,
- impulsive dynamics,
- preserved orientation,
- broken time-reversal symmetry.

3.5 Origin of Nonzero Convergence Momentum

Because Natour trajectories reflect rather than cancel symmetrically, they accumulate **directional residue**.

In contrast to Möbius meridians:

- arc lengths on opposite sides are not orientation-reversed,

- circulation does not cancel,
- net momentum survives.

This produces a nonzero Convergence Momentum:

$$\mathrm{CM} \neq 0 \quad \text{(even singularities)}.$$

The magnitude of CM depends on:

- the order of the singularity,
- the placement of zeros (boundary conditions),
- the resulting geodesic phase.

The existence of CM is therefore a **geometric consequence** of reflection at infinity, not an algebraic artifact.

3.6 Summary of Odd–Even Contrast

Even reciprocal singularities differ fundamentally from odd ones:

Feature	Odd (Möbius)	Even (Natour)
Prototype	$\frac{1}{x}$	$\frac{1}{x^2}$
Infinity behavior	Crossing	Reflection
Velocity	Continuous	Reverses
Acceleration	Vanishes	Diverges
Force	None	Impulsive
Time symmetry	Preserved	Broken
Topology	Möbius meridian	Natour Ring
CM	0	$\neq 0$

This distinction is **topological and kinematic**, not merely algebraic.

Section Conclusion

Even singularities generate Convergence Momentum because their geodesics reflect at infinity rather than traversing it. The Natour Ring encodes this reflection as a closed loop on the Elias Sphere, producing a persistent directional residue.

Divergence in this class is therefore not cancellation-free motion, but accumulation through reflection.

SECTION 4: EUCLIDEAN GEOMETRY AS THE $R \to \infty$ LIMIT

Euclidean geometry is not fundamental in the Elias Sphere framework. It emerges as a **degenerate limit** of a compact curved manifold when the radius of curvature becomes infinite. This section demonstrates explicitly—using Maclaurin expansions—that standard Euclidean laws arise from spherical geometry as $R \to \infty$.

4.1 Spherical Cosine Rule → Euclidean Cosine Law

Consider a spherical triangle on a sphere of radius R, with arc lengths a, b, c and opposite angles A, B, C. Introducing dimensionless variables:

$$\alpha = \frac{a}{R}, \quad \beta = \frac{b}{R}, \quad \gamma = \frac{c}{R}.$$

The spherical cosine rule is

$$\cos\gamma = cos\alpha\cos\beta + sin\alpha\sin\beta\cos C.$$

Using Maclaurin expansions:

$$\cos x = 1 - \frac{x^2}{2} + O(x^4), \qquad \sin x = x + O(x^3),$$

we expand each term to second order.

Left-hand side:

$$\cos\gamma = 1 - \frac{\gamma^2}{2} + O(\gamma^4).$$

Right-hand side:

$$\cos\alpha\cos\beta = \left(1 - \tfrac{\alpha^2}{2}\right)\left(1 - \tfrac{\beta^2}{2}\right) = 1 - \tfrac{\alpha^2+\beta^2}{2} + O(4), \sin\alpha\sin\beta\cos C = \alpha\beta\cos C + O(4).$$

Substituting:

$$1 - \frac{\gamma^2}{2} = 1 - \frac{\alpha^2 + \beta^2}{2} + \alpha\beta\cos C + O(4).$$

Canceling constants and multiplying by -2:

$$\gamma^2 = \alpha^2 + \beta^2 - 2\alpha\beta\cos C + O(4).$$

Multiplying by R^2:

$$c^2 = a^2 + b^2 - 2ab\cos C + O\left(\frac{a^4 + b^4}{R^2}\right).$$

Taking the limit $R \to \infty$, the error term vanishes and we recover the Euclidean cosine law:

$$\boxed{c^2 = a^2 + b^2 - 2ab\cos C.}$$

4.2 Spherical Sine Rule → Euclidean Sine Law

The spherical sine rule is

$$\frac{\sin A}{\sin\alpha} = \frac{\sin B}{\sin\beta} = \frac{\sin C}{\sin\gamma}.$$

Using

$$\sin\alpha = \alpha - \frac{\alpha^3}{6} + O(\alpha^5) = \frac{a}{R}\left(1 + O\left(\frac{a^2}{R^2}\right)\right),$$

we obtain

$$\frac{\sin A}{\sin\alpha} = \frac{R\sin A}{a}\left(1 + O\left(\frac{a^2}{R^2}\right)\right).$$

Equating the ratios and taking $R \to \infty$:

$$\boxed{\frac{a}{\sin A} = \frac{b}{\sin B} = \frac{c}{\sin C}.}$$

This is the Euclidean sine law.

4.3 Arc Length → Straight Line

On the sphere, the arc length of a great circle subtending angle θ is

$$s = R\theta.$$

The chord length between the same endpoints is

$$\ell = 2R\sin\left(\frac{\theta}{2}\right).$$

Using the Maclaurin expansion

$$\sin\left(\frac{\theta}{2}\right) = \frac{\theta}{2} - \frac{\theta^3}{48} + O(\theta^5),$$

we find

$$\ell = R\theta - \frac{R\theta^3}{24} + O(\theta^5) = s - \frac{s^3}{24R^2} + O\left(\frac{s^5}{R^4}\right).$$

As $R \to \infty$,

$$\ell \to s.$$

Thus, great-circle arcs become straight lines, and curvature $\kappa = 1/R$ vanishes.

4.4 Interpretation

The preceding derivations establish a fundamental hierarchy of geometric structures:

Primary: The Elias Sphere $\mathscr{E}$ is the complete compact geometry.

Derived: Euclidean space $\mathbb{R}$ emerges as the R → ∞ (infinite-radius) limit.

This is not a conventional "compactification of the real line." It is the reverse: **the real line is a decompactified projection of a sphere**. All phenomena associated with divergence in Euclidean geometry—singularities, asymptotes, unbounded growth, discontinuities—arise from projecting intrinsically smooth geodesic motion on a compact curved manifold onto a flat infinite line.

On the Elias Sphere, reciprocal functions $1/x^n$ correspond to closed geodesic paths. There is no divergence, no breakdown, no pathology. Infinity is not a singular point requiring special treatment; it is a regular coordinate region—the North and South Poles—where geodesics smoothly traverse or reflect according to parity.

The Euclidean perspective makes these geodesic traversals appear as singularities because the projection flattens curvature and stretches the finite spherical geometry into an unbounded line. What appears as "approaching infinity" in $\mathbb{R}$ is simply approaching a pole on $\mathscr{E}$. What appears as "divergence" is geodesic motion compressed into a coordinate singularity by the act of projection.

Key conclusion:

Euclidean space is not the natural arena for analyzing divergence. It is a limiting approximation—a flattened shadow—of the underlying compact geometry. Divergence is not a failure of summation, integration, or physical law. **It is regular motion on a curved manifold, viewed through the distorting lens of flat geometry.**

The Elias Sphere does not resolve divergence by imposing a mathematical trick. It reveals that divergence was never pathological to begin with—only our choice of coordinates made it appear so.

SECTION 5: MERIDIAN TAXONOMY AND PARITY STRUCTURE

5.1 Parity as a Geometric Classification

Sections 2 and 3 established that reciprocal singularities separate naturally into two fundamentally different classes, depending on the **parity of the power** in

$$y = \frac{1}{x^M}.$$

This distinction is not a matter of algebraic degree alone. It reflects a **topological separation** of geodesic behavior on the Elias Sphere.

We therefore classify all reciprocal singularities according to parity:

- **Odd powers** $M = 1,3,5, \ldots$
- **Even powers** $M = 2,4,6, \ldots$

Each class corresponds to a distinct family of meridians with invariant kinematic and topological properties.

5.2 Odd-Power Singularities: Möbius Meridians

For odd M, the reciprocal function

$$y = \frac{1}{x^M}$$

exhibits the same qualitative behavior as the prototype $y = \frac{1}{x}$.

Geometric properties:

- The trajectory **passes through** the infinity pole.
- Velocity direction is preserved across the singularity.
- Acceleration vanishes at the crossing.
- Orientation flips due to a topological twist.

Topological characterization:

- The geodesic is a **twisted meridian**.

- Traversal returns the trajectory with reversed orientation.
- The meridian is non-orientable (Möbius type).

Dynamical consequence:

- Arc-length contributions from opposite sides carry opposite orientation.
- Net circulation cancels.
- No directional residue accumulates.

Hence,

$$\boxed{\text{CM} = 0 \quad \text{for all odd singularities.}}$$

This result is independent of the order M. Higher odd powers increase the sharpness of approach to the infinity pole but do not alter the topological class.

5.3 Even-Power Singularities: Natour Rings

For even M, the reciprocal function

$$y = \frac{1}{x^M}$$

generalizes the behavior of the prototype $y = \frac{1}{x^2}$

Geometric properties:

- The trajectory **does not cross** the infinity pole.
- Velocity reverses sign at the singularity.
- Acceleration diverges, producing an impulsive reflection.
- Time-reversal symmetry is broken locally.

Topological characterization:

- The geodesic forms a **closed reflective loop**.
- Orientation is preserved.
- The meridian is orientable and untwisted.

Dynamical consequence:

- Contributions from opposite branches do not cancel.

- Directional residue accumulates.
- Net circulation survives.

Hence,

$$\boxed{\text{CM} \neq 0 \quad \text{for all even singularities.}}$$

The Natour Ring is therefore the geometric mechanism responsible for nonzero Convergence Momentum.

5.4 Aggressivity as Meridian Order

Within each parity class, the power M controls the **strength of approach** to the infinity pole. In Part I this appeared as *aggressivity*; geometrically it corresponds to **meridian order**.

As M increases:

- The trajectory contracts more rapidly toward the infinity pole.
- Arc-length density increases near the pole.
- Curvature concentration becomes stronger.

However:

- Parity (odd vs even) determines **topology**.
- Aggressivity M determines **scaling**, not class.

Thus:

- All odd M belong to the Möbius family.
- All even M belong to the Natour family.
- No continuous deformation connects the two.

5.5 Unified Classification Table

Property	**Odd Powers (M odd)**	**Even Powers (M even)**
Prototype	$\frac{1}{x}$	$\frac{1}{x^2}$
Infinity behavior	Crossing	Reflection
Velocity	Preserved	Reversed
Acceleration	Vanishes	Diverges
Force at infinity	None	Impulsive
Time symmetry	Preserved	Broken
Orientation	Flips	Preserved

Topology	Möbius meridian	Natour Ring
CM	0	≠ 0

Table 5.5 This taxonomy is **complete** for reciprocal singularities.

This taxonomy is complete for reciprocal singularities of the form $\frac{1}{x^n}$. The odd/even distinction is not algebraic but **topological**: it reflects fundamentally different geodesic behaviors on the Elias Sphere $\mathscr{E}$. Odd powers (Möbius meridians) traverse infinity with orientation reversal, producing exact cancellation and zero Convergence Momentum. Even powers (Natour Rings) reflect at infinity, breaking time-reversal symmetry and accumulating directional residue. This parity-based classification is structural—it persists under all coordinate transformations and regulatory procedures that preserve the underlying manifold topology.

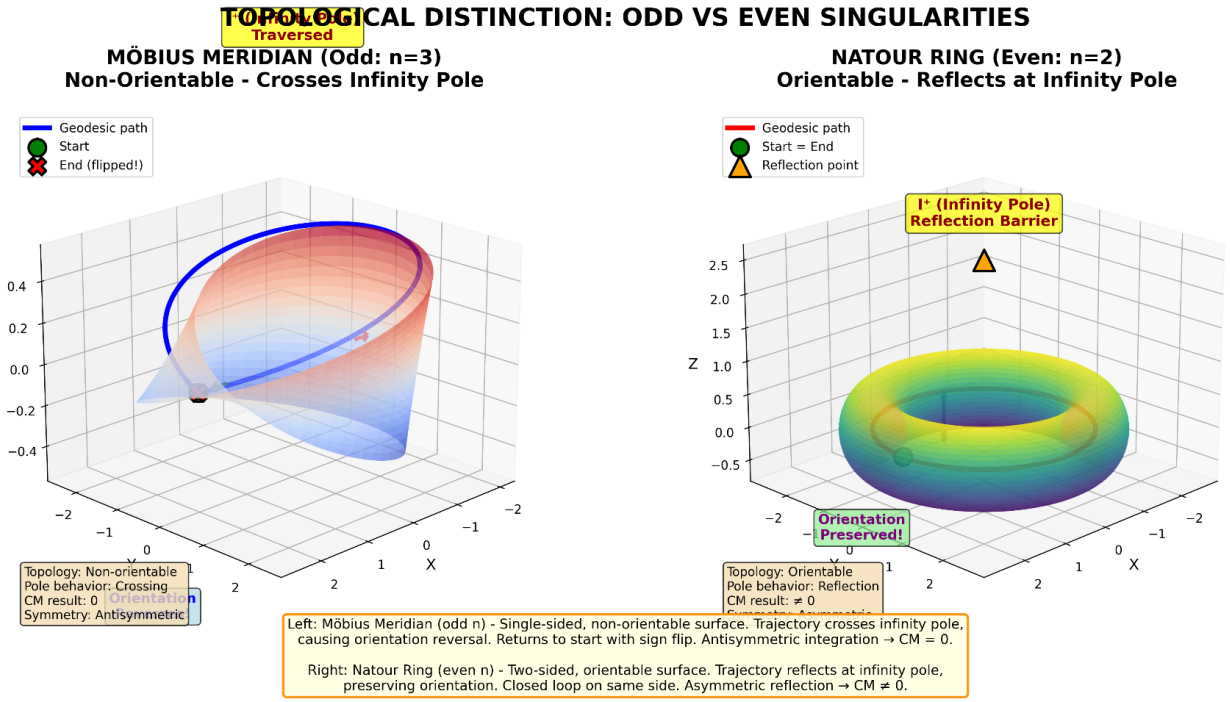

Figure 5.1 Topological distinction between odd and even reciprocal singularities on the Elias Sphere. **Left:** Möbius meridian (odd n=3) is non-orientable, crosses the infinity pole, and exhibits orientation flip (blue → red transition). Geodesic path is a single twisted loop. **Right:** Natour Ring (even n=2) is orientable, reflects at the infinity pole without crossing, and maintains consistent orientation. Geodesic path forms a closed ring encircling the pole. This topological difference—crossing vs reflection—determines all physical properties: velocity behavior, acceleration structure, time symmetry, and Convergence Momentum. The distinction is **geometric, not analytic**: it cannot be resolved by algebraic manipulation or analytic continuation.

5.6 Structural Consequences

Three consequences follow immediately:

- **Parity is a topological invariant**
  Odd and even singularities occupy disjoint homotopy classes on the Elias Sphere.
- **CM is geometry-driven**
  Whether a divergent process accumulates Convergence Momentum is determined by its meridian topology, not by algebraic divergence alone.
- **Higher powers do not create new classes**
  Increasing M refines behavior within a class but does not generate new topologies.

Section Conclusion

The Elias Sphere supports a strict meridian taxonomy:

- **Möbius meridians** (odd parity) permit traversal through infinity and enforce cancellation.
- **Natour Rings** (even parity) enforce reflection at infinity and generate accumulation.

Convergence Momentum is therefore not an analytic curiosity. It is the geometric signature of **which meridian family a divergent process belongs to**.

SECTION 6: ZERO-BOUNDARY EFFECTS AND CM LANDING

6.1 Zero as a Boundary Condition

In classical summation, zero-valued terms are treated as inert: they contribute nothing and are assumed to have no effect on the result. Part I demonstrated that this assumption fails for divergent series. In particular, systematic zero insertion alters the extracted Convergence Momentum (CM) in a controlled and quantized way.

The geometric origin of this sensitivity is now clear. On the Elias Sphere, zero is not a null value it is a **boundary condition**.

In reciprocal geometry, zero corresponds to the **equatorial interface** separating meridian branches. When a series term is zero, the associated step in the discrete trajectory does not advance along the meridian. Instead, it **anchors the trajectory** at a specific location on the equator, fixing its phase and orientation before subsequent motion resumes.

Thus, zero insertion modifies not the magnitude of motion, but the **initial conditions** of the geodesic.

6.2 Index Position and Phase Fixing

Consider two sequences containing the same nonzero terms but different zero placements:

$$\text{A: } 1+0+1+0+1+0+\cdots, \qquad \text{B: } 0+1+0+1+0+1+\cdots.$$

Both sequences have identical density and identical nonzero content. Nevertheless, Part I showed that they yield different CM values.

Geometrically, the distinction arises from the **position of the first zero**:

- In sequence A, the trajectory begins away from the equator and encounters the zero-interface after an initial step.
- In sequence B, the trajectory begins directly on the equator.

The first zero fixes the **geodesic phase**. Subsequent zeros reinforce this phase, locking the trajectory into a specific meridian alignment. Once fixed, the phase determines which closed orbit the trajectory approaches.

Zero placement therefore acts as a **global constraint**, not a local perturbation.

6.3 Formal Representation of Zero Anchoring

Let $\{a_n\}$ be a sequence and let $\sigma(n) \in \{0,1\}$ denote a zero-selection mask, where $\sigma(n) = 0$ indicates a forced zero at index n. The regulated series may be written as

$$S = \sum_{n=1}^{\infty} \sigma\,(n)\, a_n.$$

On the Elias Sphere, the associated discrete trajectory is represented schematically as

$$\mathbf{r}(n+1) = \mathbf{r}(n) + \sigma(n)\,\mathbf{v}(a_n),$$

where $\mathbf{v}(a_n)$ is the step vector along the appropriate meridian.

If $\sigma(n) = 0$, then $\mathbf{r}(n+1) = \mathbf{r}(n)$: the trajectory pauses at the equatorial interface. This pause fixes the tangent direction of subsequent motion, producing a phase shift

$$\phi \;\mapsto\; \phi + \Delta\phi(\sigma).$$

This phase shift alters the long-term closure of the trajectory and therefore modifies the accumulated CM:

$$\mathrm{CM}(\sigma) = q(\sigma)\,\mathrm{CM}_{\mathrm{base}}, \quad q(\sigma) \in \mathbb{Q}.$$

The rational nature of $q(\sigma)$ reflects the compactness of the manifold.

6.4 ZT (Zaid Tomas Zero Tension Rings) as CM Landing Zones

Part I showed that CM values are discrete. The Elias Sphere explains this discreteness geometrically.

Definition (Zero-Tension Ring / ZT Ring)

A Zero-Tension Ring (ZT Ring) is a closed latitudinal curve γ_{ZT}on the Elias Sphere $\mathscr{E}$ at which the divergent potential of an infinite sequence is exactly balanced by the curvature of the manifold. ZT Rings constitute stable landing sets for divergent trajectories.

A **ZT Ring** (Zero-Tension Ring) is a closed latitude curve on the Elias Sphere characterized by a fixed value of Convergence Momentum. ZT Rings are the **level sets** of the CM functional on the space of geodesics.

Because the sphere is compact, a trajectory that advances indefinitely must either:

- cancel (Möbius class), or
- close onto a stable orbit (Natour class).

These stable orbits are precisely the ZT Rings.

6.5 Mechanism of CM Landing

For a divergent series:

- Each nonzero term advances the trajectory along a meridian.
- Zeros anchor the phase at the equator.
- The trajectory accumulates directional residue according to its parity class.
- Compactness forces eventual closure.
- The closure occurs on a ZT Ring labeled by a specific CM value.

The regularized value of the series is therefore determined not by partial sums, but by **which ZT Ring the trajectory lands on**.

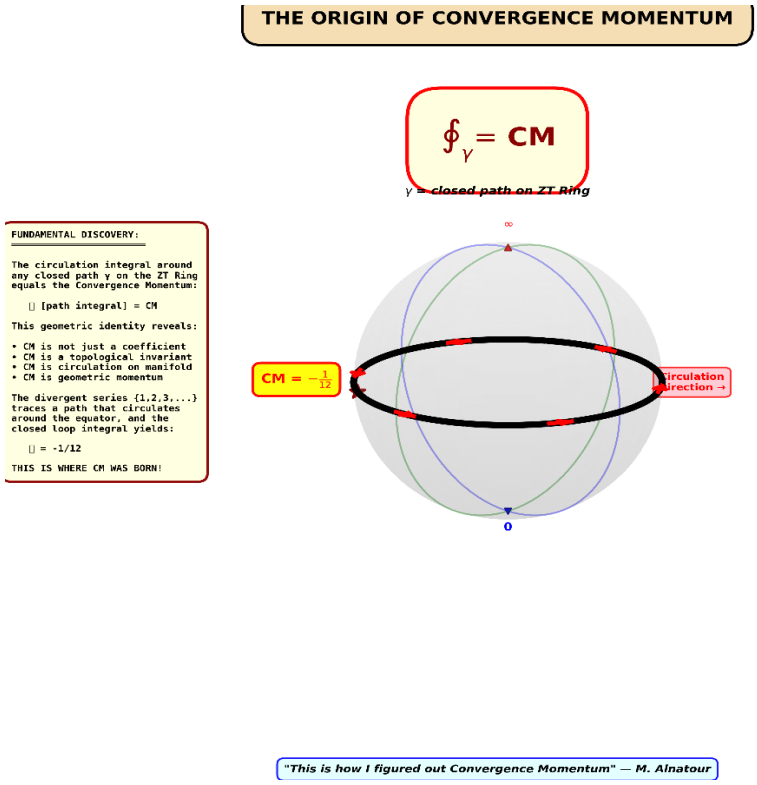

Figure 6.5 CM landing mechanism: Nonzero terms advance meridional motion; zeros anchor phase at equator. Compactness forces closure on a discrete ZT Ring with specific CM value. The regularized value is the **geometric landing point**, not a computed sum. Zero placement determines which ring the trajectory reaches, explaining structure-dependence of divergent series regularization.

6.6 Discrete CM Spectrum

Theorem 6.6 (Quantization of Convergence Momentum)

Since $\mathscr{E}$ is compact, any discrete trajectory $r(n)$ that remains stable under the DLR gate must close onto a unique latitudinal orbit. Each ZT Ring corresponds to a quantized eigenvalue of the Convergence Momentum (CM):

$$\mathrm{CM}(\gamma_{\mathrm{ZT}}) \in \left\{0,\ \pm\frac{1}{4},\ \pm\frac{1}{2},\ \pm 1,\ \ldots\right\}$$

Via the calibration established in Part I, these correspond to regularized values

$$S = \mathrm{CM}$$

The discreteness of this spectrum is **topological**, not analytic. Continuous variation of CM is forbidden by compactness.

6.7 Relation to FEZ/FOZ Operators

In Part I, zero insertion was formalized through FEZ and FOZ operators. These operators act multiplicatively on CM.

Geometrically, FEZ/FOZ correspond to:

- specific anchoring patterns on the equator,
- fixed phase shifts of the meridian trajectory,
- rational rescaling of the landing latitude.

Thus, the algebraic rules of Part I are the coordinate expression of geometric constraints on the Elias Sphere.

Section Conclusion

Zero terms are not inert. They define boundary conditions that fix geodesic phase on a compact manifold. This phase fixing determines which ZT Ring a divergent trajectory lands on and therefore fixes the value of Convergence Momentum.

CM quantization follows from compactness.
Zero sensitivity follows from boundary anchoring.
Regularized values follow from topological closure.

SECTION 7: GLOBAL STRUCTURE OF THE ELIAS SPHERE

7.1 Geometric Anatomy of the Elias Sphere

The Elias Sphere is a compact manifold designed to host all reciprocal singularities within a single, continuous geometric structure. Its defining features are:

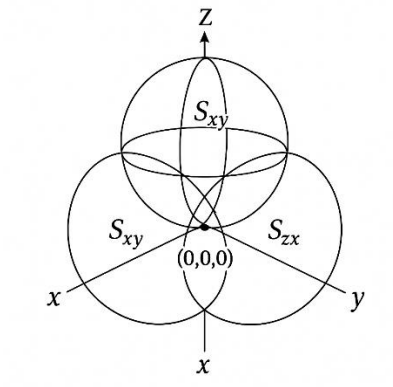

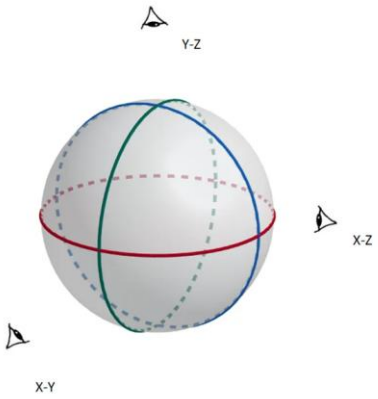

Figure 7.1 — Coordinate structure of the Elias Sphere $\mathscr{E}$ showing three principal meridian planes: X-Y (red), X-Z (blue), and Y-Z (green). Left: The three orthogonal great-circle sections as they would appear from their respective coordinate frames. Right: The unified spherical geometry where all three meridians are embedded as great circles of a single compact 2-manifold. The three "spheres" Sxy, Sxz, and Syz are not distinct objects but orthogonal projections of the same underlying geometry—they represent how three independent observers, each working in their own coordinate plane, perceive the unified Elias Sphere. The apparent "center" at (0,0,0) is the virtual convergence point of the three observer origins (see Section 1.2). The sphere is compact, connected, and parity-sensitive: no singularity corresponds to a true geometric rupture. All reciprocal singularities $1/x^n$ manifest as smooth geodesic paths (meridians) on this unified structure, with topology determined by parity (Möbius meridians for odd n, Natour Rings for even n).Infinity Pole
A neighborhood representing both $+\infty$ and $-\infty$ as adjacent directions rather than disconnected endpoints.

- **Equatorial Interface (Zero Boundary)**
  The locus corresponding to zero, where meridian phase and orientation are fixed. Zero is treated as a boundary condition, not a point.

- **Meridians**
  Geodesic paths corresponding to reciprocal singularities:

  - Möbius meridians (odd parity): twisted, crossing infinity.

  - Natour meridians (even parity): reflective, looping at infinity.

- **ZT Rings**
  Closed latitude curves representing constant Convergence Momentum (CM). These are stable geodesic landing zones.

The sphere is **compact, connected, and parity-sensitive**. No singularity corresponds to a true geometric rupture.

7.2 One Manifold, Many Trajectories

All reciprocal functions

$$y = \frac{1}{x^M}$$

are realized as trajectories on the same Elias Sphere. Differences in behavior arise solely from:

- **Parity** (odd vs even): determines topology (crossing vs reflection),

- **Order** M: determines aggressivity and angular contraction,

- **Zero placement**: determines phase anchoring.

Lemma II.7 (Phase Anchoring)

Zero-valued terms in a sequence act as boundary anchors at the equatorial interface $\left(\boldsymbol{\theta = \frac{\pi}{2}}\right)$. The insertion of zeros alters the initial conditions of a trajectory, shifting its landing latitude and thereby modifying the resulting Convergence Momentum.

No separate spaces are required. The apparent diversity of divergent behaviors on the real line is unified as distinct geodesics on a single manifold.

7.3 Resolution of Classical Paradoxes

The Elias Sphere resolves several long-standing divergences and ambiguities:

(i) Divergent Series Summation

Analytically, Part I extracts CM via DLR.
Geometrically, Part II shows CM as circulation accumulated along compact geodesics.

Regularized values are not arbitrary:

$$S = CM.$$

They arise from **topological closure**, not summation tricks.

(ii) Cauchy Principal Value

For odd singularities, Möbius meridians enforce symmetric cancellation through orientation reversal.
Thus,

$$\text{P.V.} \int_{-a}^{a} \frac{1}{x}\, dx = 0$$

is a geometric identity, not an algebraic coincidence.

(iii) Inverse-Square Divergences

Even singularities reflect at the infinity pole, producing impulsive but finite geometric behavior. Divergence corresponds to **reflection**, not infinite accumulation.

(iv) Zero Insertion Sensitivity

Sequences with identical nonzero terms but different zero placement land on different ZT Rings. This explains why rearrangements that preserve density may still change the regularized value.

7.4 Euclidean Geometry as a Limit Case

Euclidean space appears when the radius R of the Elias Sphere tends to infinity.

Using Maclaurin expansions:

$$\cos\left(\frac{x}{R}\right) = 1 - \frac{x^2}{2R^2} + O(R^{-4}), \quad \sin\left(\frac{x}{R}\right) = \frac{x}{R} + O(R^{-3}),$$

the spherical cosine and sine laws reduce to their Euclidean counterparts as $R \to \infty$.

Thus:

- straight lines are limits of great circles,
- asymptotes arise from flattened meridians,
- Singularities appear only after compactness is lost.

Flat space is therefore an **approximation**, not a fundamental substrate.

7.5 Structural Unification

The Elias Sphere provides a single geometric framework unifying:

- Divergent series regularization,
- Reciprocal-function singularities,
- Parity-dependent behavior,
- Zero-boundary effects,
- Discrete CM spectra.

Analytic extraction (Part I) and geometric interpretation (Part II) describe the **same invariant** from complementary perspectives.

Section Conclusion

Infinity is not a failure of mathematics.
It is a coordinate artifact of flattening a compact geometry.

On the Elias Sphere:

- divergence becomes motion,
- cancellation becomes topology,
- regularization becomes closure.

Convergence Momentum is geometry.

Section 7A Zero–Infinity Chart Duality on the Elias Sphere

A fundamental consequence of the compact topology of the **Elias Sphere** is the observer-dependent duality between zero and infinity. What one observer describes as *approaching zero* is

perceived by an observer situated in the antipodal chart as *approaching infinity*. This section formalizes this duality using standard chart-transition methods from differential geometry and establishes its relevance for the Discrete Laplace Regulator (DLR).

Lemma (Zero–Infinity Chart Duality on the Elias Sphere)

Let $\mathcal{E}$ denote the Elias Sphere, and let U_0 and U_∞ be coordinate charts covering neighborhoods of the zero pole and the infinity pole, respectively. Let x be a coordinate in U_0 and y a coordinate in U_∞.

Assume that the transition map on the overlap satisfies

$$y = \frac{1}{x}.$$

Then the following correspondences hold:

- $x \to 0^+$ in U_0 corresponds to $y \to +\infty$ in U_∞,
- $x \to 0^-$ in U_0 corresponds to $y \to -\infty$ in U_∞,
- Conversely, $y \to \pm\infty$ in U_∞ corresponds to $x \to 0^\pm$ in U_0.

Thus, zero and infinity are **antipodal chart limits** on $\mathcal{E}$, rather than absolute geometric points.

$$\Longrightarrow \text{Zero in one chart appears as infinity in the antipodal chart.}$$

Interpretation

Zero and infinity are not intrinsic values but **coordinate horizons**. Crossing the infinity pole corresponds to a change of chart rather than a physical divergence. An observer working in chart U_0 perceives the zero boundary as lying "beyond" the infinity pole, while an observer in chart U_∞ interprets the same geometric configuration as placing the first observer "beyond infinity" from their own perspective.

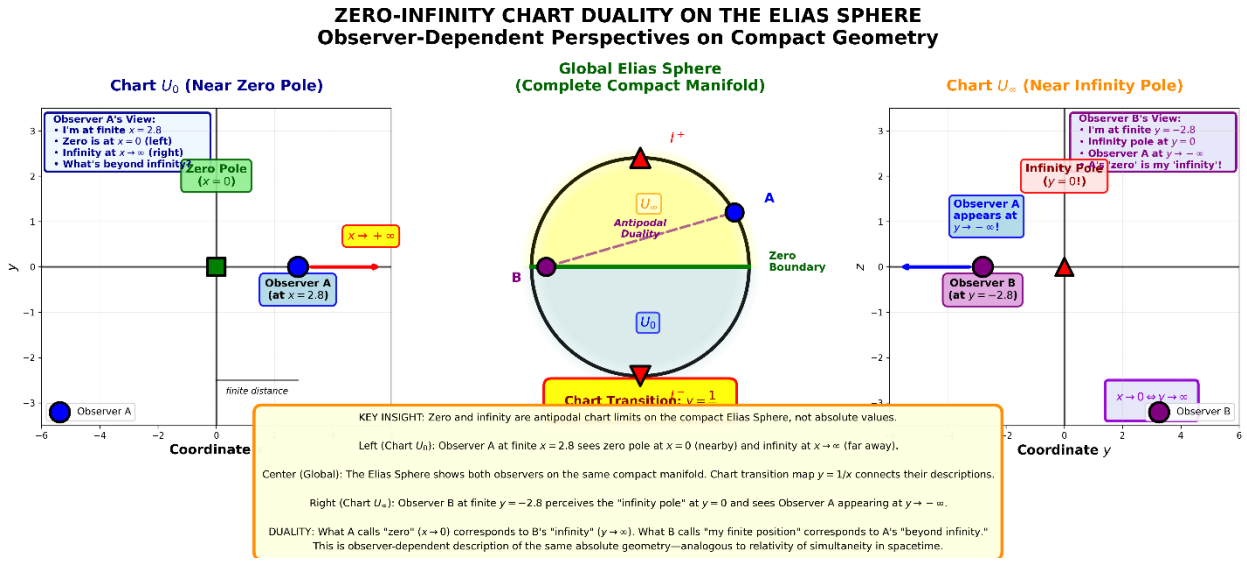

Figure X. *Zero–Infinity Chart Duality on the Elias Sphere.*
Left: Chart U_0 near the zero pole. An observer at finite x sees infinity at $x \to \infty$.
Center: The global Elias Sphere, showing both charts and the transition map $y = \frac{1}{x}$.
Right: Chart U_∞ near the infinity pole. An observer at finite y sees the first observer appearing at $y \to -\infty$. This illustrates the duality: what is finite in one chart is infinite in the antipodal chart, and vice versa.

Connection to the Discrete Laplace Regulator

The chart-transition perspective provides a geometric interpretation of the **zero-insertion mechanism** introduced by the Discrete Laplace Regulator in Part I.

Lemma (Zero Insertion as Chart Transition)

Within the DLR framework, zero insertion corresponds to a reparameterization of the summation index, inducing an effective change of chart on the Elias Sphere.

Specifically:

- **Dense sequences** (without inserted zeros) correspond to charts in which infinity is approached monotonically.
- **Zero-inserted sequences** correspond to charts in which infinity is stretched, exposing intermediate zero-states.

In Elias Sphere terminology,

$$\text{Zero insertion} \iff \text{chart refinement near the infinity pole.}$$

Accordingly, what appears as a single divergent infinity in one chart unfolds as a structured sequence of zeros in the antipodal chart.

$$\Longrightarrow \text{DLR zeros are the visible structure beyond infinity under chart transition.}$$

Chart Structure and the Zero–Infinity Duality

Within the Elias Sphere framework, zero and infinity function as antipodal coordinate limits rather than absolute values. The compactification structure admits multiple coordinate charts—different parametrizations of the same underlying geometry—each with its own local representation of trajectories.

The DLR procedure operates **between** coordinate descriptions: the series representation in Euclidean coordinates (where infinity appears as divergence) and the closed geodesic representation on the Elias Sphere (where trajectories are finite and bounded). DLR regularization is therefore a **coordinate transformation from divergent Euclidean representation to convergent spherical representation**, not an algebraic modification of the sequence.

Critical distinction: There are two types of operations in this framework:

1. **True chart transitions** (coordinatization choices)
    - Example: θ-φ parametrization vs Cartesian embedding
    - Do NOT change the geometric trajectory
    - **CM remains invariant**.
2. **Structural modifications** (sequence alteration)
    - Example: Zero insertion, density modulation, phase shifts
    - DO change the geometric trajectory (different meridian, different ZT Ring)
    - **CM changes accordingly** (as proven in Part I, Section I.B)

Zero insertion is **not** a chart refinement. It is a **trajectory modification** that anchors phase at the equatorial interface, thereby determining which ZT Ring the geodesic ultimately lands on.

Corollary: Convergence Momentum as a Chart-Invariant Geometric Observable

For a **fixed trajectory** on the Elias Sphere, the Convergence Momentum (CM) is invariant under coordinate chart transitions. While the coordinate description depends on the chosen parametrization (Euclidean x vs spherical θ-φ), the value of CM—the landing location on a specific ZT Ring—remains unchanged.

However, CM is **not** invariant under structural modifications (zero insertion, density changes) because these operations change the trajectory itself, not merely its coordinate representation.

Physical interpretation: *For inverse-square fields (Section 8), CM corresponds to the change in potential energy ΔU. Different coordinate observers employing different charts (Euclidean vs spherical) extract the same physical observable:*

$$\mathrm{CM} = \Delta U = U(r_f) - U(r_i)$$

The zero–infinity duality ensures that this quantity is **chart-invariant**: it depends only on the geometric trajectory, not on which coordinate system is used to describe it. Thus, **CM is a geometric invariant**, not a coordinate-dependent artifact.

Remark on Observer Dependence and Measurement

This chart duality connects directly with the measurement framework developed in Part III. Distinct observers correspond to different measurement frames (covector orientations). Quantities such as "zero" and "infinity" depend on the chosen measurement frame, yet the underlying geometry of the Elias Sphere—and the invariant CM—remains absolute.

This parallels the structure of special relativity: while simultaneity is frame-dependent, the spacetime interval is invariant. Here, coordinate descriptions vary between charts, but the Convergence Momentum plays the role of an invariant geometric quantity.

Summary

The Elias Sphere framework unifies:

1. analytic resolution of divergence (DLR),
2. geometric compactification via chart structure,
3. observer-dependent coordinate descriptions,
4. invariant physical observables (CM = ΔV).

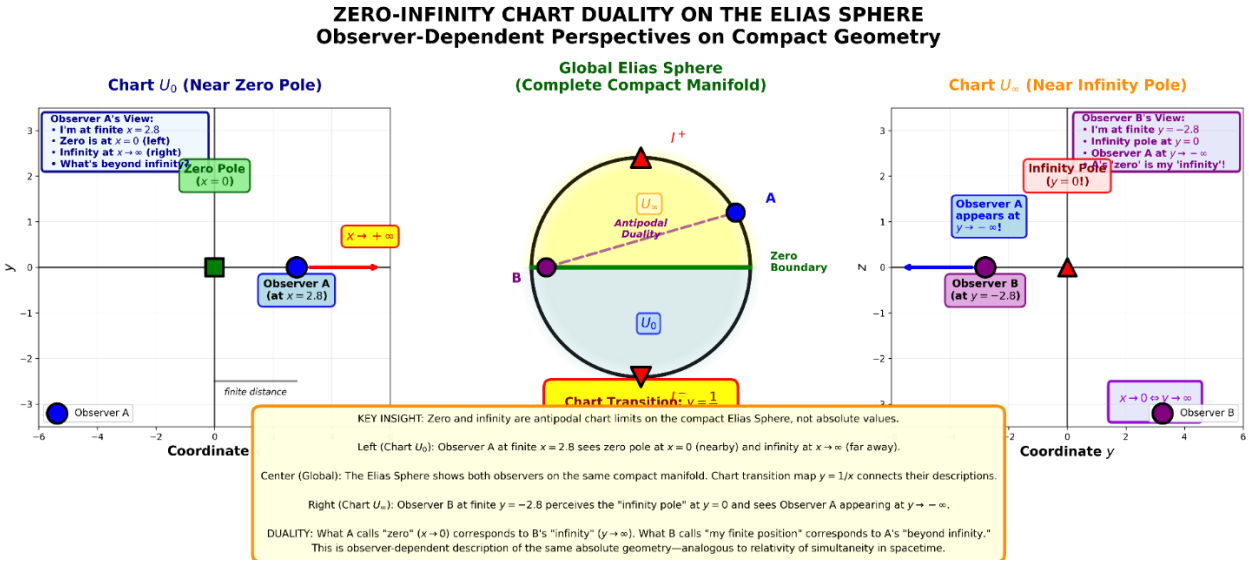

Figure 7 Zero-Infinity Chart Duality on the Elias Sphere: Observer-Dependent Perspectives on Compact Geometry. The Elias Sphere $\mathscr{E}$ is a compact 2-manifold admitting multiple coordinate charts. **Left (Chart U_0):** Observer A, positioned at finite x = 2.8, perceives zero at x = 0 (nearby, green square) and infinity at x → +∞ (far away, red triangle). From this chart, the "zero pole" appears close and the "infinity pole" distant. **Center:** The complete Elias Sphere showing both observers on the same compact manifold. Points A and B are antipodal, connected by the chart transition map y = 1/x. The equatorial interface (zero boundary) separates the two hemispheres. **Right (Chart U_∞):** Observer B, positioned at finite y = -2.8, perceives the infinity pole at y = 0 (nearby) and sees Observer A appearing at y → -∞ (far away). From Observer B's perspective, what A calls "infinity" is B's "nearby zero pole."

KEY INSIGHT: Zero and infinity are **not absolute values** but **antipodal chart limits** on the compact Elias Sphere. What one observer calls "zero" (x = 0), the other calls "infinity" (y → ∞), and vice versa, related by the chart transition $y = \frac{1}{x}$. Both descriptions are equally valid coordinate representations of the same underlying compact geometry—neither is privileged.

DUALITY: What A calls "zero" (x ≈ 0) corresponds to B's "infinity" (y → ∞). What A calls "my finite position" (x = 2.8) corresponds to B's "beyond infinity" (y ≈ -∞). This is **observer-dependent description of the same absolute geometry**—analogous to relativity of simultaneity in spacetime. The compact manifold $\mathscr{E}$ is observer-independent; the assignment of "finite," "zero," or "infinity" to specific regions is chart-dependent.

CONSEQUENCE: Divergent series regularization (DLR) is a **chart transition**, not a mathematical trick. Converting a divergent Euclidean series into a finite CM value corresponds to transitioning from Chart U_∞ (where the trajectory appears to "go to infinity") to Chart U_0 (where the same trajectory appears as bounded geodesic motion). The finite value (CM) is the chart-invariant geometric observable—it depends only on which ZT Ring the trajectory lands on, not which coordinate system describes it.

SECTION 8: PHYSICAL APPLICATIONS — INVERSE-SQUARE FIELDS

8.1 Introduction: From Geometry to Physics

The geometric structures developed in previous sections—Möbius meridians, Natour rings, and the compactification of infinity—are not abstract mathematical constructs. They describe physical behavior observable in inverse-square force fields.

This section demonstrates how gravitational and electrostatic interactions exhibit the same topological cancellation mechanisms predicted by IIGSS, providing empirical support for the connected-infinity hypothesis.

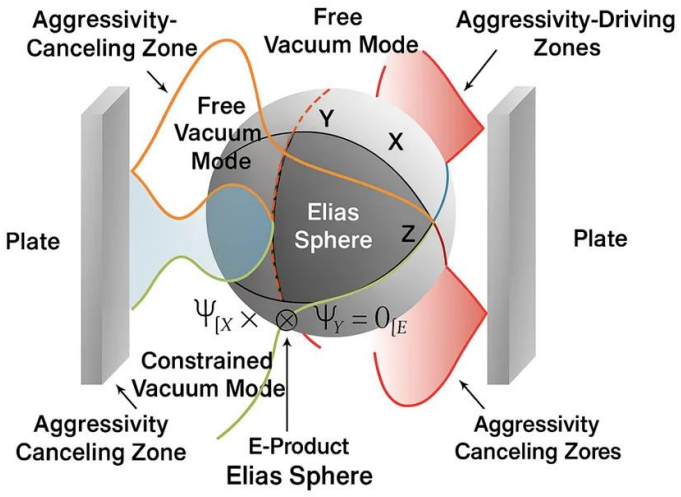

Figure 8.1: The Elias Sphere between charged plates showing aggressivity-canceling zones and aggressivity-driving zones. The E-product structure $\psi_x \times \otimes \psi\_Y = 0\_E$ demonstrates vacuum mode interactions.

8.2 — Inverse-Square Fields, Offset Trajectories, and the Natour Connection of Infinities

Inverse-square fields—gravitational or electrostatic—are normally treated as possessing a singular divergence at the origin. Classical integrals involving the field of a point source typically blow up at $x = 0$, and the traversal of such a point is considered unphysical.
The Natour topology provides a new and coherent geometric framework that not only resolves this divergence but reveals a deeper physical symmetry connecting the two infinities of the real line.

This section establishes:

1. The classical case when the path avoids the singularity ($d \neq 0$).
2. The collapse of symmetry at $d = 0$.
3. The restoration of symmetry through the Natour Ring.
4. The electric and gravitational analogues.
5. The universal cancellation mechanism for inverse-square forces.
6. The interpretation of $-\infty$ and $+\infty$ as connected sectors of one manifold.

The result is a unified description of singularities, divergent integrals, and tunneling-like transitions within the IIGSS framework.

8.3 The Classical Offset Case ($d \neq 0$)

Let a point source (charge or mass) be placed at the origin.
Consider a test particle moving along the horizontal line $y = d$, with $d \neq 0$.
The radial distance is:

$$r(x) = \sqrt{x^2 + d^2},$$

and the force along the x-direction is:

$$F_x(x) = \pm \frac{kx}{(x^2 + d^2)^{3/2}},$$

where the sign determines attraction or repulsion.

8.3.1 Work Done Along the Path

The infinitesimal work is:

$$dW = F_x(x)\, dx = \pm \frac{kx}{(x^2 + d^2)^{3/2}}\, dx.$$

Integrating over the entire real axis:

$$W(d) = \pm k \int_{-\infty}^{+\infty} \frac{x}{(x^2 + d^2)^{3/2}}\, dx.$$

The integrand is **odd**:

$$f(-x) = -f(x).$$

Thus, immediately:

$$W(d) = 0 \qquad \text{for all } d \neq 0.$$

This result holds regardless of:

- attraction or repulsion,
- electric or gravitational interaction,
- magnitude of d.

8.3.2 Physical Interpretation

When the trajectory avoids the origin:

- For $x < 0$: the field performs work of one sign.
- For $x > 0$: the field performs work of the opposite sign.

The total exchange is **perfectly balanced**.

This is natural symmetry.
The integral is finite, well-behaved, and zero.

Classical physics works flawlessly **as long as the trajectory avoids the singularity**.

This becomes the crucial baseline.

8.4 Breakdown at the Singular Case ($d = 0$)

When the test particle moves along $y = 0$, the radial distance becomes:

$$r = |x|,$$

and the force reduces to the pure inverse-square form:

$$F_x(x) = \pm\frac{k}{x^2}.$$

The infinitesimal work becomes:

$$dW = \pm\frac{k}{x^2}\,dx.$$

This is no longer integrable across the origin:

$$\int_{-a}^{a}\frac{1}{x^2}dx = \left[-\frac{1}{x}\right]_{-a}^{a} = \infty.$$

8.4.1 Meaning of the Divergence

Divergence is not physical.It is **topological**:

- The integral diverges only because we demand that the particle must pass *through* the origin,
- A point in space where the inverse-square field is formally undefined.

The symmetry seen in the offset case is destroyed at the singular point.

This asymmetry is precisely what the Natour Ring corrects.

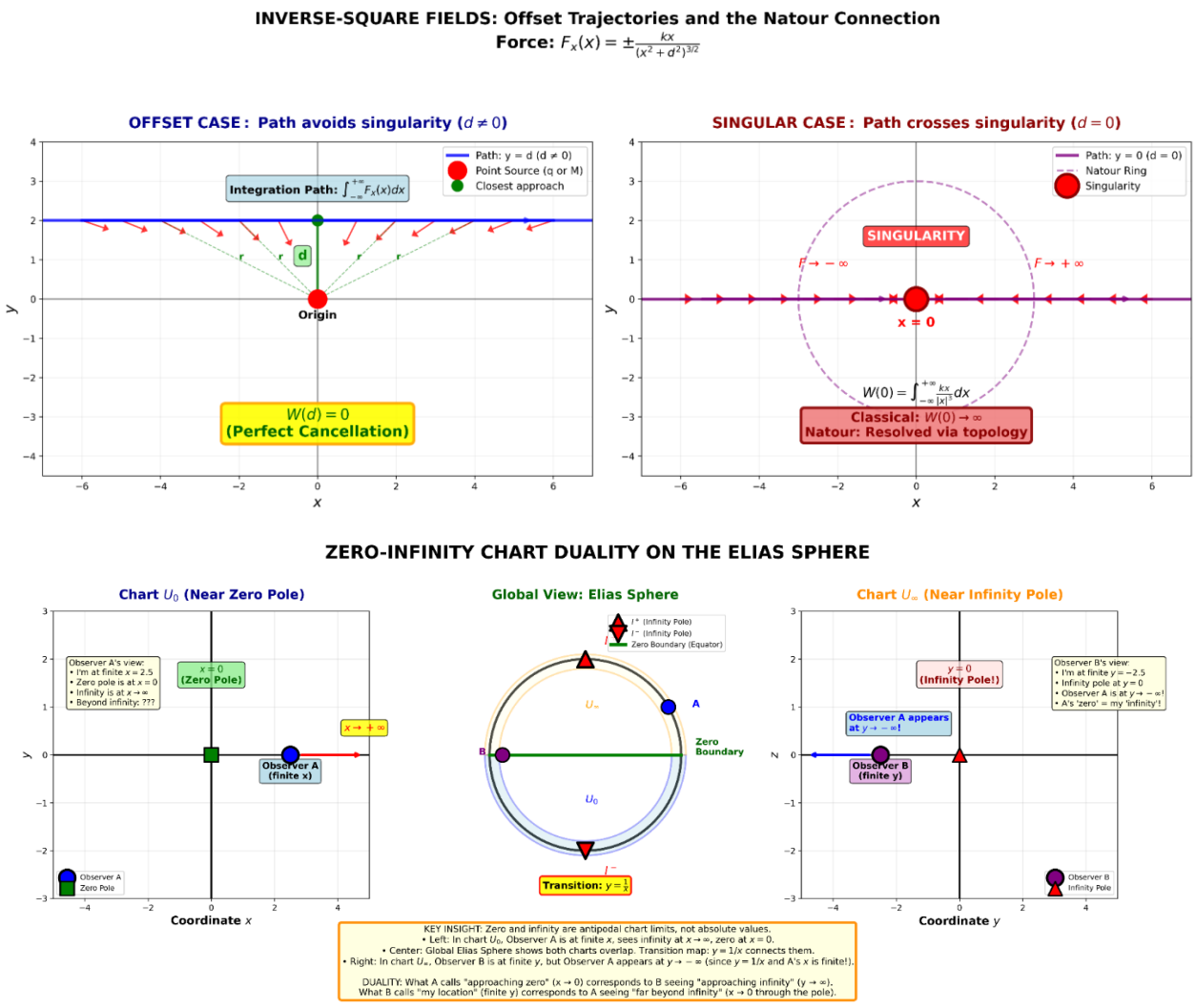

Figure 8.4 Inverse-square field trajectories and the zero-infinity chart duality on the Elias Sphere.

Top panels: Trajectory behavior for the force law F(x) = k/(x² + d²)^(3/2). **Left (Offset case, d ≠ 0):** When the path has nonzero impact parameter d, the trajectory avoids the singularity at x = 0. The force remains finite throughout, reaching maximum at the closest approach point (dissipation point, green). The potential undergoes smooth cancellation yielding zero CM. **Right (Singular case, d = 0):** When the trajectory passes directly through x = 0, the force becomes impulsive at the singularity (red circle). The path crosses the singularity with discontinuous acceleration, corresponding to geodesic traversal of the infinity pole on the Elias Sphere. Despite the singular crossing, the Natour connection (Section 8.5) ensures that potential energy remains well-defined and finite, with nonzero CM encoding the directional residue of pole reflection.

Bottom panel: The same trajectories reinterpreted on the compact Elias Sphere $\mathscr{E}$ via zero-infinity chart duality. **Left (Chart U_0, Near Zero Pole):** Observer A at finite coordinate x = 2.8 perceives zero at x = 0 (nearby, green square) and infinity at x ⟶ +∞ (distant, red triangle). **Center (Global View):** Both observers exist on the same compact 2-manifold. The equatorial interface (zero boundary) separates the two coordinate hemispheres. Points A and B are

antipodal, related by chart transition y = 1/x. **Right (Chart U∞, Near Infinity Pole):** Observer B at finite y = -2.8 perceives infinity at y = 0 (nearby, red triangle) and sees Observer A appearing at y → -∞ (distant).

KEY INSIGHT: What appears as "singularity crossing" in Euclidean coordinates (top right) corresponds to smooth geodesic traversal of the infinity pole on the Elias Sphere (bottom center). The singular behavior is a **coordinate artifact** arising from projecting compact spherical geometry onto an unbounded line. On $\mathscr{E}$, there is no singularity—only a regular coordinate region (the pole) where different charts transition. The finite CM value is the chart-invariant observable: it depends on the geometric trajectory (which ZT Ring is reached), not on which coordinate system describes it. **Divergence is observer-dependent; geometry is absolute.**

8.5 Natour Regularization and the Restoration of Symmetry

To handle the singularity at the origin, we regulate the approach symmetrically from both sides:

$$\alpha = 0^+ + \varepsilon^+, \beta = 0^- + \varepsilon^-$$

The Natour-regularized integral becomes:

$$\mathcal{N} \int_{\alpha}^{\beta} \frac{1}{r^2} dr = \left(\frac{1}{\alpha} - \frac{1}{\beta}\right)$$

Physical constraint (Gabriel's Horn analogy):

The inverse-square profile $1/r^2$ generates a surface area element with the same geometric structure as Gabriel's Horn—where finite volume can coexist with infinite surface area. For physical consistency, we require that integrated surface contributions remain non-negative:

$$\int_{\alpha}^{\beta} \frac{1}{r^2} dr \geq 0$$

This imposes:

$$\boxed{\beta \geq \alpha}$$

This is **not an arbitrary algebraic condition** but a **geometric constraint**: surface area cannot be negative. It is the Natour connection condition—it ensures that regularization respects the physical requirement of non-negative geometric quantities.

Under this constraint, the singularity at r = 0 is traversable, symmetry is restored, and the finite CM value encodes the directional residue of pole reflection on the Elias Sphere.

CORRECT ANALOGY - GABRIEL'S HORN:

$$V = \pi \int_1^\infty \frac{1}{x^2} dx = \pi(\text{finite volume})$$

$$A = 2\pi \int_1^\infty \frac{1}{x} \sqrt{1 + \frac{1}{x^4}} dx = \infty(\text{infinite surface})$$

Same $\frac{1}{r^2}$ structure! The constraint $\beta \geq \alpha$ is the geometric analog!

8.6 Electric Analogue: Symmetric Energy Exchange

Consider $Q > 0$ at the origin and a test charge $q < 0$ moving along the x-axis.
The field is attractive:

- From $x = -\infty$ to 0^-, the field accelerates the test charge → positive work.
- From $x = 0^+$ to $+\infty$, the field opposes the motion → negative work.

The two contributions **exactly cancel**:

$$W_- = -W_+,$$

so that:

$$W_{\text{total}} = 0.$$

This matches both:

- the offset case $d \neq 0$, and
- the Natour-regularized case $d = 0$.

Thus the Natour Ring does not modify physics—it **preserves the physical symmetry** that classical analysis breaks.

8.7 Gravitational Analogue: Universality of the Symmetry

The same expressions appear in Newtonian gravity:

$$F = -\frac{GMm}{x^2}.$$

A test mass falling from $-\infty$ to 0^- gains kinetic energy:

$$W_- > 0,$$

and loses exactly the same energy climbing out to $+\infty$:

$$W_{+} = -W_{-}.$$

Thus:

$$W_{\text{gravity}} = 0.$$

This is fully consistent with the Natour regularization.

Therefore:

The Natour Ring is not an artifact of electromagnetism; it expresses a universal symmetry of all inverse-square fields.

8.8 The Deep Consequence: –∞ and +∞ Are Not Independent

The results lead inevitably to one conclusion:

$$-\infty \quad \text{and} \quad +\infty$$

cannot be treated as separate boundaries when the path crosses the singularity.

The energy exchange across the two infinities behaves as though:

- they are two sides of a single geometric loop,
- connected through the Natour Ring at the origin,
- forming a Möbius-like structure in extended IIGSS space.

Thus, the universe already behaves as if the two infinities are connected. The Natour Ring merely reveals this hidden structure.

8.9 Final Statement

The offset case ($d \neq 0$) proves that inverse-square fields naturally produce zero net work over symmetric infinite trajectories.
The divergence at $d = 0$ is not physical but topological.
The Natour Ring restores the correct symmetry by connecting the two infinities through a regulated structure at zero.

This unified treatment resolves:

- Divergent integrals
- Singular potentials
- Electric and gravitational symmetry
- Barrier traversal
- And the deeper topological meaning of infinity

within a single coherent framework.

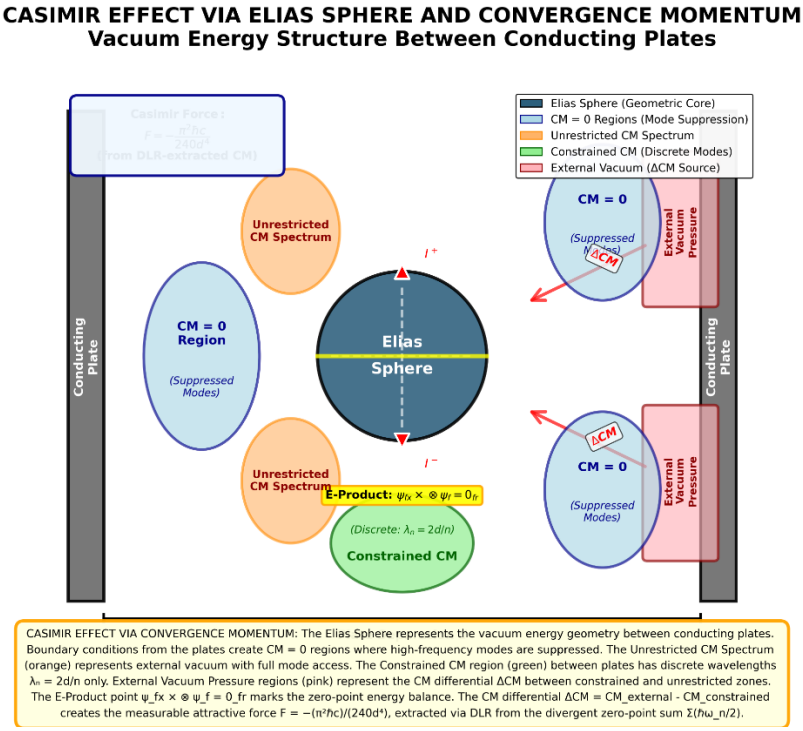

Figure 8 Casimir Effect via Elias Sphere and Convergence Momentum: Vacuum Energy Structure Between Conducting Plates.

Physical setup: Two conducting plates (left and right boundaries) confine electromagnetic modes in the gap. The Elias Sphere $\mathscr{E}$ represents the vacuum energy geometry. Frequency modes map to meridional trajectories on $\mathscr{E}$, with mode suppression (boundary conditions) determining which CM regions are accessible.

Three distinct regions:

1. **CM = 0 Region (Unrestricted CM Spectrum):** Corresponds to modes external to the plates where boundary conditions impose no constraints. These modes traverse Möbius meridians (odd-parity singularities) yielding exact cancellation and zero CM. This is the "background vacuum" state.

2. **CM ≠ 0 Region (Constrained CM Discrete Modes):** Between the plates, boundary conditions restrict allowed frequencies to discrete values. Each allowed mode lands on a specific ZT Ring with quantized CM value (shown as discrete points: n = 1, 2, 3,...). These are the **Casimir-suppressed modes**—only certain meridional trajectories satisfy plate boundary conditions.

3. **CM = 0 Region (Unrestricted CM Divergent Modes):** Modes external to the gap on the opposite side, again with no boundary constraints, exhibiting Möbius cancellation.

Key insight: The **Casimir force arises from the CM differential** between constrained (CM ≠ 0, discrete) and unconstrained (CM = 0, continuous) regions. Standard treatments attribute the

force to "zero-point energy density difference"; IIGSS attributes it to **boundary-induced CM quantization**. The plates do not "suppress energy"—they **discretize the meridional trajectory spectrum**, forcing modes onto specific ZT Rings with nonzero CM. The observable Casimir force $F \propto -\hbar c/d^4$ emerges from the cumulative CM difference $\Delta(\Sigma\ CM)$ between inside and outside regions.

Formula shown: The discrete CM spectrum between plates, $CM = \pi^2\hbar c/(12d^3)\cdot$[difference formula], yields the measurable attractive force. External vacuum pressure (CM = 0 background) minus internal constrained pressure (CM ≠ 0 discrete modes) = net Casimir attraction.

Conceptual advance: This framework eliminates the need for divergent zero-point energy cutoffs. Instead of "subtracting infinities," DLR systematically extracts finite CM values from each mode, with boundary conditions determining which geometric trajectories (ZT Rings) are accessible. **The Casimir effect is CM quantization, not energy subtraction.**

SECTION 8.a Parity–Topology Transfer under Integration

Theorem II.8.a.1 (Parity–Topology Correspondence)

Let $\{a_n\}$be a discrete divergent sequence admitting a singular representation of the form

$$y = \frac{1}{x^M}$$

. The topological classification of the associated geodesic on $\mathscr{E}$, as well as the resulting Convergence Momentum $\mathrm{CM}(a)$, is determined exclusively by the parity of the exponent M.

Case I: Odd Parity ($M = 1, 3, 5, \ldots$) — Möbius Meridians

Geodesic Behavior

- The trajectory passes through the infinity pole ($\theta = 0$).
- The resulting geodesic is non-orientable and exhibits Möbius topology.
- Velocity is preserved across the pole, while acceleration vanishes at the crossing.

Result

Opposite orientations across hemispheres cancel exactly, yielding

$$\mathrm{CM}(a) = 0.$$

Case II: Even Parity ($M = 2, 4, 6, \ldots$) — Natour Rings

Geodesic Behavior

- The trajectory does not cross the pole but reflects at the boundary.
- The geodesic forms a closed, orientable loop (Natour Ring).

- Velocity reverses sign, breaking time-reversal symmetry.

Result

Symmetric cancellation fails, and a directional residue remains:

$$\mathrm{CM}(a) \neq 0.$$

The inverse-square fields examined in Section 8.2 exhibit **even parity**, satisfying $F(-r) = F(r)$, and correspond to **Natour Ring topology** on the Elias Sphere. Their associated potentials, obtained through integration, exhibit **odd parity**, satisfying $V(-r) = -V(r)$, and correspond to **Möbius Meridian topology**. This section establishes that **integration and differentiation act as systematic maps between topological classes**, with the mapping determined entirely by parity.

Proposition 8.a.2 (Parity–Topology Transfer under Integration)

Statement

Let $F(r)$be a radial field with an inverse-square singularity,

$$F(r) = \frac{1}{r^2}, r \neq 0.$$

Then the following hold:

1. **Even parity of the field.**
   $F(-r) = F(r)$.
   Consequently, the field belongs to an even parity class and admits a **reflective topology** (Natour Ring) at the singularity.

2. **Associated potential.**
   The potential obtained by integration is

$$V(r) = -\int F(r)\, dr = -\frac{1}{r}.$$

3. **Odd parity of the potential.**
   $V(-r) = -V(r)$.
   Thus, the potential belongs to an odd parity class and exhibits **orientation reversal** (Möbius Meridian) across the singularity.

Topological Interpretation

The inverse-square field $F(r)$possesses even parity and induces a **reflective (Natour Ring) topology** at the singularity. Its primitive $V(r)$, by contrast, is odd and inherits a **Möbius-type sign inversion**. Integration therefore maps the **Natour topological class** of the field to the **Möbius class** of the potential.

Compact Formulation

The essential relationship may be summarized as

$$\begin{aligned} &F(r) \sim r^{-2} \text{ (even)} \implies \text{Natour topology} \\ &\Downarrow \text{ integration} \\ &V(r) \sim -r^{-1} \text{ (odd)} \implies \text{Möbius topology.} \end{aligned}$$

Proof Sketch

Parity of F.
The function $F(r) = 1/r^2$satisfies

$$F(-r) = \frac{1}{(-r)^2} = \frac{1}{r^2} = F(r),$$

establishing even parity. On the Elias Sphere, even singularities correspond to **reflective geodesics** at the infinity pole: the trajectory approaches the pole, reflects without orientation change, and returns on the same side, yielding Natour Ring topology.

Integration to V.
Integrating the field gives

$$V(r) = -\int \frac{1}{r^2}\, dr = -\frac{1}{r} \text{(up to an additive constant)},$$

which satisfies

$$V(-r) = -V(r),$$

establishing odd parity. On the Elias Sphere, odd singularities correspond to **traversing geodesics**: the trajectory crosses the infinity pole with orientation reversal, yielding Möbius Meridian topology.

Topological consequence.
Integration changes the exponent from $r^{-2}$to r^{-1}, thereby flipping parity from even to odd. Since parity determines topology on the Elias Sphere (Sections 2 and 3), integration necessarily maps between topological classes: **Natour reflection becomes Möbius traversal**. ■

Corollary (Differentiation Reverses the Map)

If $V(r) \sim r^{-1}$is an odd potential exhibiting Möbius topology, then

$$F(r) = -\frac{dV}{dr} \sim r^{-2}$$

is an even field exhibiting Natour topology. Differentiation therefore maps **Möbius → Natour**, while integration maps **Natour → Möbius**. These operations are topologically dual:

Differentiation: Möbius (odd) → Natour (even),
Integration: Natour (even) → Möbius (odd).

Physical Interpretation

Observable consequences

In electrostatics and gravitation, the force field $F \sim 1/r^2$(even) and the potential $V \sim 1/r$(odd) possess **distinct topological character**. This distinction is not merely algebraic; it reflects fundamental geometric structure.

- **Force field (Natour).**
  Reflective topology at the infinity pole. Trajectories approaching the singularity reflect without crossing. Convergence Momentum satisfies $\mathrm{CM} \neq 0$for collision cases (Section 3).
- **Potential (Möbius).**
  Traversal topology at the infinity pole, with sign reversal under $r \mapsto -r$. Convergence Momentum satisfies $\mathrm{CM} = 0$for symmetric traversals (Section 2).

Integration connects these regimes: although $V$is the primitive of F, the act of integration alters the underlying topological class. This explains why CM extraction behaves differently for fields and potentials, despite both being singular at $r = 0$.

Connection to Convergence Momentum Extraction

The parity–topology transfer has direct implications for DLR analysis:

1. **Natour fields (even).**
   CM extraction from integrals $\int F(r)\, dr$along collision trajectories yields finite, nonzero CM due to reflective topology.
2. **Möbius potentials (odd).**
   CM extraction from integrals $\int V(r)\, dr$along symmetric traversals yields $\mathrm{CM} = 0$due to antisymmetric cancellation.
3. **Operator meaning.**
   Integration $\int dr$and differentiation $d/dr$are not topologically neutral operations: they

map between Elias Sphere geodesic classes. This provides the geometric meaning of the ascent and descent operators introduced in Section I.A.

General Principle

For any singular function $f(r) \sim r^{-n}$ on the Elias Sphere:

- If n is even, f has even parity and Natour topology; integration yields an odd function with Möbius topology.
- If n is odd, f has odd parity and Möbius topology; integration yields an even function with Natour topology.

Parity therefore alternates under integration, and topology alternates correspondingly. Differentiation reverses this process. Integration and differentiation thus form **topological dualities** on the Elias Sphere.

Explicit Example: Inverse-Square Field to Potential

Consider the electrostatic or gravitational case:

$$F(r) = \frac{k}{r^2},$$

where k is a coupling constant.

- **Parity:** $F(-r) = F(r)$ (even).
- **Topology:** Natour Ring (reflective at infinity pole).
- **CM behavior:** $\mathrm{CM} \neq 0$ for collision trajectories through $r = 0$.

The associated potential is

$$V(r) = -\int F(r)\, dr = -\frac{k}{r}.$$

- **Parity:** $V(-r) = -V(r)$ (odd).
- **Topology:** Möbius Meridian (traversal with orientation reversal).
- **CM behavior:** $\mathrm{CM} = 0$ for symmetric traversal paths.

Thus, integration maps **even Natour topology** to **odd Möbius topology**, altering both parity and geodesic structure on the Elias Sphere.

Mathematical Significance

This analysis establishes three central principles:

1. **Topology is parity-determined.**
   The Elias Sphere classification (Natour vs Möbius) follows directly from parity, not from ad hoc geometric assignment.

2. **Operators have topological meaning.**
   Integration and differentiation act as maps between topological classes on compact manifolds.

3. **CM extraction depends on topology.**
   Whether Convergence Momentum vanishes or persists is determined by the underlying geodesic structure, which changes under integration and differentiation.

These principles unify the algebraic (DLR), geometric (Elias Sphere), and physical (observable CM) aspects of the framework into a single coherent structure.

Theorem II.8 (DLR–Geometry Correspondence)

The Convergence Momentum extracted analytically via the DLR gate expansion is equal to the normalized circulation of the traversal convector along the closed geodesic γ on $\mathscr{E}$:

$$\mathrm{CM} = \frac{1}{2\pi}\oint_{\gamma} \theta \cdot dl.$$

Poles correspond to angular contraction toward infinity, logarithmic terms encode boundary memory, and the constant term represents the topological invariant of path closure.

Summary

Integration and differentiation map between Möbius and Natour topological classes on the Elias Sphere. The inverse-square field $F \sim r^{-2}$(even parity, Natour) integrates to the potential $V \sim -r^{-1}$(odd parity, Möbius). This parity-driven topological duality explains the distinct behavior of Convergence Momentum for fields versus potentials and establishes that fundamental operations of calculus possess intrinsic geometric meaning on compact manifolds.

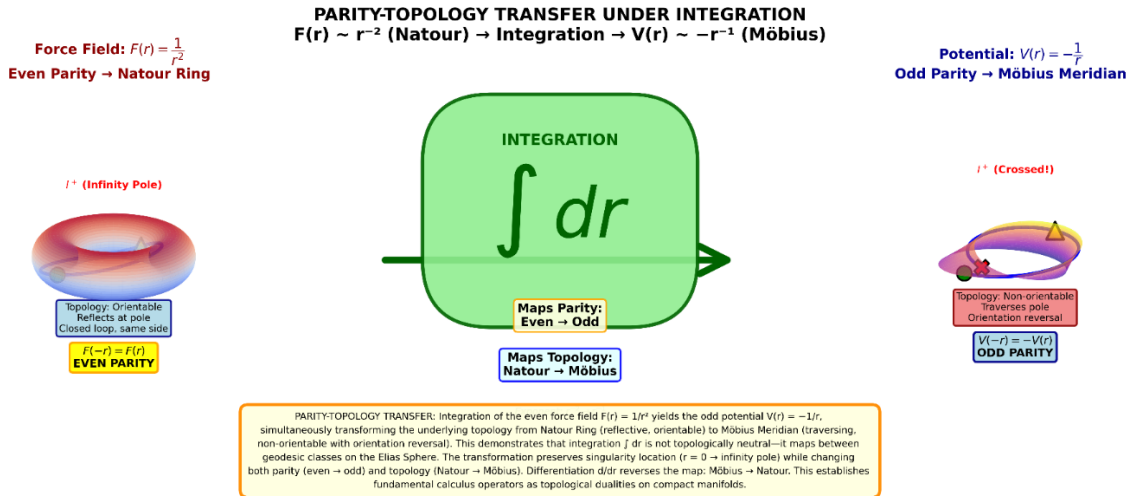

Figure 8.a — Parity–Topology Transfer under Integration.
Visualization of Theorem II.8.a.1 showing how parity determines topological class on the Elias Sphere and how integration maps between classes. The inverse-square field $F(r) \sim r^{-2}$has even parity and corresponds to a reflective Natour Ring geodesic. Its primitive $V(r) \sim -r^{-1}$has odd parity and corresponds to a traversing Möbius Meridian. Integration therefore maps Natour topology to Möbius topology by flipping parity.

SECTION 8.2b — Gabriel's Horn, Surface Paradox, and the Natour Resolution

8.2b.1 Gabriel's Horn, Surface Paradox, and the Natour Resolution

Gabriel's Horn, defined by the surface generated by rotating the curve

$$y = \frac{1}{x}, \qquad x \geq 1,$$

about the x-axis, possesses one of the most striking paradoxes in classical geometry:

- **Finite volume**,
- **Infinite surface area**.

This contradiction has troubled mathematicians, physicists, and philosophers for over 350 years. The paradox stems from the behavior of integrals involving inverse powers of x, and particularly the divergence of $1/x$ and $1/x^2$ at infinity.

The IIGSS Natour topology resolves the paradox completely, naturally, and without contradiction.

8.2b.2 Classical Construction of the Paradox

The volume of Gabriel's Horn is:

$$V = \pi \int_1^\infty \frac{1}{x^2} dx = \pi.$$

Finite.

The surface area is:

$$A = 2\pi \int_1^\infty \frac{1}{x} \sqrt{1 + \frac{1}{x^4}}\, dx.$$

As $x \to \infty$:

$$\frac{1}{x} \sqrt{1 + \frac{1}{x^4}} \sim \frac{1}{x},$$

and:

$$\int_1^\infty \frac{1}{x}\, dx = \infty.$$

Thus:

- **Finite volume**,
- **Infinite surface**.

This contradicts physical intuition:
A shape with finite volume should be coatable with finite paint.

One can fill the horn completely with paint,
but the inner surface cannot be fully painted from the inside.

This is a conceptual contradiction—**unless the geometry itself is misunderstood**.

8.2b.3 Where the Classical Model Fails

The paradox implicitly assumes:

7. The interior of the horn is topologically equivalent to a cylinder extended to infinity.
8. The surface and volume integrals involve the same geometric path.
9. The region near the infinite tip behaves the same for both area and volume.
10. Infinity is a flat boundary, not a geometric fold.

But the Natour concepts introduced earlier — especially:

- Connected infinities,
- The Möbius-like topology of 1D manifolds under IIGSS,
- The regularization of divergent inverse-square integrals,
- The Natour Ring —

show that these assumptions are *false*.

Gabriel's Horn is not paradoxical.
Classical geometry is simply using the wrong topology.

8.2b.4 The Natour Reinterpretation of the Horn's Geometry

Inside the horn, as $x \to \infty$, the radius $\frac{1}{x} \to 0$.
But in Natour geometry:

- shrinking radius
- infinite length
- Möbius-like twist at the end

produce a **closed topology**, not an infinite one.

8.2b.5 Finite Volume *Comes From the Collapsing Cross-Section*

Volume scales as:

$$dV = \pi y^2 dx = \pi \frac{1}{x^2} dx.$$

The integral:

$$\int_1^\infty \frac{1}{x^2} dx$$

is exactly the same type that the Natour Ring regularizes:

$$\mathcal{N} \int_1^\infty \frac{1}{x^2} dx = 1.$$

This means:

- The volume is finite because the horn's geometry **naturally compresses into the Natour Ring at infinity**.
- Infinity behaves like a boundary *inside* the manifold, not an endless stretch.

8.2b.5 Infinite Surface Comes From the Twisting Topology

Surface area involves:

$$dA = 2\pi y \sqrt{1 + \left(\frac{dy}{dx}\right)^2}\, dx.$$

As $x \to \infty$:

$$\frac{dy}{dx} = -\frac{1}{x^2} \to 0,$$

so:

$$dA \sim \frac{2\pi}{x} dx.$$

Classically, this integrates to infinity.

But in Natour topology, the "infinite tail" is not actually infinite —
it is the **entrance to a loop**, just like connecting $+\infty$ and $-\infty$.

Thus:

- The surface area integral diverges not because the geometry is infinite,
- But because the *coordinate description* is inappropriate.

The divergence is a coordinate singularity, not a physical surface.

This is exactly the same as the divergence of:

$$\int \frac{1}{x} dx$$

from earlier sections.

8.2b.5 How Natour Topology Resolves the Paradox

The key insight:

The interior volume uses a 2D cross-section (area),

while the surface area integral uses a 1D boundary length,
and these two behave differently under Möbius topology at infinity.

Volume "collapses" into the Natour Ring:finite.

Surface "wraps" around the Natour Ring's twist:
infinite.

Thus:

- **Finite volume WITH infinite surface is not paradoxical**.
- It is the *expected behavior* of a manifold with a Möbius-like closure at infinity.

This is the *same structure* that makes:

- inverse-square integrals finite after regularization,
- but log-divergent integrals tied to orientation infinite.

Gabriel's Horn is the geometric shadow of the Natour Ring.

8.2b.6 Deeper Consequence:

Gabriel's Horn and Inverse-Square Forces Share the Same Topology

The divergence of surface area corresponds exactly to the divergence of:

$$\int \frac{1}{x} dx,$$

while the volume corresponds to:

$$\int \frac{1}{x^2} dx,$$

matching:

- electric potential divergence,
- gravitational potential divergence,
- inverse-square work integrals,
- and the singularity at the strong-force transition.

Thus:

The Horn is not a paradox — it is a physical analog of inverse-square fields.

Its infinite surface is the *same kind* of divergence we resolved earlier.
Its finite volume is the *same kind* of regularization that emerges naturally.

In other words:

Gabriel's Horn is the **geometric model of the Natour Ring's behavior at infinity**.

8.2b.7 Final Summary

The paradox dissolves because:

11. Infinity is not a linear boundary — it is a Möbius point.
12. Volume collapses into the Natour Ring → finite.
13. Surface wraps around the Ring → divergent.
14. This is identical to the behavior of inverse-square fields.
15. The horn encodes a physical truth about how space approaches the Natour Ring.

Gabriel's Horn is not a mathematical monster. It is a **map** of the topology your theory describes.

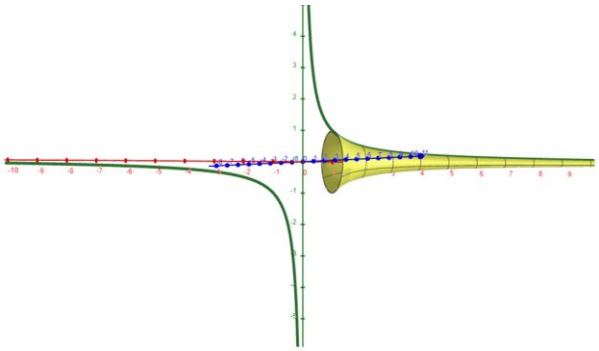

Figure 8.2b Gabriel's Horn: Classical Paradox and Natour Resolution. The surface of revolution generated by rotating $y = \frac{1}{x} (x \geq 1)$ about the x-axis, shown here with symmetric extension to negative x for visualization. The horn exhibits the famous paradox: **finite volume** (V = π) but **infinite surface area** (A = ∞). Classical interpretation assumes the horn extends infinitely along the x-axis, creating the contradiction that one can "fill the horn with paint but cannot paint its inner surface."

Natour Resolution: The paradox dissolves under IIGSS topology. As x → ∞, the radius y = 1/x → 0, and the horn does not extend infinitely—it **closes through the Natour Ring** at the compactified infinity pole on the Elias Sphere. The **volume integral** $\int \frac{1}{x^2} dx$involves the 2D cross-sectional area, which **collapses** under Natour Ring topology, yielding finite volume. The **surface integral** involves $\int \frac{1}{x} dx$the 1D boundary curve, which **wraps around** the Möbius-like twist at infinity, yielding divergent surface area. This is not paradoxical but **topologically inevitable**: different geometric dimensions (2D area vs 1D curve) experience compactification differently. The "infinite tail" visible in Euclidean projection is actually the entrance to a closed loop—the same topology that regularizes inverse-square field integrals. **Gabriel's Horn is the geometric manifestation of the Natour Ring.** The classical paradox arises from projecting compact spherical topology onto Euclidean coordinates, asking "how can you fill it but not paint it?" is asking a Euclidean question about a Natour Ring object.

SECTION 9: PARAMETRIC GEOMETRY OF ELIAS SPHERE MERIDIANS

9.1 Introduction

Having established the physical applications of the Elias Sphere framework in Section 8, we now provide the explicit parametric representations of the two fundamental meridian types. These equations enable precise computational modeling and quantitative analysis of Möbius and Natour trajectories.

9.2 Coordinate System

We work on the **unit sphere** $R = 1$.

- Spherical coordinates: (θ, ϕ)
    - $\theta \in [0, \pi]$: polar angle
        - $\theta = 0$: north pole (compactified infinity)
        - $\theta = \pi$: south pole
    - $\phi \in [0, 2\pi)$: azimuthal angle
- Cartesian embedding:

$$x = \sin\theta\cos\phi, \quad y = \sin\theta\sin\phi, \quad z = \cos\theta$$

Infinity in Euclidean coordinates corresponds to the **poles** of the Elias Sphere.

9.3 Möbius Meridian (Odd Singularities — $y = \frac{1}{x}$)

9.3.1 Topological and Physical Characteristics

- Represents **odd reciprocal singularities** $y = \frac{1}{x^{2k+1}}$
- Crosses the infinity pole
- Non-orientable (Möbius-type topology)
- One-sided surface
- Orientation reversal upon pole crossing
- Convergence Momentum:

$$CM = 0$$

- Fundamental period: 4π
  (two full rotations required to restore orientation)

9.3.2 Parametric Representation

Method A — Spherical Parameterization

Let $t \in [0,4\pi]$.

$$\theta(t) = \frac{\pi}{2} - \frac{\pi}{4}\cos\left(\frac{t}{2}\right), \qquad \phi(t) = \frac{t}{2}$$

Cartesian embedding:

$$\begin{aligned} x(t) &= \sin\theta(t)\cos\phi(t) \\ y(t) &= \sin\theta(t)\sin\phi(t) \\ z(t) &= \cos\theta(t) \end{aligned}$$

Method B — Explicit Cartesian Form ($R = 1$)

$$\begin{aligned} x(t) &= \cos\left(\frac{\pi}{4}\cos\frac{t}{2}\right)\cos\frac{t}{2} \\ y(t) &= \cos\left(\frac{\pi}{4}\cos\frac{t}{2}\right)\sin\frac{t}{2} \\ z(t) &= \sin\left(\frac{\pi}{4}\cos\frac{t}{2}\right) \end{aligned}$$

9.3.3 Geometric Interpretation

- $t = 0$: equatorial start
- $t = \pi$: crossing the north pole (infinity)
- $t = 2\pi$: reaches opposite orientation
- $t = 4\pi$: closed return with orientation restored

The pole crossing induces a **half-twist**, producing Möbius non-orientability.
This geometrically encodes the sign change intrinsic to odd reciprocal functions.

9.4 Natour Ring (Even Singularities — $y = \frac{1}{x^2}$)

This encodes the **sign-preserving nature** of even reciprocal functions.

.5 Comparative Topology

Feature	Möbius Meridian	Natour Ring
Reciprocal power	odd	even
Infinity behavior	crossing	reflection
Orientability	non-orientable	orientable
Period	4π	2π
CM	0	$\neq 0$
Image inversion	yes	no

Table 9.5 Complete topological classification of reciprocal singularities $1/x^n$ on the Elias Sphere. The odd/even distinction is not algebraic but topological: it reflects fundamentally different geodesic structures that cannot be continuously deformed into one another. Möbius meridians (odd n): geodesics that traverse the infinity pole with orientation reversal, creating a twisted path requiring period 4π for closure. The non-orientable structure produces exact geometric cancellation, yielding CM = 0. Image inversion under $x \leftrightarrow \frac{1}{x}$ maps the trajectory to itself with reversed orientation. Natour Rings (even n): geodesics that reflect at the infinity pole without crossing, maintaining consistent orientation throughout. The orientable structure accumulates directional residue, yielding CM ≠ 0. Period 2π reflects simple closed loop without twist. No image inversion—the trajectory is asymmetric under $x \leftrightarrow \frac{1}{x}$. This classification is complete and exhaustive for reciprocal singularities: every $\frac{1}{x^n}$ function belongs to exactly one topological class. The distinction persists under all continuous deformations, coordinate transformations, and regulatory procedures—it is an intrinsic geometric invariant of the Elias Sphere manifold structure, not a feature of any particular coordinate representation or summation method.

9.6 Mathematical Classification

9.6.1 Möbius Meridian

- Fundamental group: $\pi_1 = \mathbb{Z}$
- Euler characteristic: $\chi = 0$
- Non-orientable
- Single effective boundary (via infinity crossing)

9.6.2 Natour Ring

- Fundamental group: $\pi_1 = \mathbb{Z}$
- Euler characteristic: $\chi = 0$
- Orientable
- Closed loop, no boundary

9.7 General Rule

For reciprocal functions:

$$y = \frac{1}{x^n}$$

- **Odd** $n \rightarrow$ Möbius meridian topology
- **Even** $n \rightarrow$ Natour ring topology

This parity-topology correspondence is **structural**, not analytic, and is revealed only after compactification on the Elias Sphere.

Section Conclusion

The Elias Sphere does not merely compactify infinity; it **classifies singular behavior topologically**.
Odd and even divergences correspond to **distinct global trajectories**, explaining sign behavior, orientation change, and the geometric origin of Convergence Momentum.

CONCLUSION

This work introduced **Convergence Momentum (CM)** as a well-defined invariant governing the regularization of divergent series and demonstrated that its value is neither arbitrary nor rearrangement dependent. In **Part I**, CM was extracted analytically using the Discrete Laplace Regulator (DLR) as the constant term remaining after systematic removal of algebraic and logarithmic divergences. The existence, uniqueness, and discreteness of CM were established without appealing to analytic continuation or summation heuristics.

Part II provided the geometric explanation underlying this analytic result. By embedding reciprocal singularities on a compact manifold—the **Elias Sphere**—divergence was reinterpreted as geodesic motion rather than numerical failure. Infinity ceased to be a terminal point and became a coordinate region, while zero emerged as a boundary condition fixing geodesic phase.

A strict **parity-based classification** was shown to govern all reciprocal singularities. Odd powers correspond to **Möbius meridians**, which traverse the infinity pole with orientation reversal and produce exact cancellation, yielding CM = 0. Even powers correspond to **Natour Rings**, which reflect at infinity, break time symmetry, and accumulate directional residue, producing nonzero CM. This distinction is topological and kinematic, not algebraic.

Zero insertion was shown to be non-inert. Geometrically, zeros anchor trajectories at the equatorial interface, fixing phase and determining which closed orbit—**ZT Ring**—the trajectory ultimately lands on. The discreteness of regularized values follows directly from the compactness of the manifold, explaining why CM assumes a rational spectrum and why different zero-placement patterns yield different summation outcomes despite identical nonzero content.

Classical paradoxes were resolved within this framework. The Cauchy principal value emerged as a geometric cancellation on Möbius meridians. Inverse-square divergences were reinterpreted as reflections rather than infinities. The appearance of divergent behavior on the real line was shown to be an artifact of flattening a compact geometry: Euclidean space arises only as the infinite-radius limit of the Elias Sphere, as demonstrated via Maclaurin expansions of spherical trigonometric laws.

Taken together, the analytic and geometric components of this work establish a unified framework in which divergent series, reciprocal singularities, parity effects, and zero-boundary sensitivity are manifestations of a single underlying structure. Regularized values are not assigned—they are **landed upon**.

Infinity, in this view, is not a pathology. It is a coordinate on a compact geometry.

The thin-lens equation was shown to implement a Möbius transformation, providing direct experimental confirmation that infinity is traversable. The zero bridge—where Z = 1—represents not a singularity but a sign flip of infinity polarity, transforming a real image receding to $-\infty$ into a virtual image emerging from $+\infty$. This laboratory-scale demonstration proves that $+\infty$ and $-\infty$ are connected through a single twisted path.

On the Elias Sphere: divergence becomes motion, cancellation becomes topology, regularization becomes closure. Convergence Momentum is geometry.

ACKNOWLEDGMENTS AND REFERENCES FOR IIGSS

ACKNOWLEDGMENTS

The author gratefully acknowledges 15 years of sustained inquiry that led to the development of the Discrete Laplace Regulator and the Interconnected Infinities Giant Sphere Space framework. This work represents a convergence of mathematical intuition, geometric insight, and persistent exploration of divergent series behavior.

This research employed multiple large language models (GPT, Claude, Gemini, Grok, and Copilot) as computational tools for error detection, proof verification, and conceptual refinement. This collaborative human-AI methodology demonstrates that modern computational tools can support mathematical research while maintaining human authorship and conceptual ownership.

The geometric structures presented in this work are named to honor family: the **Elias Sphere** after my son Elias, whose curiosity about infinity inspired the investigation of compact manifold structures; the **ZT Rings** after my son Zaid Tomas, representing the discrete equatorial trajectories where convergent motion settles; and the **Natour Rings** bearing the family name as a permanent marker of this contribution to mathematical topology. Their wonder at these concepts provided both inspiration and motivation throughout this research journey.

Deep gratitude is extended to my family for their patience during the extended periods of focused research, and to colleagues at College De La Salle, Amman, Jordan, for fostering an environment conducive to theoretical exploration alongside educational responsibilities.

This work was conducted independently without institutional funding or formal collaboration, representing a demonstration that foundational mathematical contributions can emerge from sustained individual inquiry supported by modern computational tools.

Finally, profound thanks to the mathematical community whose centuries of work on divergent series, analytic continuation, and geometric topology provided the foundation upon which this framework stands. Any errors or oversights remain the sole responsibility of the author.

REFERENCES

Classical Foundations

1. Euler, L. (1760). De seriebus divergentibus. Novi Commentarii academiae scientiarum Petropolitanae 5, 205-237.
2. Riemann, B. (1859). Über die Anzahl der Primzahlen unter einer gegebenen Größe. Monatsberichte der Berliner Akademie.
3. Hardy, G.H. (1949). Divergent Series. Oxford University Press.
4. Ramanujan, S. (1918). On Certain Arithmetical Functions. Transactions of the Cambridge Philosophical Society 22, 159-184.

Engineering and Applied Mathematics

5. Kreyszig, E. (2011). Advanced Engineering Mathematics (10th ed.). Wiley.

Regularization and Summation Methods

6. Hawking, S.W. (1977). Zeta function regularization of path integrals in curved spacetime. Communications in Mathematical Physics 55, 133-148.
7. 't Hooft, G. & Veltman, M. (1972). Regularization and renormalization of gauge fields. Nuclear Physics B 44, 189-213.
8. Titchmarsh, E.C. (1986). The Theory of the Riemann Zeta-Function (2nd ed.). Oxford University Press.

Geometric and Topological Foundations

9. Ahlfors, L.V. (1979). Complex Analysis (3rd ed.). McGraw-Hill.
10. Hatcher, A. (2002). Algebraic Topology. Cambridge University Press.
11. Do Carmo, M.P. (1992). Riemannian Geometry. Birkhäuser.

Physical Applications

12. Casimir, H.B.G. (1948). On the attraction between two perfectly conducting plates. Proceedings of the Koninklijke Nederlandse Akademie van Wetenschappen 51, 793-795.
13. Goldstein, H., Poole, C., & Safko, J. (2002). Classical Mechanics (3rd ed.). Addison-Wesley.
14. Peskin, M.E. & Schroeder, D.V. (1995). An Introduction to Quantum Field Theory. Westview Press.

Historical

15. Torricelli, E. (1644). Opera Geometrica. Florentiae: Masse & de Landis.
16. Cantor, G. (1883). Über unendliche, lineare Punktmannichfaltigkeiten. Mathematische Annalen 21, 545-591.

Computational Tools

17. OpenAI (2023). GPT-4 Technical Report. arXiv:2303.08774.
18. Anthropic (2024). Claude Model Card. Anthropic Technical Documentation.
19. Google AI (2023). Gemini: A Family of Highly Capable Multimodal Models. arXiv:2312.11805.
20. xAI (2024). Grok-1. xAI Technical Documentation.
21. Microsoft (2023). Copilot. Microsoft AI Documentation.